

SOLID SORBENT CONTROL OF NITROGEN OXIDES (NO<sub>x</sub>)

By

MAXWELL RICHARDSON MENTZER LEE

A DISSERTATION PRESENTED TO THE GRADUATE SCHOOL  
OF THE UNIVERSITY OF FLORIDA IN PARTIAL FULFILLMENT  
OF THE REQUIREMENTS FOR THE DEGREE OF  
DOCTOR OF PHILOSOPHY

UNIVERSITY OF FLORIDA

1999

This work is dedicated to my father, John Augustus Lee,  
for his firm belief in the value of education  
that laid the foundation of this achievement.

## ACKNOWLEDGMENTS

My sincere gratitude is given to Professor Eric R. Allen for his support and guidance in this academic endeavor. His knowledge and patience expressing such knowledge have proven the meaning of an advisor. During our meetings and conversations his advice has been demonstrative of issues much more than only this research. To Professor Dale Lundgren, I have appreciated his quick wit and pragmatism to real-world issues of air pollution. I offer my sincere appreciation to Professor Gar Hoflund for his continual interest in this research and support of new ideas. To Professor Emmett Bolch, I offer my gratitude for serving as a committee member and as the professor whom I initially met in the Environmental Engineering Department. That initial conversation helped persuade me to pursue a career in this field. As well, I give thanks to the numerous graduate students of the Air Pollution Program, present and past. I especially thank Larry Kimm for his encouragement to continue on with his research.

The advice of Joseph Wander through email and conference meetings has given me an additional point of view one can only have as an experienced manager and scientist. His friendship and advice have covered sage-like knowledge to the whimsical note.

XPS analysis and laboratory assistance of John Wolan and other members of Professor Hoflund's research group, and the added value of the work and experience that they have provided to this research are sincerely appreciated. Regarding technical

assistance, I wish to thank Professor B. Moudgil, UF Materials Science Engineering Department, for the use of the BET analyzer, including instrument training by his graduate student, Josh Adler. As well, the use of an FTIR from Professor K. Williams, which included the assistance of Mr. Russ Pierce, is appreciated.

I wish to thank the numerous undergraduate assistants I have had the opportunity to work with: John Lindsay, Tyler Crone, Michael Diehl, Tiffany Burns, Paul Dehart, and Jacob Mauldin. I give special thanks to undergraduate assistant Jacob Mauldin, who has worked with me during a major portion of this research. His talents in construction and design as well as computer skills have proven invaluable. The computer work of Dr. George Harder to create a successful data-acquisition program is appreciated.

Regarding the persons outside of the academic arena, I wish to thank Nancy Szabo for support of this endeavor and commitment to me. I also give thanks to my family including my nine brothers and sisters, who have taught me many things including the valuable lessons of working with others.

I would like to thank the United States Air Force, Armstrong Laboratory, Tyndall AFB, Florida, for the financial support to perform this research project. Also, financial support received from the National Science Foundation is appreciated.



## TABLE OF CONTENTS

|  | <u>page</u> |
|--|-------------|
| ACKNOWLEDGMENTS .....  | iii         |
| LIST OF TABLES .....   | viii        |
| LIST OF FIGURES.....   | ix          |
| ABSTRACT.....  | xiv         |
| <br>CHAPTERS   |             |
| 1 INTRODUCTION.....  | 1           |
| Chemical and Physical Properties of NO <sub>x</sub> .....      | 3           |
| NO <sub>x</sub> Related Atmospheric Chemistry.....             | 4           |
| Formation of Combustion NO <sub>x</sub> .....                  | 4           |
| Thermal NO <sub>x</sub> Formation .....                        | 4           |
| Fuel NO <sub>x</sub> Formation .....                           | 9           |
| Prompt NO <sub>x</sub> .....                                   | 11          |
| Detrimental Effects of NO and NO <sub>2</sub> .....            | 11          |
| Biological Effects.....  | 11          |
| Material Effects.....  | 13          |
| Government Regulations Related to NO <sub>x</sub> Control..... | 13          |
| NO <sub>x</sub> Control Technologies .....                     | 17          |
| Combustion Modification.....                                   | 17          |
| Flue-Gas Treatment.....  | 18          |
| Reduction Methods.....   | 19          |
| Sorption Methods .....   | 21          |
| Wet Sorption .....   | 21          |
| Dry Sorption .....   | 22          |
| Applied methods of dry sorption .....                          | 24          |
| Hybrid Systems .....   | 27          |
| Related SO <sub>2</sub> -Control Methods.....                  | 29          |
| Other NO <sub>x</sub> -Control Methods .....                   | 29          |
| Research Justification.....                                    | 30          |
| Research Objectives.....                                       | 31          |

|  |     |
|--|-----|
| 2 EXPERIMENTAL .....   | 32  |
| Fixed-Bed Reactor System.....  | 32  |
| Initial Fixed-Bed Reactor System .....   | 32  |
| Redesigned System: Single and Triple Bed .....                                       | 35  |
| Triple bed.....  | 37  |
| Water injection .....  | 38  |
| System automation .....  | 38  |
| Fixed-bed reactor system: experimental error.....                                    | 39  |
| Redesigned system .....  | 40  |
| General Fixed-Bed Reactor Experimental Procedure .....                               | 43  |
| Experimental Conditions .....  | 43  |
| Sample Preparation .....   | 46  |
| Magnesium-Oxide Coated Vermiculite (MgO/v).....                                      | 46  |
| $\gamma$ -Alumina: Untreated and Treated.....  | 48  |
| Ion-Specific Electrode (ISE) Measurements .....                                      | 50  |
| X-ray Photoelectron Spectroscopy .....   | 55  |
| BET Analyses .....   | 57  |
| Fourier Transform Infrared (FTIR) Analyses.....                                      | 60  |
| 3 RESULTS AND DISCUSSION .....   | 62  |
| Initial MgO/v Laboratory Experiments.....  | 64  |
| NO <sub>x</sub> Sorption: MgO/v .....  | 65  |
| MgO/v: Internal Diffusion of NO <sub>2</sub> .....                                   | 66  |
| MgO/v: External Diffusion .....  | 69  |
| MgO/v: Sorption of NO .....  | 69  |
| MgO/v: Effect of Water on NO <sub>x</sub> Sorption.....                              | 70  |
| Comparison of MgO/v and Alumina Sorbents .....                                       | 78  |
| MgO/v vs. Alumina: NO <sub>x</sub> Sorption .....                                    | 78  |
| Formation of NO.....   | 81  |
| Initial Studies of Untreated and KOH-Treated $\gamma$ -Alumina.....                  | 83  |
| Different Sources of $\gamma$ -Alumina .....   | 83  |
| Alumina: Removal of Gaseous NO.....  | 87  |
| X-ray Photoelectron Spectroscopy (XPS) Analysis of Untreated $\gamma$ -Alumina ..... | 87  |
| KOH-Treated $\gamma$ -Alumina: Initial Testing.....                                  | 89  |
| KOH Treatment Parameters: NO <sub>x</sub> -Sorption Effects .....                    | 98  |
| Studies of Group I-Treated $\gamma$ -Alumina .....                                   | 100 |
| NO <sub>x</sub> Sorption: Temperature Effects .....                                  | 107 |
| NO <sub>x</sub> Sorption: Concentration Effects .....                                | 107 |
| NO <sub>x</sub> Sorption: Saturation.....  | 115 |
| Comparison of Alkali Compounds: NO <sub>x</sub> Sorption.....                        | 115 |
| Alkali-Hydroxide Treatments .....  | 116 |
| Alkali-Carbonate Treatments.....   | 116 |
| Cesium Treatments.....   | 116 |

|  |     |
|--|-----|
| Alkali-Treated Alumina: Surface Area Measurements.....   | 123 |
| Relation of Alkali Element Ionization Potential to NO <sub>x</sub> Sorption.....                   | 127 |
| Sorption Studies of the Effect of Varying NO and NO <sub>2</sub> Concentrations.....               | 127 |
| Initial Tests on Sorption of Gaseous NO .....  | 130 |
| Interaction of NO with Sorbents following NO <sub>2</sub> Sorption .....                           | 130 |
| Effect of Varying the Inlet NO Concentration.....  | 135 |
| Effect of Varying Inlet NO <sub>2</sub> Concentrations .....                                       | 137 |
| Gas and Surface Profile for the Sorption Process.....  | 138 |
| Molar Ratio of Nitrite to Nitrate.....   | 146 |
| Trends in $\Delta\text{NO}_2$ sorbed/ $\Delta\text{NO}$ formed: Untreated and Treated Alumina..... | 148 |
| Proposed Reaction Mechanisms of NO <sub>x</sub> with Alkali-Treated or Untreated                   |     |
| Alumina .....  | 148 |
| Untreated $\gamma$ -Alumina .....  | 152 |
| KOH-Treated $\gamma$ -Alumina .....  | 153 |
| K <sub>2</sub> CO <sub>3</sub> -Treated $\gamma$ -Alumina.....                                     | 154 |
| Confirmation of NO Production from Nitrite-NO <sub>2</sub> Interaction.....                        | 154 |
| Fourier Transform Infrared (FTIR) Spectroscopy Confirmation of ISE                                 |     |
| Measurements.....  | 155 |
| Thermal Decomposition Studies.....   | 167 |
| Decomposition of NO <sub>2</sub> -Exposed Sorbents: Varied Exposure Time .....                     | 168 |
| Decomposition of Pure Compounds Treated onto $\gamma$ -Alumina.....                                | 170 |
| Decomposition of Pure Salts .....  | 171 |
| Effect of Additional Gases on NO <sub>x</sub> Sorption.....  | 179 |
| Added H <sub>2</sub> O vapor .....   | 179 |
| Added O <sub>2</sub> gas.....  | 180 |
| Added CO <sub>2</sub> gas .....  | 181 |
| Added SO <sub>2</sub> gas.....   | 181 |
| 4 CONCLUSIONS AND RECOMMENDATIONS.....   | 183 |
| REFERENCES.....  | 193 |
| APPENDICES   |     |
| A NO <sub>x</sub> SORPTION: CONSTANT NO (500 PPM), VARIED NO <sub>2</sub>                          |     |
| CONCENTRATION .....  | 201 |
| B NO <sub>x</sub> SORPTION: CONSTANT NO <sub>2</sub> (500 PPM), VARIED NO                          |     |
| CONCENTRATION .....  | 217 |
| C ADDED GASES, SO <sub>2</sub> AND H <sub>2</sub> O .....  | 233 |
| BIOGRAPHICAL SKETCH .....  | 249 |

## LIST OF TABLES

| Table  | page |
|--|------|
| 1-1. General properties of nitrogen oxide ( $N_xO_y$ ) species (US EPA, 1993). ....  | 5    |
| 1-2. Theoretical estimates of equilibrium concentrations for NO and $NO_2$ in air (21% $O_2$ ) and 50% relative humidity (US EPA, 1993).....   | 8    |
| 2-1. Physical properties of sorbent materials studied.....   | 49   |
| 2-2. ISE measurement error of $NO_x$ -exposed untreated, $K_2CO_3$ -treated and KOH-treated alumina samples .....  | 54   |
| 2-3. Cumulative measurement error of fixed-bed reactor testing and subsequent ISE measurement of three samples of $NO_x$ -exposed untreated, $K_2CO_3$ -treated and KOH-treated alumina..... | 56   |
| 3-1. $NO_x$ saturation capacity of untreated and KOH-treated $\gamma$ -alumina.....  | 97   |
| 3-2. Saturation capacity of treated alumina samples.....   | 117  |
| 3-3. BET surface area measurement of treated $\gamma$ -alumina sorbents. ....  | 124  |
| 3-4. Fractional $NO_2$ removal of Group-I treated alumina and element ionization potential.....  | 129  |
| 3-5. Fractional recovery of surface nitrogen species ( $NO_2^-$ and $NO_3^-$ ) to sorbed $NO_x$ gas. ....  | 147  |

## LIST OF FIGURES

| Figure  | page |
|---|------|
| 1-1. Schematic diagram of the combined reactions of nitrogen, oxygen, and hydrogen (Carmichael and Peters, 1984).....   | 6    |
| 1-2. Production of hydrocarbons, carbon monoxide, and nitrogen oxides as a function of A/F ratio (Heywood, 1988).....   | 10   |
| 2-1. Experimental system developed by Kimm (1995) to study NO <sub>x</sub> removal by magnesium oxide coated vermiculite (MgO/v) sorbent.....   | 33   |
| 2-2. Redesigned experimental arrangement for fixed-bed reactor system. ....   | 36   |
| 2-3. Sorbent tube temperature profile of triple fixed-bed reactor system. ....  | 42   |
| 2-4. Experimental reproducibility tests: a) simultaneously run samples of untreated alumina, b) consecutively run samples of untreated alumina. ....  | 44   |
| 2-5. Reproducibility of decomposed samples separately sorption tested. ....   | 47   |
| 2-6. Samples prepared by different coating methods with similar mass amounts of coating showing similar NO <sub>x</sub> sorption characteristics .....  | 51   |
| 2-7. XPS survey spectra obtained from (a) untreated $\gamma$ -alumina, NO <sub>x</sub> saturated (b) untreated $\gamma$ -alumina after KOH-coating and NO <sub>x</sub> -saturated (c) untreated $\gamma$ -alumina, NO <sub>x</sub> saturated (d) untreated $\gamma$ -alumina after KOH coating and NO <sub>x</sub> saturated..... | 58   |
| 2-8. FTIR reproducibility of Cs <sub>2</sub> CO <sub>3</sub> -treated alumina a) initial survey, b) second survey after mixing sample. ....   | 61   |
| 3-1. NO <sub>x</sub> -sorption test for MgO/v compared with Kimm's (1995) data.....   | 67   |
| 3-2. NO <sub>x</sub> -sorption tests for sieved MgO/v samples .....   | 68   |
| 3-3. External mass transfer test for NO <sub>x</sub> sorption on MgO/v.....   | 71   |
| 3-4. Variation of NO <sub>x</sub> sorption at 0, 5 and 25% water additions to MgO/v at 1-second residence time at 50 °C.....  | 73   |

|  |     |
|--|-----|
| 3-5. Variation of NO <sub>x</sub> sorption at 0, 5 and 25% water additions to MgO/v at 2-second residence time at 50 °C.....   | 74  |
| 3-6. Variation of NO <sub>x</sub> sorption at 0, 5 and 25% water additions to MgO/v at 1-second residence time at 200 °C.....  | 75  |
| 3-7. Variation of NO <sub>x</sub> sorption at 0, 5 and 25% water additions to MgO/v at 2-second residence time at 200 °C.....  | 76  |
| 3-8. NO <sub>x</sub> -saturation study of MgO/v and added water at 200 °C.....   | 77  |
| 3-9. NO <sub>x</sub> sorption by MgO/v and untreated $\gamma$ -alumina (Al <sub>2</sub> O <sub>3</sub> ) on equal volume beds (Lee et al., 1998b).....   | 80  |
| 3-10. Sorption of NO <sub>x</sub> to Fisher Scientific <sup>®</sup> , acid, basic and neutral “pH” forms of alumina. ....  | 86  |
| 3-11. $\gamma$ -Alumina from different sources exposed to NO <sub>2</sub> .....  | 87  |
| 3-12. XPS survey spectra obtained from (a) fresh and (b) NO <sub>x</sub> -saturated $\gamma$ -alumina pressed powder samples (Lee et al., 1998b). Assignments made pertain to both spectra. ....           | 90  |
| 3-13. Bed outlet NO and NO <sub>2</sub> concentrations as a function of time for untreated and KOH-treated $\gamma$ -alumina (Lee et al., 1998b).....  | 92  |
| 3-14. XPS survey spectra obtained from (a) KOH-impregnated and (b) NO <sub>x</sub> -saturated KOH alumina pressed powder samples (Lee et al., 1998b). Assignments made pertain to both spectra.....        | 93  |
| 3-15. Unexposed (a) and NO <sub>x</sub> -saturated (b) KOH-precipitated $\gamma$ -Al <sub>2</sub> O <sub>3</sub> pressed powder samples (Lee et al., 1998b). Assignments made pertain to both spectra..... | 94  |
| 3-16. XPS (A) N 1s and (B) K 2p spectra obtained from (a) KOH-precipitated and (b) NO <sub>x</sub> -saturated KOH-precipitated alumina pressed powder samples (Lee et al., 1998b). ....                    | 95  |
| 3-17. NO <sub>x</sub> sorption by KOH-treated and untreated alumina samples at 200 °C.....   | 102 |
| 3-18. NO <sub>x</sub> sorption by NaOH-treated alumina samples at 200 °C.....  | 103 |
| 3-19. NO <sub>x</sub> sorption by K <sub>2</sub> CO <sub>3</sub> -treated alumina samples at 200 °C. ....  | 104 |
| 3-20. NO <sub>x</sub> sorption by Na <sub>2</sub> CO <sub>3</sub> -treated alumina samples at 200 °C.....  | 105 |
| 3-21. Effect of temperature on NO <sub>x</sub> sorption by KOH-treated alumina. ....   | 108 |
| 3-22. Effect of temperature on NO <sub>x</sub> sorption by NaOH-treated alumina.....   | 109 |

|   |     |
|---|-----|
| 3-23. Effect of temperature on NO <sub>x</sub> sorption by K <sub>2</sub> CO <sub>3</sub> -treated alumina. ....  | 110 |
| 3-24. Effect of temperature on NO <sub>x</sub> sorption by Na <sub>2</sub> CO <sub>3</sub> -treated alumina. ....   | 111 |
| 3-25. Effect of varied NO concentration on the sorption of NO <sub>x</sub> by KOH-treated alumina. ....   | 112 |
| 3-26. Effect of varied NO concentration on the sorption of NO <sub>x</sub> by K <sub>2</sub> CO <sub>3</sub> -treated alumina. ....   | 113 |
| 3-27. Group-I hydroxide equimolar-treated $\gamma$ -alumina sorption of NO <sub>x</sub> . ....  | 118 |
| 3-28. Group-I carbonate equimolar-treated $\gamma$ -alumina sorption of NO <sub>x</sub> . ....  | 119 |
| 3-29. Sorption of NO (balance N <sub>2</sub> ) by untreated and CsOH-treated and Cs <sub>2</sub> CO <sub>3</sub> -treated alumina. ....   | 120 |
| 3-30. Effect of varied amount of cesium carbonate treated onto $\gamma$ -alumina on the sorption of NO <sub>x</sub> . ....  | 121 |
| 3-31. Pore size distribution of a) untreated $\gamma$ -alumina, b) Cs <sub>2</sub> CO <sub>3</sub> -treated alumina, and c) NO <sub>x</sub> -saturated Cs <sub>2</sub> CO <sub>3</sub> -treated alumina. .... | 125 |
| 3-32. Incremental molar ratio of NO <sub>2</sub> /NO for Cs <sub>2</sub> CO <sub>3</sub> -treated alumina sorption of NO <sub>2</sub> . ....  | 128 |
| 3-33. Effect of presence of NO <sub>2</sub> on sorption of NO for KOH-treated and K <sub>2</sub> CO <sub>3</sub> -treated alumina. ....   | 131 |
| 3-34. Surface interaction of NO following exposure of K <sub>2</sub> CO <sub>3</sub> -treated alumina to NO <sub>2</sub> at 25 °C. ....   | 133 |
| 3-35. Nitrite and nitrate measured on incremental layers of a sorbent bed of untreated alumina. ....  | 140 |
| 3-36. Nitrite and nitrate measured on incremental layers of a sorbent bed of K <sub>2</sub> CO <sub>3</sub> -treated alumina. ....  | 141 |
| 3-37. Nitrite and nitrate measured on incremental layers of a sorbent bed of KOH-treated alumina. ....  | 142 |
| 3-38. Change of NO and NO <sub>2</sub> gas concentrations throughout a bed of untreated $\gamma$ -alumina. ....   | 143 |
| 3-39. Change of NO and NO <sub>2</sub> gas concentration throughout a bed of K <sub>2</sub> CO <sub>3</sub> -treated $\gamma$ -alumina. ....  | 144 |

|   |     |
|---|-----|
| 3-40. Change of NO and NO <sub>2</sub> gas concentrations throughout a bed of KOH-treated $\gamma$ -alumina. ....   | 145 |
| 3-41. Incremental ratio of NO <sub>2</sub> sorbed/ NO formed for successive bed layers of untreated alumina. ....   | 149 |
| 3-42. Incremental ratio of NO <sub>2</sub> sorbed/ NO formed for successive bed layers of layers of K <sub>2</sub> CO <sub>3</sub> -treated alumina. .... | 150 |
| 3-43. Incremental ratio of NO <sub>2</sub> sorbed/ NO formed for successive bed layers of layers of KOH-treated alumina. ....                             | 151 |
| 3-44. NO <sub>2</sub> sorption activity of KNO <sub>2</sub> -treated and untreated alumina. ....  | 156 |
| 3-45. Sorption of NO <sub>2</sub> to KNO <sub>2</sub> -treated alumina with subsequent ISE analysis. ....   | 158 |
| 3-46. FTIR spectrum of reagent-grade KNO <sub>2</sub> . ....  | 160 |
| 3-47. FTIR spectrum of reagent-grade KNO <sub>3</sub> . ....  | 161 |
| 3-48. FTIR spectrum of reagent-grade K <sub>2</sub> CO <sub>3</sub> . ....  | 162 |
| 3-49. FTIR spectrum of untreated alumina. ....  | 163 |
| 3-50. FTIR spectrum of K <sub>2</sub> CO <sub>3</sub> -treated alumina. ....  | 164 |
| 3-51. FTIR spectrum of K <sub>2</sub> CO <sub>3</sub> -treated alumina after exposure to NO <sub>x</sub> (1st layer)....                                  | 165 |
| 3-52. FTIR spectrum of K <sub>2</sub> CO <sub>3</sub> -treated alumina after exposure to NO <sub>x</sub> (4th layer)....                                  | 166 |
| 3-53. Representative NO <sub>x</sub> -exposure test for samples decomposed after varied NO <sub>x</sub> -exposure times. ....                             | 172 |
| 3-54. Thermal decomposition of untreated alumina after 10-min exposure to NO <sub>x</sub> . ....  | 173 |
| 3-55. Thermal decomposition of untreated alumina after 30-min exposure to NO <sub>x</sub> . ....  | 173 |
| 3-56. Thermal decomposition of untreated alumina after 120-min exposure to NO <sub>x</sub> . ....   | 174 |
| 3-57. Thermal decomposition of K <sub>2</sub> CO <sub>3</sub> -treated alumina after 10-min exposure to NO <sub>x</sub> . ....                            | 174 |
| 3-58. Thermal decomposition of K <sub>2</sub> CO <sub>3</sub> -treated alumina after 30-min exposure to NO <sub>x</sub> . ....                            | 175 |
| 3-59. Thermal decomposition of K <sub>2</sub> CO <sub>3</sub> -treated alumina after 120-min exposure to NO <sub>x</sub> . ....                           | 175 |



|  |     |
|--|-----|
| 3-60. Thermal decomposition of KOH-treated alumina after 10-min exposure<br>to NOx.....  | 176 |
| 3-61. Thermal decomposition of KOH-treated alumina after 30-min exposure<br>to NOx.....  | 176 |
| 3-62. Thermal decomposition of KOH-treated alumina after 120-min exposure<br>to NOx..... | 177 |
| 3-63. Thermal decomposition of KNO <sub>3</sub> -treated alumina. ....                   | 177 |
| 3-64. Thermal decomposition of KNO <sub>2</sub> -treated alumina. ....                   | 178 |
| 3-65. Thermal decomposition of aluminum nitrate-treated alumina. ....                    | 178 |

Abstract of Dissertation Presented to the Graduate School  
of the University of Florida in Partial Fulfillment of the  
Requirements for the Degree of Doctor of Philosophy

SOLID SORBENT CONTROL OF NITROGEN OXIDES (NO<sub>x</sub>)

By

Maxwell Richardson Mentzer Lee

May 1999

Chairman: Eric R. Allen

Major Department: Environmental Engineering Sciences

Solid materials have demonstrated applicable control of combustion-source NO<sub>x</sub>. A support material of  $\gamma$ -alumina can provide improved NO<sub>x</sub> sorption in comparison to a previously applied sorbent, magnesium-oxide-coated vermiculite. Analysis of NO<sub>x</sub>-exposed  $\gamma$ -alumina by X-ray photoelectron spectroscopy (XPS) indicated potassium impurities contribute to NO<sub>x</sub> sorption. Based on this finding and the research of others,  $\gamma$ -alumina was treated with group-I elements, as carbonates and hydroxide compounds. Treated alumina sorbents were tested (ambient pressure, 25 to 250 °C) in an isothermal tubular-flow reactor using mixed gas of nitric oxide (NO) and nitrogen dioxide (NO<sub>2</sub>) diluted in N<sub>2</sub>. None of the sorbent materials was observed to sorb NO alone. However, in the presence of NO<sub>2</sub>, treated  $\gamma$ -alumina was observed to sorb significant amounts of NO and NO<sub>2</sub>.

NO<sub>x</sub> sorption of treated  $\gamma$ -alumina correlates with the ionization potential of the group-I element. BET measures indicate reduction of surface area after treatment that relates to the atomic radius of the group-I element.

General mechanisms of NO<sub>x</sub> sorption have been developed for untreated, K<sub>2</sub>CO<sub>3</sub>-treated and KOH-treated  $\gamma$ -alumina using results of tubular-reactor tests and ion-specific electrode (ISE) measurements. ISE measurements indicate NO and NO<sub>2</sub> sorption results in formation of surface nitrite and nitrate species. Sorption of NO appears to relate to the formation of nitrite. Untreated  $\gamma$ -alumina formed little or no nitrite. For the treated  $\gamma$ -alumina, the ratio of nitrite-to-nitrate formed relates to the ratio of NO-to-NO<sub>2</sub> sorbed. Nitrite formed on treated  $\gamma$ -alumina by NO<sub>x</sub> sorption converts into nitrate and NO upon additional NO<sub>2</sub> exposure. Conversion of nitrite to nitrate correlates with the thermal stability of surface species. Thermal-decomposition tests evaluated surface-species stability. Thermal stability of nitrate salts is lowest for aluminum. In addition, thermal-decomposition tests indicated similarities of NO<sub>x</sub>-exposed sorbents to nitrite and nitrate salts. Nitrite and nitrate identified by ISE were qualitatively confirmed by Fourier transform infrared (FTIR) analyses.

Effects of additional gases (O<sub>2</sub>, SO<sub>2</sub>, CO<sub>2</sub>, or water vapor) to NO and NO<sub>2</sub> on NO<sub>x</sub> sorption at 25 and 250 °C by untreated, K<sub>2</sub>CO<sub>3</sub>-treated and KOH-treated  $\gamma$ -alumina were evaluated. Only SO<sub>2</sub> and water vapor were observed to affect NO<sub>x</sub> sorption.

## CHAPTER 1 INTRODUCTION

Nitrogen oxides ( $N_xO_y$ ) are gaseous compounds that can be produced in combustion processes. Seven oxides of nitrogen species-- $N_2O$ ,  $NO$ ,  $N_2O_3$ ,  $NO_2$ ,  $N_2O_4$ ,  $N_2O_5$ , and  $NO_3$ --exist and may be present in ambient air, but the main species of concern in the lower troposphere are  $NO$  and  $NO_2$ . These two species, collectively designated as  $NO_x$ , are key in atmospheric chemical processes producing photochemical smog and acid rain. Within the United States in 1990, 90 percent of man-made  $NO_x$  emissions originated from combustion sources (US EPA, 1993). Although the majority of nitrogen oxides in the atmosphere originate from natural sources, localized elevated concentrations of  $NO_x$  originating from man-made sources can occur at concentrations several orders of magnitude greater than ambient background levels. The United States Environmental Protection Agency (US EPA) has established primary and secondary National Ambient Air Quality Standards (NAAQS) for nitrogen dioxide ( $NO_2$ ) at  $100 \mu g NO_2/m^3$  - annual arithmetic mean, due to its proven detrimental health effects. In addition, more recently the US EPA has mandated emission reductions of  $NO_x$  from point sources to reduce ambient ozone concentrations on a regional scale.

Man-made  $NO_x$  sources include transportation, stationary-source combustion, various industrial processes, solid waste disposal, and others, such as forest fires (prescribed burning). Sources other than transportation contribute over 60% of the total

man-made NO<sub>x</sub> of which industrial and utility combustion-generated power sources account for over 95% (US EPA, 1993). Typical combustion processes result in emissions of NO and NO<sub>2</sub> in a molar ratio near 20/1 depending on the combustion parameters (Cooper and Alley, 1986). Despite the relatively small proportion of NO<sub>2</sub> in combustion exhaust, NO is an atmospheric precursor to other pollutants including NO<sub>2</sub> and ozone. Given the cumulative detrimental effects of NO<sub>x</sub>, emissions control from combustion sources is a necessary factor in the overall health and welfare of society.

Various control technologies for NO<sub>x</sub> emissions have been developed and are discussed later in this chapter. Conventional control technologies have limitations related to certain combustion conditions. As deadlines approach for the various government regulators' pollution control requirements, more cost-efficient abatement methods will be sought.

This research provides an in-depth analysis and development of NO<sub>x</sub> control using solid sorbent materials. Initial research investigated magnesium-oxide-coated on vermiculite in this application; improved sorbents consisting of treated  $\gamma$ -alumina were subsequently investigated. Based on previous research these materials had been found to provide for removal of NO<sub>x</sub> in pilot and full-scale systems. Large-scale application studies do not allow for a detailed analysis of the NO<sub>x</sub> -sorption process. Laboratory experiments were used to determine the overall chemical mechanisms for three sorbents, untreated  $\gamma$ -alumina, K<sub>2</sub>CO<sub>3</sub>-treated alumina, and KOH-treated alumina. Based on these studies, an in-depth evaluation was conducted of the effects of significant parameters that determined the limiting conditions of operation. Controlling mechanisms of adsorption

were used to determine conditions under which mass-transfer or chemical-controlling conditions are dominant.

Chapter one provides a general background on the formation, interactions and general properties of  $\text{NO}_x$ , as well as applied methods of control. Chapter two provides a detailed description of the applied experimental methods and relevant limits of the experimental systems applied. Chapter three is a chronological discussion of experimental results. Chapter four draws conclusions concerning the findings from this research and presents ideas for potential future research.

#### Chemical and Physical Properties of $\text{NO}_x$

Nitric oxide is an odorless and colorless gas. Generally, it is a more stable compound than  $\text{NO}_2$ . It is only slightly soluble in water (0.006 g/100 g of water at 25 °C and 1 atm). The covalent bonds in NO results in an uneven number of electrons causing the nitrogen atom to become slightly electropositive. Nitric oxide is a by-product of combustion through the oxidation of molecular nitrogen and fuel-bound nitrogen. Thermal production of NO can be explained by the extended Zeldovitch mechanism (Zeldovitch, 1946).

Nitrogen dioxide has a smell similar to that of chlorine and in high concentrations produces a brown-yellowish haze. Combustion  $\text{NO}_2$  is created in secondary reactions that follow NO formation. In the troposphere  $\text{NO}_2$  absorbs UV light (430-290 nm) and photodissociates to form NO and O. It reacts with water to form nitrous (HONO) and nitric ( $\text{HONO}_2$ ) acids and is highly corrosive and oxidative as an acid or in anhydrous form. It will dimerize to  $\text{N}_2\text{O}_4$  at higher concentrations and pressures and lower

temperatures, but the dimer is not significant at ambient concentrations and temperatures. General properties of  $N_xO_y$  species are provided in Table 1-1.

### NO<sub>x</sub> Related Atmospheric Chemistry

Nitrogen oxides help to regulate the amount of free radicals in the troposphere and therefore help regulate the oxidizing potential of the atmosphere. Figure 1-1 provides a flow diagram of significant tropospheric reactions of NO<sub>x</sub>. From this diagram the concentration of NO<sub>x</sub> can be observed to affect tropospheric ozone and organic chemistry as well as acidification of the atmosphere.

### Formation of Combustion NO<sub>x</sub>

Oxides of nitrogen (NO<sub>x</sub>) created by combustion processes are formed through chemical reaction between oxygen in combustion air and nitrogen compounds, which are present in both the combustion air and fuel. Formation of NO<sub>2</sub> in combustion processes is secondary to NO formation, NO and molecular oxygen combining to form NO<sub>2</sub>. Typically exhaust gases contain a ratio of NO/NO<sub>2</sub> near 20/1. However, this ratio can vary significantly depending on combustion conditions. Three major mechanisms of combustion contribute to the formation of NO<sub>x</sub> during fossil fuel combustion.

### Thermal NO<sub>x</sub> Formation

Thermal NO<sub>x</sub> results from formation of NO<sub>x</sub> due to the reaction of molecular nitrogen with atomic oxygen as described by the Zeldovitch mechanism. The rate-limiting step in the production of thermally-produced NO is described by



Table 1-1. General properties of nitrogen oxide ( $N_xO_y$ ) species (US EPA, 1993).

| Oxide type                    | Mol. weight | Melting point (°C) | Boiling point (°C) | Henry's Law coeff. at 25 °C (M/atm) | Solubility in water (cm <sup>3</sup> /100 g) at 0 °C, 1 atm | Thermodynamic Functions (Ideal Gas, 25 °C, 1 atm) |                                | Theoretical conc. at equilibrium with N <sub>2</sub> , O <sub>2</sub> and water in air (25 °C, 1 atm, 50% rel. hum.) (ppm) |                                   |
|-------------------------------|-------------|--------------------|--------------------|-------------------------------------|---|---|--------------------------------|--|-----------------------------------|
|                               |             |                    |                    |                                     |   | Enthalpy of formation (kcal/mol)                  | Entropy of form. (cal/mol-deg) | Equilibrium  | Sunlight-irradiated polluted atm. |
| NO                            | 30.01       | -163.6             | -151.8             | $1.93 \times 10^{-3}$               | 7.34  | 21.58   | 50.35                          | $2.69 \times 10^{-10}$   | $10^{-1}$                         |
| NO <sub>2</sub>               | 46.01       | -11.2              | 21.2               | $1.2 \times 10^{-2}$                | forms HONO and HONO <sub>2</sub>                            | 7.91  | 57.34                          | $1.91 \times 10^{-4}$  | $10^{-1}$                         |
| N <sub>2</sub> O              | 44.01       | -90.8              | -88.5              | $2.47 \times 10^{-2}$               | 130.52  | 19.61   | 52.55                          |  |                                   |
| N <sub>2</sub> O <sub>3</sub> | 76.01       | -102               | 47 (decomp)        | $0.6 \pm 0.2$                       | forms HONO  | 19.80   | 73.91                          | $2.96 \times 10^{-20}$   | $10^{-2} - 10^{-4}$               |
| N <sub>2</sub> O <sub>4</sub> | 92.02       | -11.3              | 21.2               | $1.4 \pm 0.8$                       | forms HONO and HONO <sub>2</sub>                            | 2.17  | 72.72                          | $2.48 \times 10^{-13}$   | $10^{-4} - 10^{-7}$               |
| N <sub>2</sub> O <sub>5</sub> | 108.01      | 30                 | 3.24 (decomp)      |                                     | forms HONO <sub>2</sub>                                     | 2.7   | 82.8                           | $3.16 \times 10^{-17}$   | $10^{-4} - 10^{-3}$               |



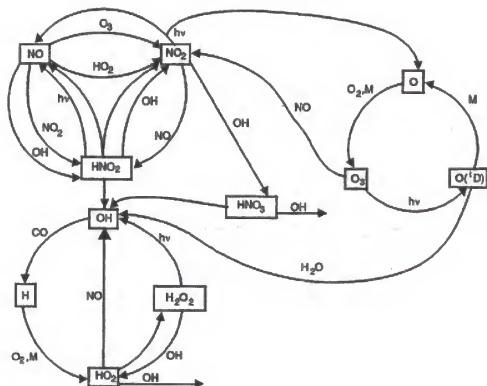


Figure 1-1. Schematic diagram of the combined reactions of nitrogen, oxygen, and hydrogen (Carmichael and Peters, 1984).

The high activation energy (75 kcal/mol) necessary to break the triple-bond of molecular nitrogen is extremely temperature sensitive (Bowman, 1973). The concentration of atomic oxygen is also highly temperature sensitive and dependent on the air-to-fuel ratio (A/F). Thermally-formed NO<sub>x</sub> is dependent not on reaction equilibrium but on gas kinetics. Table 1-2 shows estimates of the equilibrium concentrations of NO and NO<sub>2</sub> that would be expected at various temperatures.

When comparing the data in Table 2 with real situations, it appears that the concentration of NO<sub>x</sub> in actual combustion systems does not reach equilibrium. The rate of reaction (1-1) is not fast enough to reach equilibrium in the high-temperature flame zone. However, the removal mechanisms for NO are even slower to reach equilibrium. If the available heat produced from combustion is not used to produce useful work then the NO<sub>x</sub> species formed would result in lower concentrations. Thus, rapid cooling of the combustion flame zone "freezes" the NO<sub>x</sub> formed at concentrations characteristic of the high-temperature combustion zone. As a result, control of thermal NO<sub>x</sub> is a function of combustion time as well as temperature.

The air-to-fuel (A/F) ratio defines the stoichiometric weight ratio of the combustion reactants in the influent mixture. A high or "lean" A/F ratio provides excess air that can increase power output and also the concentration of oxygen available to react and form NO<sub>x</sub>. However, high A/F ratios provide excess air conditions that act to cool the combustion zone, thus controlling peak temperatures and reducing thermal NO<sub>x</sub> production. A low or "rich" A/F ratio reduces the concentration of oxygen available and thus reduces NO<sub>x</sub>. However, in this case the combustion efficiency is reduced due to a

Table 1-2. Theoretical estimates of equilibrium concentrations for NO and NO<sub>2</sub> in air (21% O<sub>2</sub>) and 50% relative humidity (US EPA, 1993).

| Temperature (K) | Concentration ( ppm)   |                                     |
|-----------------|------------------------|-------------------------------------|
|                 | Nitric Oxide (NO)      | Nitrogen Dioxide (NO <sub>2</sub> ) |
| 298             | $2.63 \times 10^{-10}$ | $1.88 \times 10^{-4}$               |
| 500             | $6.54 \times 10^{-4}$  | $3.86 \times 10^{-2}$               |
| 1000            | 34.4                   | 1.80                                |
| 1500            | 1,296                  | 6.57                                |
| 2000            | 7,957                  | 12.7                                |

lack of available oxygen. Figure 1-2 shows the effect of varying the A/F ratio on the concentrations of pollutants in the exhaust gas.

Also, in Figure 1-2 it can be seen that by modifying the A/F ratio some pollutants can be reduced while others are increased. Several NO<sub>x</sub> control strategies utilize the A/F ratio to control NO<sub>x</sub> formation and are discussed later in the section NO<sub>x</sub> Control Methods. To minimize thermal NO<sub>x</sub> formation, it is necessary to reduce combustion zone temperatures and residence time, minimizing atomic oxygen concentrations in the combustion process.

Thermal NO<sub>x</sub> formation from combustion of heavy fuel oil represents approximately 40-20% of the total NO<sub>x</sub> produced. For coal, thermal NO<sub>x</sub> can comprise approximately 50-20% of the total NO<sub>x</sub> generated from conventional pulverized coal boilers. This contribution can vary significantly depending on boiler design and fuel properties. For fuels that contain no inherent nitrogen (e.g., natural gas), essentially 100% of NO<sub>x</sub> is thermal NO<sub>x</sub>.

#### Fuel NO<sub>x</sub> Formation

Fuel NO<sub>x</sub> pertains to NO<sub>x</sub> emissions resulting from the conversion of nitrogen organically bound in the fuel. Reaction mechanisms have been developed for the numerous fuel-bound nitrogen (FBN) species (US EPA, 1993). Considering only FBN compounds, a 'lean' A/F ratio results in high NO formation, while fuel 'rich' conditions tend to produce N<sub>2</sub>. This mechanism represents 80-50% of the NO<sub>x</sub> produced from heavy fuel oil combustion, and approximately 80-60% of the NO<sub>x</sub> produced from pulverized coal combustion. Formation of fuel NO<sub>x</sub> is also affected by burner design, and type of boiler employed.

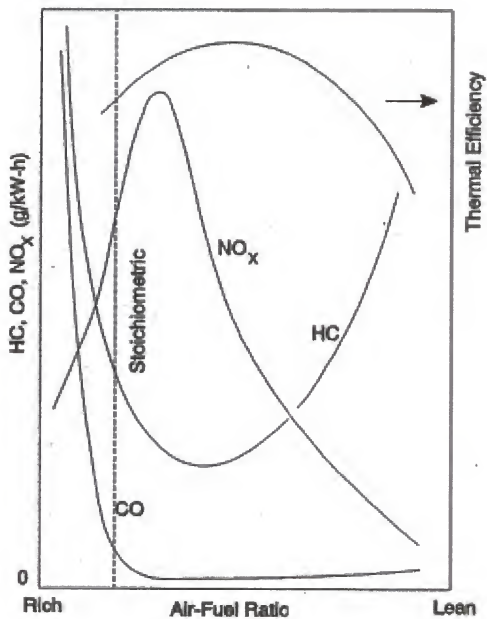


Figure 1-2. Production of hydrocarbons, carbon monoxide, and nitrogen oxides as a function of A/F ratio (Heywood, 1988).

### Prompt NO<sub>x</sub>

Another mechanism that typically produces a minor portion of NO<sub>x</sub> during fuel combustion involves combustion-formed hydrocarbon radicals that can split the N<sub>2</sub> triple bond as shown below:



This type of reaction can proceed at a relatively low activation energy and may precede the Zeldovitch mechanism thus, the term “prompt.” The contribution of prompt NO<sub>x</sub> to the overall NO<sub>x</sub> emissions is usually small for most combustion processes (Buonicore et al., 1991).

### Detrimental Effects of NO and NO<sub>2</sub>

#### Biological Effects

Nitrogen dioxide (NO<sub>2</sub>) is the most toxic of the NO<sub>x</sub> species. Its primary effect on mammals is lung damage. At concentrations greater than 100 ppm NO<sub>2</sub> is lethal to most exposed mammals, 90% being subject to pulmonary edema (US EPA, 1993). Short-term non-lethal exposures to NO<sub>2</sub> have been shown to cause pulmonary-function change in the lungs of monkeys (Henry et al., 1965). Pathological lesions have been observed in lungs of animals after short- and long-term NO<sub>2</sub> exposures. Similar symptoms to chronic lung disease have been observed in animals after NO<sub>2</sub> exposure suggesting that chronic effects on humans may result from long-term low-level NO<sub>2</sub> exposures. Exposure of monkeys to

15 to 50 ppm  $\text{NO}_2$  for two hours produced damage to the lungs, heart, liver, and kidneys, and pulmonary changes resembling human emphysema (US EPA, 1993).

Epidemiological surveys for residential areas in Chattanooga, Tennessee, showed an increased occurrence in acute respiratory illness after 6 months of 24-hr averaged concentrations from 0.109 to 0.062 ppm  $\text{NO}_2$ . The frequency of infant acute bronchitis cases also increased in the same area of Chattanooga for  $\text{NO}_2$  concentrations in the range from 0.063 to 0.083 ppm over a 6-month period (Shy et al., 1970).

Detrimental effects of exposure to NO are less well studied. A 12-minute exposure of mice to 2500 ppm NO proved lethal (Flury and Zernick, 1931). Exposure to lower NO concentrations (~ 20 ppm) appeared to inhibit bacterial enzymatic activity (Krasna and Rittenburg, 1954). Although toxicological effects have been demonstrated for NO exposure, the detrimental health effects potential of NO at ambient concentration result primarily from its oxidation to  $\text{NO}_2$  (US EPA, 1993).

Effects of plant sensitivity to  $\text{NO}_x$  have been separated into three categories: (1) acute injury, (2) chronic injury, and (3) physiological effects. Acute injuries in which necrotic patterns result within 48 hours have been observed on agricultural crops exposed to 1 ppm  $\text{NO}_2$  for 48 hours (Van Haut and Stramann, 1967). Such conditions are expected only for direct exposure near stationary sources. However, greenhouse studies simulating smog conditions in the Los Angeles basin have suggested that  $\text{NO}_x$ , not ozone, contributes to significant leaf-dropping (Glaser, 1970). Detrimental physiological effects of exposure to NO and/or  $\text{NO}_2$  appear to be reduced photosynthesis and  $\text{CO}_2$  fumigation (Hill and Bennett, 1970).

### Material Effects

Loss of color has been observed in cotton and rayon fabrics due to NO<sub>x</sub> (0.6 to 2 ppm) created from natural gas-heated domestic dryers (McLendon and Richardson, 1965). Cotton and nylon textiles fibers can deteriorate from exposure to elevated ambient NO<sub>x</sub> concentrations (Morris et al., 1964). Increased metal failures, which were observed in the Los Angeles area, were suspected to be due to elevated particulate nitrate and NO<sub>x</sub> concentrations (Hermance et al., 1970).

### Government Regulations Related to NO<sub>x</sub> Control

A decisive impetus for NO<sub>x</sub>-control research was the development of government regulations. Currently federal and state agencies enforce NO<sub>x</sub>-related regulations that have been promulgated by legislative acts. The effects of NO and NO<sub>2</sub> as precursors to photochemical smog and contributors to acid rain as well as their being a public health threat have led to NO<sub>x</sub> regulation for both ambient concentration levels and point and mobile source emissions. Federal NO<sub>x</sub>-related regulations established by the United States Environmental Protection Agency (US EPA) are based on the Clean Air Act (CAA) of 1963 and subsequent amendments promulgated in 1970, 1977, and 1990.

The 1970 CAA amendments established the national ambient air quality standards (NAAQS) which set primary and secondary standards for ambient NO<sub>2</sub> concentrations of 100 µg/m<sup>3</sup> (annual arithmetic mean). Areas exceeding the NAAQS standard were designated as "non-attainment." Within areas attaining the standard, new or modified major sources were subject to best available control technology (BACT) standards and were defined as being a listed source with the potential to emit more than 100 ton/yr of an



individual pollutant or emitting 250 ton/yr total pollutants (Buonicore et al., 1991). Through negotiations with regulating agencies, a major-source operator will select the BACT technology through evaluation of various contemporary control technologies, estimation of the reduction of emissions, energy consumed, and cost per pollutant removed. New source performance standards (NSPS) that were established under section 111 of the 1977 CAA amendments generally include the BACT requirements for sources and assist in the decision process.

In non-attainment areas NO<sub>x</sub> pollution controls were required to achieve the lowest achievable emission rate (LAER) for new or modified major sources and reasonable available control technology (RACT) for existing sources. The technology decision process was similar to BACT negotiations (Heinsohn and Kabel, 1999).

The 1977 CAA amendments established a classification of major urban areas based on their degrees of non-attainment with deadlines set to reach attainment. State implementation plans (SIPs) were created by state governments to achieve attainment. Title IV of the 1990 CAA amendments addresses the acid-rain issue and requires NO<sub>x</sub> reductions in two phase-in periods for coal-fired utility boilers generating electricity exceeding 25 MW, to cut NO<sub>x</sub> emissions by 30% from 1980 levels by the year 2000 (Grano, 1995).

Title II of the 1990 CAA amendments sets forth mobile-source regulations that are directed toward improved fuels and advanced sensor-activated controls for combustion and exhaust conditions. The application of catalytic converters, while greatly improved over past years, is limited because of narrow operational conditions ( $A/F$  ratio,

temperature, etc.) and expensive precious metals that can be poisoned. While sorbent techniques have been evaluated for certain unique semi-mobile sources (Nelson et al., 1994), inherent difficulties in the application of sorbent methods for NO<sub>x</sub> control have not been thoroughly investigated to provide practical applications to mobile sources. Space limitations and sorbent regeneration are key issues to be addressed.

States may establish stricter regulations than the federal government. California, for example, is commonly known to have some of the nation's strictest air pollution standards, because four of the top five non-attainment areas in the US are located in California (Heinsohn and Kabel, 1999). To further address the seemingly persistent air quality problems, California legislation has considered controls for various uncommon NO<sub>x</sub> sources, such as small marine-vessel and lawn mower engines.

The current nature of governmental regulation is becoming more regionally oriented in both control and implementation of air pollution programs. Observations that there is considerable transport of ground-level ozone and ozone precursors (NO<sub>x</sub> and volatile organic compounds (VOC)) between states has become increasingly evident (US EPA, 1998). Realizing that several states would not meet the 1-hr ozone standard by the November 1994 deadline set forth in the 1990 CAA Amendments, The US EPA extended and reconsidered the deadline. The Ozone Transport Assessment Group (OTAG) was formed in 1995 in response to the ozone non-attainment situation as a partnership between US EPA, the Environmental Council of the States (ECOS) and various industry and environmental groups. The goal of this partnership is to develop an assessment and a consensus for reducing ground-level ozone and the pollutants that cause ground-level

ozone, including NO<sub>x</sub>. OTAG explicitly addresses ozone transport over the Eastern United States.

Recommendations from OTAG in its final report guided a recent ruling by US EPA mandating reduction of NO<sub>x</sub> emissions in 22 states and the District of Columbia to reduce regional ozone transport and help areas reach the new NAAQS ozone standard (US EPA, 1998). Significant, smaller sources of NO<sub>x</sub> that were identified by OTAG include, non-utility boilers, reciprocating internal combustion (IC) engines, gas turbines, residential fuel combustion, cement manufacturing, metals processing, wood/pulp/paper manufacturing, oil and gas production, and waste incineration. Despite the fact that these sources operate at greater variability in conditions compared to larger stationary sources, suggested controls in the OTAG final report for most of these sources, which are primarily combustion sources, are NO<sub>x</sub>-reduction techniques. The report recognizes the inadequacies of conventional reduction technologies under highly variable operating conditions that are more typical for smaller sources, but does not provide specific methods to improve existing NO<sub>x</sub>-reduction techniques.

In the future, regulating agencies may require NO<sub>x</sub> controls on smaller and non-conventional NO<sub>x</sub>-sources if current regulations fail to achieve the desired goals. One study of non-conventional NO<sub>x</sub> sources for which control ideas have been thoroughly investigated by the United States Air Force (USAF) is jet engine test cells (Kimm, 1995; Kimm et al., 1995; Kittrell, 1991; Nelson et al., 1989, 1992, 1993, and 1994; Petrik, 1991). Thus, novel control methods are likely to be of commercial interest based on past and present trends in NO<sub>x</sub> regulations. Control of NO<sub>x</sub> from non-conventional sources

may be economically feasible only if an effective and inexpensive control technology is available that is capable of functioning over varied combustion and exhaust conditions.

### NO<sub>x</sub> Control Technologies

NO<sub>x</sub> control technologies may be conveniently divided into two major categories: combustion modification and flue gas treatment. In addition, hybrid systems have evolved, which include a variety of NO<sub>x</sub> control methods that in combination provide enhanced NO<sub>x</sub> control and system flexibility.

#### Combustion Modification

The formation of NO<sub>x</sub> in combustion processes, as previously discussed, is a complex phenomenon based on three mechanisms: thermal NO<sub>x</sub>, fuel NO<sub>x</sub>, and prompt NO<sub>x</sub>. The relative contribution from each of these mechanisms to the overall NO<sub>x</sub> in exhaust gases must be determined to evaluate beneficial combustion modifications. The following factors affect the amount of NO<sub>x</sub> formed from combustion: the air-to-fuel (A/F) ratio, the nitrogen content of fuel (fuel-bound nitrogen (FBN)), the amount of pre-mixing of reactants, burner design, and gas residence time in the high-temperature zone of combustion.

For fuels that have little to no fuel-bound nitrogen (FBN) the formation of NO<sub>x</sub> is dominated by the Zeldovitch mechanism (reaction (1-1)). To reduce combustion-formed NO<sub>x</sub> according to the Zeldovitch mechanism implies a reduction in peak flame temperature, limiting gas residence time at peak temperatures, and reducing the concentration of atomic oxygen at the peak temperature. Common methods that apply

these concepts are flue gas recirculation, reducing the combustion load, lower combustion air preheat temperatures, water injection, and reduced excess air (US EPA, 1993).

Combustion modification methods for NO<sub>x</sub> control of fuels with high FBN include limiting available oxygen to the FBN evolved during combustion. Applications that limit available oxygen include fuel-rich firing, staged combustion or burner designs that control the mixing rate of fuel and air streams.

Prompt NO<sub>x</sub> is a function of hydrocarbon radicals and molecular nitrogen. Unlike the Zeldovitch mechanism prompt NO<sub>x</sub> forms at lower temperatures and at rates similar to the oxidation process. Thus, controlling prompt NO<sub>x</sub> cannot be achieved as effectively by methods recommended for thermal NO<sub>x</sub>. However, limiting the available oxygen in the gas will prevent the formed N species from reacting with the oxygen. Thus, fuel-NO<sub>x</sub> control mechanisms should help limit prompt NO<sub>x</sub>.

### Flue-Gas Treatment

In the past, combustion modification has been the method of choice to reduce NO<sub>x</sub> emissions in commercial applications. Combustion modifications are less expensive than flue-gas treatments if they provide initial reductions of near 50% (Buonicore et al., 1991; Staudt, 1996). However, certain economic and/or physical limitations may render combustion modification impractical (Staudt, 1996).

The two general chemical mechanisms for flue-gas NO<sub>x</sub> control are reduction and oxidation. These mechanism have evolved into a variety of processes that may include both oxidation and reduction reactions with various system configurations. The final goal of any of these processes is to convert the flue-gas NO<sub>x</sub> to either inert gases or to a

palpable (liquid and solid-phase) product. Catalysts are commonly used to improve the rate of the desired reaction.

Sorbents are common commercially-applied for  $\text{SO}_2$  control and have also been studied to provide combined  $\text{SO}_2/\text{NO}_x$  control in recent years. Hybrid systems as well have grown in use that encompass various flue-gas treatment systems as well as combustion modifications. One of the most common  $\text{NO}_x$  control methods involves the reduction of  $\text{NO}_x$  to inert species.

### Reduction Methods

Major  $\text{NO}_x$  sources, such as power plants, that operate at close to steady-state conditions typically employ selective reduction methods for flue gas treatment. The methods are “selective” to reactions only with  $\text{NO}_x$  and the reaction reduces the  $\text{NO}_x$  species to molecular nitrogen ( $\text{N}_2$ ) and other inert species. The two selective reduction methods differ by either exclusion or inclusion of a catalyst (commonly zeolite, titanium, tungsten, and/or vanadium oxides) in the reaction. The methods are called SNCR (selective non-catalytic reduction) and SCR (selective catalytic reduction) methods, respectively (Cooper and Alley, 1986). The catalyst acts to reduce the required reaction temperature and increase the overall removal efficiency, but introduces additional costs and operational limitations. Selective reduction methods are highly temperature sensitive and operate in the ranges 400-300 °C (dependent of catalyst type) and 900-800 °C for SCR and SNCR, respectively.

The typical  $\text{NO}_x$ -reduction reaction uses ammonia ( $\text{NH}_3$ ) and is represented by



Various reducing compounds (such as  $\text{NH}_3$ ,  $\text{CO}$ ,  $\text{H}_2$ , and urea) have been evaluated for this application (US EPA, 1994). Assuming that the gas-phase reduction in reaction (1-3) is conducted stoichiometrically and with complete mixing, the emission products will be  $\text{N}_2$  and water. However, adequate gas mixing and injecting the correct ratio of reducing gas is critical and difficult to achieve under variable  $\text{NO}_x$  concentrations and emission rates. The result of not achieving these requirements is the emission of additional  $\text{NO}_x$  from oxidation of the reducing gas or the emission ["slip"] of reducing gas, which itself is a pollutant.

Some inexpensive solid materials have been tested that can perform at lower temperatures with reducing gas, to provide cheaper alternative  $\text{NO}_x$  reduction methods. Activated carbon has been tested at 230-220 °C with  $\text{NH}_3$  injection to simultaneously reduce  $\text{NO}_x$  to  $\text{N}_2$  and oxidize  $\text{SO}_2$  to  $\text{H}_2\text{SO}_4$  (Cooper and Alley, 1986). Copper oxide-impregnated alumina in the presence of  $\text{SO}_2$  and  $\text{O}_2$  will form copper sulfate and either material acts as a catalyst for reducing  $\text{NO}_x$  with  $\text{NH}_3$ . This control method has been applied in oil-fired boilers in Japan with 90%  $\text{SO}_x$  removal and 70%  $\text{NO}_x$  removal (Cooper and Alley, 1986; Markussen and Livengood, 1995).

The Parsons Process simultaneously and catalytically reduces  $\text{SO}_2$  to  $\text{H}_2\text{S}$  and  $\text{NO}_x$  to  $\text{N}_2$  in a hydrogenation reactor using steam-reformer gas. Removal efficiencies for a high-sulfur coal pilot plant were 98% for  $\text{SO}_2$  and 96-92% for  $\text{NO}_x$  (Markussen and Livengood, 1995).

Disadvantages of selective-reduction methods include combustion must be performed at known steady-state conditions, catalyst deactivation through continued use and/or poisoning from other flue-gas constituents (particulate, etc.), high start-up capital costs, and continual reducing-gas costs. Regarding SCR, the required reaction temperature usually mandates that the catalyst be placed in-line prior to particulate control treatment and thus particulate poisoning becomes a major detriment to catalytic activity.

### Sorption Methods

Sorption is essentially a process to reversibly collect gaseous NO<sub>x</sub> species onto a solid surface or into a liquid. For both wet and dry sorption, the oxidation of NO to NO<sub>2</sub> vastly enhances the removal of NO<sub>x</sub> (Cooper and Alley, 1986). After collection the trapped NO<sub>x</sub> species can be handled under specified conditions outside the exhaust gas system. An added benefit of sorption methods is that both SO<sub>2</sub> and NO<sub>x</sub> can be removed simultaneously using certain sorbent materials with possible synergistic effects on removal efficiency.

#### Wet Sorption

Wet sorption has been applied to SO<sub>2</sub> control with considerable success and is a standard control technology. However, the solubility of SO<sub>2</sub> in water is much higher than that of NO. While NO<sub>2</sub> is soluble in water it is typically only a small fraction (approx. 5%) of the total amount of NO<sub>x</sub> in combustion exhaust. Nitric acid manufacturing typically applies wet scrubbing of NO<sub>2</sub> to produce nitric acid. Counce and Perona (1980) have studied in detail the NO<sub>x</sub>-HNO<sub>3</sub>-H<sub>2</sub>O process in nitric acid manufacturing. However, the concentrations are much higher and temperatures much lower than those experienced in



combustion-exhaust NO<sub>x</sub>. Chemical enhancements have been studied to improve the solubility of NO, that include KMnO<sub>4</sub>/NaOH and Na<sub>2</sub>SO<sub>3</sub>/FeSO<sub>4</sub> solutions (Cooper and Alley, 1986). However, due to various limitations, this particular technology has not gained widespread acceptance. Some metal chelates, such as Fe(II)•EDTA have been found to readily remove any absorbed NO and allow for the maximum absorption driving force. Problems have occurred with oxidation of the iron to the inactive ferric state. Antioxidants are added for improved performance. In pilot-scale tests at a 1.5-MW plant, nitrogen oxides were reduced 60% and SO<sub>2</sub> near 100% (Markussen and Livengood, 1995). Wet sorption of NO<sub>x</sub> produces a liquid product that cannot be handled as easily as a dry material for on-site or off-site transportation and disposal. Typical costs of water treatment are higher than land disposal for non-hazardous wastes. Additional regulations may be imposed for wet solution supply, storage and handling.

Measurement methods for NO<sub>x</sub> were developed using wet sorption, and suggested possible interaction with alkaline materials. A method developed by Jacobs and Hocheiser (1958) collected ambient NO<sub>2</sub> gas by absorption into a solution of NaOH. Standard wet sorption methods for the detection of NO<sub>x</sub> have been under development since the beginning of this century (Keiser and McMaster, 1908, Cook, 1936, Jacobs, 1949).

### Dry Sorption

Dry sorption methods have been studied using a variety of materials. The advantages of dry sorption include operational simplicity, ease of waste effluent handling, inexpensive sorbent cost (depending on regenerability of sorbent) and low maintenance

costs. Dry sorption is essentially gas filtration achieved by chemically sorbing NO<sub>x</sub> to the sorbent surface.

Past research and application work has shown that dry sorption methods have the potential to effectively control NO<sub>x</sub>. Ganz (1958) evaluated NO<sub>x</sub> removal by various compounds including activated carbon, aluminosilicate, silica gel, manganese oxide, copper dioxide and coke. He found aluminosilicates to be the most efficient NO<sub>x</sub> sorbent. James and Hughes (1977) used calcined limestone and dolomite to remove high-concentration NO with good results. A review of dry basic sorbents suggests that other materials such as MgO and ZnO are possible sorbents of NO<sub>x</sub> (Komppa, 1986). Kimm researched NO<sub>x</sub> sorption to MgO-coated vermiculite (MgO/v); specifically, his results showed the MgO/v sorption of NO<sub>2</sub> (Kimm, 1995, Kimm et al., 1995).

Patented processes for sorbent NO<sub>x</sub> control are numerous and point to the generally perceived benefits of dry sorption. Lott et al. (US Patent 5,795,553, 1998) has patented a material comprised of (potassium or sodium) alkali metal and copper-doped hydrous zirconium oxide that is coated on to a honeycomb cordereite monolith to adsorb NO<sub>x</sub> emissions under lean-burn operations of mobile sources. Golden et al. (US Patent 5,779,767, 1998) describe the use of an adsorbent of alumina/zeolite treated with basic alkali metal compounds to control NO<sub>x</sub>. The most preferred treatment material in this process is potassium carbonate. Bortz and Podlenski (US Patent 5,165,902, 1992) apply injected dry sodium (NaHCO<sub>3</sub> and/or other basic sodium materials) additives, under controlled moisture additions, to remove NO<sub>2</sub> and SO<sub>2</sub> emissions from stationary sources. Lever et al. (US Patent 5,096,871, 1990) patented a procedure for making a general acid-gas adsorber consisting of activated alumina and an amorphous alkali aluminum silicate.

Materials capable of sorbing acid gases have been considered using activated alumina with additions of alkali metal materials (US Patent 5,096,871, 1992). Additions of iron oxide to synthetic layered double hydroxide sorbents to enhance oxidation greatly improved the utilization of sorbents. The sorbents include varying amounts of aluminum, carbonates, and hydroxides (US Patent 5,116,587, 1992). Nelli and Rochelle have studied the combined removal of  $\text{NO}_2$  and  $\text{SO}_2$  using a patented mixture of calcium hydroxide and silicate (Nelli and Rochelle, 1998).

Cryogenic gas-purification patents for the removal of oxides of nitrogen apply alumina and zeolite adsorbents (US Patent 5,779,767, 1998) with additions of alkali hydroxide materials to improve the removal of unwanted gases, including  $\text{NO}_x$ . Many other applications relating alumina to cryogenic-gas purification can be found in this patent.

Polymeric materials have been tested for the removal of  $\text{NO}$  and  $\text{NO}_2$ . Kikkinides and Yang (1991) tested a weak-base macrorecticular resin to simultaneously remove  $\text{NO}_2$  and  $\text{SO}_2$ .

#### Applied methods of dry sorption

The ADVACATE process uses an activated sorbent of lime and fly ash that has been pilot-scale tested for  $\text{SO}_2$  control. However, laboratory studies have found that significant  $\text{NO}_x$  control may also be possible (Nelli and Rochelle, 1996).

The NOXSO process uses sodium-impregnated alumina beads of sorbent in a fluidized bed system (Ma et al., 1995). Removal of  $\text{SO}_2$  and  $\text{NO}_x$  has been studied in small-scale process tests where 90%  $\text{SO}_2$  and 90-70%  $\text{NO}_x$  removals were observed. Adsorbed  $\text{NO}_x$  is removed by heating the sorbent to 600 °C in a second fluidized bed.

After heating, the sorbent is treated with a reducing gas, such as methane and steam to produce  $\text{SO}_2$  and  $\text{H}_2\text{S}$  that can be converted to elemental sulfur via the Claus process. Reburning of the desorbed concentrated  $\text{NO}_x$ -laden gas from the saturated sorbent has also been a process which was recommended over conventional adsorption/catalytic methods (Regalbutto, 1994). Improvements upon this process have been achieved and described in a patent in which additions of silica as a strength enhancer and hydrothermal stabilizer is included with an active ingredient of an alkali or earth alkali material (US Patent 5,585,082, 1996).

The LILAC process uses a sorbent composed of fly ash, lime, and gypsum. The sorbent is injected into the flue gas duct. Solids are collected in either a baghouse or ESP. Pilot-plant tests in Japan showed removal of 75%  $\text{SO}_2$  and 55%  $\text{NO}_x$  using a 2.9 Ca/S weight ratio (Markussen and Livengood, 1995).

NaTec Resources Inc. has tested dry sodium carbonate injection into coal-fired boilers at commercial installations in several industrial sites. Removal efficiencies for  $\text{SO}_2$  and  $\text{NO}_x$  were near 70% and 40-0%, respectively, in systems equipped with electrostatic precipitators (ESPs). Systems with baghouses showed removals of  $\text{SO}_2$  and  $\text{NO}_x$  near 90% and 25%, respectively (Markussen and Livengood, 1995).

Spray dryer FGD technology utilizes alkali sorbent in the form of a slurry injected into the flue gas and collected as dry particulate. The particulate is collected and disposed of in landfills. Very little  $\text{NO}_x$  is removed under normal conditions but researchers at the Pittsburgh Energy Technology Center (PETC) have found that additions of  $\text{NaOH}$  promote significant  $\text{NO}_x$  removal at elevated dryer-exit temperatures (Markussen and

Livengood, 1995). Demonstration tests at 20-MW high-sulfur burning coal plants with 10 to 3 % weight additions of NaOH reduced the required lime and improved NO<sub>x</sub> removal to near 35%. Removal occurred mostly in the baghouse over extended intervals. NO<sub>x</sub> removal was higher under higher SO<sub>2</sub>/NO<sub>x</sub> ratios.

Small-scale sorbent systems for domestic coal-fired combustors were designed by Arthur D. Little Inc. (Benedeck, and Flytzani-Stephanopoulos, 1994). Of the sorbents considered, copper-alumina was the most promising. The NO<sub>x</sub>/SO<sub>2</sub>-control units are designed for domestic use in coal-fired combustors and are applied in the form of a cross-flow filter unit.

The USAF has promoted a number of studies for controlling the highly variable emissions of NO<sub>x</sub> from jet engine test cells (Kitrell, 1989; Lyon, 1989, 1991; Nelson et al., 1989, 1992, 1993, and 1994; Petrik, 1992). From these studies, a dry sorbent material of magnesium oxide coated onto vermiculite (MgO/v) was found to be effective in controlling NO<sub>x</sub> emissions. Development of this sorbent material was the impetus for the current research that has expanded on previous sorbent research in this laboratory.

Adaptation of these dry sorption methods has demonstrated that the practical application of NO<sub>x</sub> sorbents is possible. The greatest benefit derived from dry sorption in comparison to other methods is their lack of sensitivity to highly variable operational conditions. The output NO<sub>x</sub> concentration, gas flowrate, and temperature fluctuations need only be monitored to track the amount of sorbent necessary to maintain a desired removal efficiency. Supplies of reducing gas are not necessary. Thus, the emission of ammonia or other reducing gas is not an issue. Sorbents can perform over a range of temperatures that are lower than those required by SCR and thus allow the system to be

located after flue-gas particulate controls. This feature reduces the effect of particulate on reactive gas sorption. Sorbents are normally regenerable and with further research the number of cycles of use may be improved and thus sorbent consumption reduced. Dry material handling and simple system structure design have obvious benefits over wet sorption methods. The design of sorbent controls for smaller systems can be quite simple and thus reduce start-up cost in comparison to other reduction methods.

### Hybrid Systems

Hybrid systems have been under investigation from laboratory-scale up to full-scale studies. The benefits of combining technologies of combustion modification with flue-gas treatment has enabled >95% removal of NO<sub>x</sub>. Described below are several of the better developed and field-tested applications.

A 32-MW "Federal Cogeneration" natural-gas turbine power plant facility owned by Sunlaw Cogeneration Partners in Vernon, California uses a hybrid system of water injection and a patented "SCONOX" process to achieve NO<sub>x</sub> emissions less than 2 ppm. Water injection reduces the exhaust NO<sub>x</sub> to near 25 ppm. The SCONOX process uses catalytic oxidation of exhaust CO to CO<sub>2</sub> followed by catalytic oxidation of NO to NO<sub>2</sub> (US Patent 5,607,650). The oxidized NO<sub>2</sub> then adsorbs to a bed of potassium carbonate-treated alumina. The sorbent is regenerated with H<sub>2</sub> and CO<sub>2</sub> to emit H<sub>2</sub>O and N<sub>2</sub> and regenerate the K<sub>2</sub>CO<sub>3</sub>. This system has been acknowledged by the EPA as having achieved the Lowest Achievable Emission Rate (LAER) for combined-cycle gas turbine systems firing natural gas. A more recent patent describes a combined catalytic/adsorber in which an alkali or alkaline earth carbonate or bicarbonate, preferably potassium carbonate, is coated to a platinum coated high-surface area alumina (US Patent 5,665,321,

1997). This material performs in a similar manner to layered double-hydroxide sorbents (US Patent 5,116,587, 1992).

Integrated dry injection using low-NO<sub>x</sub> burners, dry injection of alcohol–water hydrated lime for SO<sub>2</sub> capture, and dry injection of commercial-grade sodium carbonate for additional SO<sub>2</sub> removal and NO<sub>x</sub> removal has been tested. Research–Cottrell Environmental Services and Riley Stoker achieved 90% SO<sub>2</sub> and 15% NO<sub>x</sub> removal using a proof-of-concept unit following low-NO<sub>x</sub> burners (US DOE, 1997).

The LIMB (Limestone Injection Multistage Burner) process uses Ca(OH)<sub>2</sub> injected dry sorbent to control SO<sub>2</sub> with low-NO<sub>x</sub> burners for NO<sub>x</sub> control. The system has been pilot-scale tested on coal-fired boilers with 70% NO<sub>x</sub> and SO<sub>2</sub> control using a combined improved removal system by adding NaOH or Na<sub>2</sub>CO<sub>3</sub> to the injected sorbent (US DOE, 1997).

Other processes include the SNRB process which combines sorbent injection with a hot catalytic baghouse to adsorb SO<sub>2</sub> and convert NO<sub>x</sub> to N<sub>2</sub> and water (Markussen and Livengood, 1995). The SNOX process catalytically removes SO<sub>2</sub> and NO<sub>x</sub> in the flue gas while producing salable concentrated sulfuric acid. Selective catalytic reduction of NO<sub>x</sub> to N<sub>2</sub> and water using NH<sub>3</sub> is followed by catalytic oxidation of SO<sub>2</sub> to SO<sub>3</sub>. The SO<sub>3</sub> is hydrated in a glass condenser and the exothermic process energy recouped. A 30-MW petroleum–coke fired boiler in Italy maintains greater than 96% removal of both SO<sub>2</sub> and NO<sub>x</sub>. A demonstration project as part of a DOE Clean Coal Technology Program has continued to show 95% SO<sub>2</sub> and 94% NO<sub>x</sub> removal. A similar process called DESONOX

uses a single tower containing both reduction and oxidation catalysts. Removals for low-sulfur coals are near 80% for NO<sub>x</sub> and 94% for SO<sub>2</sub> (Markussen and Livengood, 1995).

#### Related SO<sub>2</sub>-Control Methods

The efforts to control SO<sub>2</sub> emissions from various sources are more detailed and extensive than research for improved NO<sub>x</sub> control. This difference in research efforts is partly due to the historically known effects of SO<sub>2</sub> sorption relative to studies of NO<sub>x</sub> sorption. The research on SO<sub>2</sub> control is related in several ways to NO<sub>x</sub> control. A number of control application sorbents apply to both SO<sub>2</sub> and NO<sub>2</sub> through observed performance measures (US Patents 5,665,321, 1997, 5,585,082, 1996 5,165,902, 1992, 5,120,508, 1992, 5,116,587, 1992, 5,096,871, 1990, 4,721,582, 1987). Gaseous SO<sub>2</sub>, NO and NO<sub>2</sub> are considered "acid" gases in that hydration of these gases result in acid formation. The United States Bureau of Mines has investigated the use of alkalized alumina for the control of SO<sub>2</sub> emitted from coal-fired power plants (Murphy, 1973). Regeneration temperature of the alkalized alumina destroyed the material and thus further studies were not pursued. Numerous patents have been granted for various aluminas and alkali and alkaline-earth treatments ( US Patents 2,992,884, 3,501,264, 3,8535,031, 3,699,037, 3,974,256, 4,002,720, 4,259,179, 5,002,742) to control gaseous sulfur emissions.

#### Other NO<sub>x</sub>-Control Methods

Electron beam irradiation initiates reactions that oxidize SO<sub>2</sub> to SO<sub>3</sub> and NO to NO<sub>2</sub> (Cooper and Alley, 1986). The oxidized compounds are easily reacted further to



form salts. However, the cost of the energy required is significantly higher than for other methods. Methods are under investigation to reduce these additional energy costs.

Given the variety of methods being tested and those currently in use, improved system design has become a very specific practice according to the type of combustion process being considered. If current regulation strategies require stricter NO<sub>x</sub> controls for combustion sources having more-variable outputs, single, conventional NO<sub>x</sub> reduction methods will be ineffective and either hybrid systems or new technologies will be needed. A dry filter material may serve to provide NO<sub>x</sub> control that could be regenerated on a regular basis.

#### Research Justification

Past research of solid sorbent materials indicates that practical application of sorbent materials is possible despite the limited understanding of current sorbent material sorption properties. The various pilot-scale studies have indicated that a sorbent material has distinct advantages over conventional NO<sub>x</sub> control methods. Also, laboratory studies related to this topic have proposed various mechanisms of NO<sub>x</sub> sorption by solid sorbents. No other research has provided an in-depth study of the mechanisms involved in NO<sub>x</sub> sorption to such common material as untreated  $\gamma$ -alumina, K<sub>2</sub>CO<sub>3</sub>-treated alumina, and KOH-treated alumina. The kinetics of the sorption process has not been studied from both gas- and solid-phase analyses. The stability of these compounds has not been studied at temperatures experienced under real conditions. In addition, tests of the effects of other gases on NO<sub>x</sub> sorption have not been performed for these materials in a comprehensive

manner. Applicable improvements to solid-sorption control of nitrogen oxides must be accompanied by fundamental research on the sorption processes.

### Research Objectives

Based upon the justification for this basic research, the objectives of this study are as follows:

- Qualify and quantify NO<sub>x</sub> sorption for the most promising sorbent materials.
- Evaluate the controlling mechanism(s) of sorption (diffusion or reaction).
- Determine controlling factors in the sorption potential of alkali compounds
- Evaluate and compare saturation characteristics of sorbents.
- Evaluate the progression of gas and solid conditions over exposure time.
- Measure nitrogen surface species formed on sorbent materials.
- Determine the affects of additional gases, such as O<sub>2</sub>, CO<sub>2</sub>, SO<sub>2</sub>, and H<sub>2</sub>O on the NO<sub>x</sub> sorption process.

## CHAPTER 2 EXPERIMENTAL

### Fixed-Bed Reactor System

Laboratory experiments to measure NO<sub>x</sub> sorption to solid sorbents were performed using a fixed-bed reactor system. The design of the fixed-bed reactor system was modified during the course of experimental work. A reactor system, that was used by a previous researcher (Kimm, 1995), was initially used in this research for comparison of data with the results of Kimm. Studies of magnesium oxide-coated vermiculite (MgO/v) sorbent with added water were performed using the redesigned system, including a redesigned sorbent reactor tube. After the study of added-water effects on MgO/v sorbent was completed, the redesigned system was modified once more to accommodate three sorbent reactor tubes in parallel in the furnace. The experimental errors associated with these three system designs differ and are discussed within the detailed description of each system.

### Initial Fixed-Bed Reactor System

Initial studies of NO<sub>x</sub>-sorption onto MgO/v were performed using a laboratory-scale, single fixed-bed reactor system operated under isothermal conditions. The system has been previously described (Kimm, 1995). This laboratory system is shown in Figure 2-1. Certified cylinder gases (BOC Gases, Murray Hill, New Jersey) sources consisting of diluted NO and NO<sub>2</sub> (balance N<sub>2</sub>) are mixed/diluted by measurement of flow

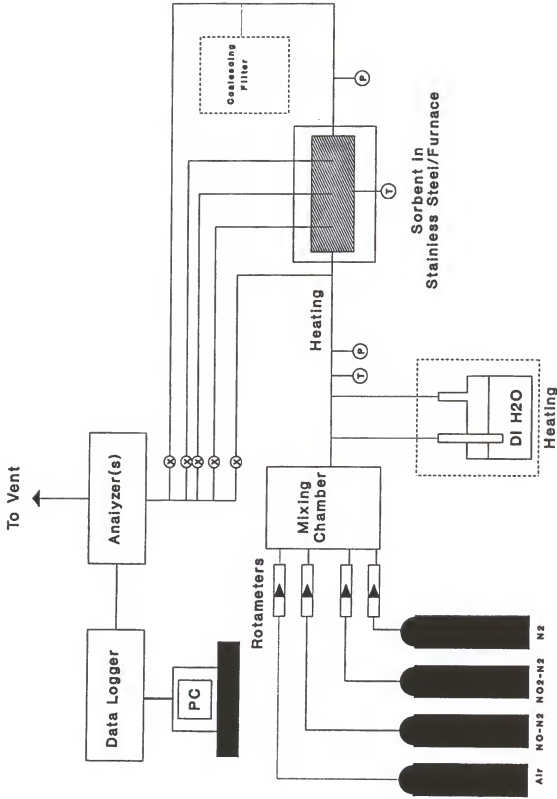


Figure 2-1. Experimental system developed by Kimm (1995) to study NOx removal by magnesium oxide-coated vermiculite (MgO/v) sorbent.

through in-line calibrated rotameters (Omega Engineering, Inc., Stamford, Connecticut) prior to entering the bypass line or the reactor bed. Rotameter calibrations were performed regularly on a quarterly basis using a primary standard bubble meter (Gillibrator, Gillian Instrument Inc., Wayne, New Jersey). The reactor bed enclosure is a 1-in. diameter, 18-in. long 316 stainless steel tube fitted with NPT-Swagelok® fittings and placed vertically inside a tubular furnace (Model 421135, Thermolyne, Dubuque, Iowa). A type-K thermocouple (Model KQSS-116 -24 and -18, Omega, Stamford, Connecticut) is clamped to the outside of the reactor tube to measure the reactor bed temperature. Sorbent material was weighed and then poured down into the reactor tube to rest upon a 316 stainless steel mesh wire (Tyler screen size 325) support. The tube was flushed with deionized water and air dried before each test. Preliminary measurements were made to quantify the possible interaction of gases in a clean reactor bed. After cleaning the reactor bed outlet concentration was 99+% of the bypass line concentration. For quality assurance purposes, the latter test was performed periodically.

Gas can be continuously sampled for NO and NO<sub>2</sub> content from the bypass or the bed outlet line using a chemiluminescent NO<sub>x</sub> analyzer (Model 42H, Thermo Environmental Incorporated, Franklin, Massachusetts). NO<sub>x</sub> concentration checks are performed before and after each test using the NO<sub>x</sub>-test gas concentration flowing through the bypass line. Daily NO<sub>x</sub> analyzer calibrations were performed with N<sub>2</sub> (zero value) and NO and NO<sub>2</sub> gases certified by manufacturer analysis having a concentration of near 80% of analyzer full-scale range (span value). Control charts of zero and span check values were created and used such that values diverging more than three standard

deviations from the mean without an acceptable reason required recalibration of the analyzer. The response times of the NO<sub>x</sub> analyzer in measuring gases flowing from the bed were delayed for about 30 seconds to one minute, depending on flow rates, and data were corrected for the delay.

Three forms of graphical information are used to describe data collected from fixed-bed reactor experiments. One format provides qualitative comparisons of the data collected from the reactor bed gas (NO and NO<sub>2</sub>) as bed outlet concentration of gases. A second format of graphics gives quantitative information of the data as accumulated moles of gas sorbed or produced per mass of bed ( $\mu\text{mole/g}$ ). The third format shows the rates of gas sorbed/produced to indicate trends of gas conversion.

#### Redesigned System: Single and Triple Bed

The original laboratory-scale single fixed-bed reactor (Kimm, 1995) was redesigned to improve the operation, reliability and performance of the system. The redesigned system is shown in Figure 2-2.

System features can be described using Figure 2-2. Gas flows are obtained from certified gas cylinders as in the original system. Five rotameters, having various flow ranges, that are used to mix the gases, are placed on a supporting frame with quick-connect fittings to the inlets. One rotameter can supply N<sub>2</sub> gas to the H<sub>2</sub>O saturation vessel for water vapor-effect studies. A mass flow meter (Model FC-280, Tylan, Rancho Dominguez, California) is set in line following the mixing rotameters to measure total gas flow. A three-way valve allows the gas to flow either to the bypass line or to the reactor beds. A quick-connect fitting was added to the line for flushing the reactor bed(s) without

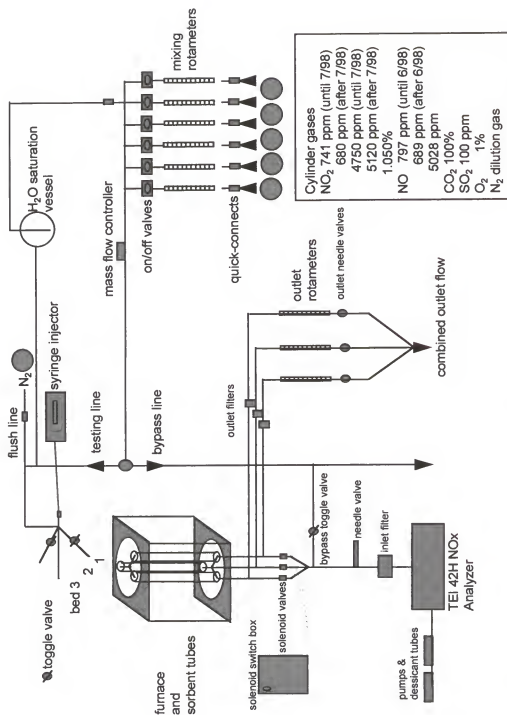


Figure 2-2. Redesigned experimental arrangement for fixed-bed reactor system.

interfering with the inlet mixing gas that is directed to the bypass line. A clam shell type furnace (Model F79325, Thermolyne, Dubuque, Iowa) was purchased to replace the original smaller tubular furnace.

### Triple bed

Initially, the redesigned system included only one redesigned sorbent reactor tube. The studies of  $\text{MgO}/\text{v}$  with added water (see Results and Discussion) were performed using the single redesigned sorbent reactor tube. The redesigned reactor tube was a 0.65 in. I.D., 18-in. long 316 stainless steel tube (0.049 in. thickness) with airtight thermocouple insert ports located above and below the 4-in. bed.

Following the  $\text{MgO}/\text{v}-\text{H}_2\text{O}$  study, the single-bed tube reactor configuration was replaced with three parallel reactor bed tubes. In addition, the single inlet line was modified to incorporate a three-way manifold. Reactor bed #3 had an optional connection to be used for water injection. Inlet lines leading to beds #2 and #1 had on/off toggle valves to allow the use of either one or two beds at a time. A remote controlled solenoid valve was placed at the outlet of each reactor bed to sample effluent gas from that bed. The sequence and time of gas sampling from each bed was adjusted using developed computer software programmed in Visual Basic<sup>™</sup>. The flow of gas leaving each bed was measured using an outlet line rotameter. Inert filters (47 mm diam., 5  $\mu\text{m}$  pore size, PTFE, Gelman Sciences, Ann Arbor, Michigan) were placed after the sampling lines to trap particulate material that escaped from the beds and might have contaminate the rotameters and the  $\text{NO}_x$  analyzer. The outlet tubing configuration also helped prevent particulate entering into the gas-sampling solenoid valves.



Adjustable features were one of the primary benefits derived from the redesigned reactor system. Additional cylinder gases could be easily added to the existing gas mixtures via Swagelok™ quick-connects to one of the five inlet rotameters.

#### Water injection

Water vapor would be added to the gas mixture via two optional connections. A syringe could be used [as needed] to inject additional water vapor into the gas via bed #3. Also, bed #3 had a heat-tape-wrapped injection line that would be activated when introducing a known amount of water vapor. The heat rising from the furnace further ensured that the water vaporized. Furthermore, lesser amounts of water vapor could be added to the gas mixture via an alternative connection in the reactor line. Here the water vapor was produced using the saturation pressure of deionized water in a glass bulb with a fritted-bubbler. A portion of the inlet  $N_2$  gas was diverted through the glass bulb to obtain the desired low-concentrations of water vapor. Measurements were made to ensure complete  $N_2$  gas saturation with water at the flow rates used. The theoretical saturation water vapor pressure was obtained within experimental error.

#### System automation

Certain aspects of the reactor system were automated. A computer data acquisition card (Model PC-LPM-16, National Instruments Inc., Austin, Texas) was purchased to allow for automatic collection of data from the  $NO_x$  analyzer and the thermocouples, and for switching of the solenoid valves. A Microsoft® Visual Basic™ program was created to control the DAQ card and provide for collection of data.

To ensure that the computer recorded accurate data from the NO<sub>x</sub> analyzer, voltage output settings on the analyzer were initially adjusted and checked on a quarterly basis. No observable errors have occurred in collected computer data when compared to the displayed NO<sub>x</sub> analyzer concentration readings. The thermocouple signals were attenuated with additional equipment obtained from the thermocouple manufacturer (Model CCT-23, Omega, Stamford, Connecticut). The attenuator was adjusted to provide a linear, accurate and measurable voltage signal to the DAQ card. The attenuator was adjusted such that a calibrated, hand-held temperature readout device (Model HH23, Omega Inc., Stamford, Connecticut) matched the computer readout values.

#### Fixed-bed reactor system: experimental error

Given that the initial reactor system was used only to perform comparative testing with the work of Kimm. Detailed analysis of that system error was less in comparison to later studies.

The systematic errors in the fixed-bed reactor system were due to variations of bed temperature, flow mixing, and analyzer calibration. Temperature measures were obtained using an 18-in. type K thermocouple inserted through the bottom of the temporarily opened end of the sorbent reactor tube. Temperature at the horizontal center of the bed at vertical positions of 8 and 12 in. in the sorbent tube was measured three times at a furnace temperature setting of 170 °C for gas flowrates of 0.3 and 3 standard liters per minute (sLpm), respectively. The 8- and 12-in. average measurements for 0.3 sLpm were 189.6 and 206.5 °C and for 3.0 sLpm 193.8 and 204.1 °C. No alterations to the position of the bed were made because the bed positions were chosen and used in the work by a previous

researcher (Kimm et al., 1995) and comparison studies required the system to remain unaltered (Kimm, 1995). Cylinder gas  $N_2$  was used for gas flow variation tests.

Test errors due to flow mixing were found to be the most significant experimental error source when gas dilutions greater than 10:1 were used. One must consider the measurable flow parameters used to perform sorption tests: rotameter values and total flow. To test the effect of flow parameters on the input,  $NO_x$  flow control settings were varied over extreme ranges of dilution for typical  $NO_x$  concentrations and the  $NO_x$  measured. The greatest dilutions were 10:1 for any cylinder gas. Control of dilution is dependent on the precision of the rotameter and the relative position of the rotameter ball. The precision of reading the rotameters was found to be near 1% of full-scale flow. Thus, a maximum dilution of 10:1 would be expected to vary the gas concentration by 10%. Testing of the flow controls showed that a 10% variation does occur at the maximum dilution.

The principal  $NO_x$  analyzer parameter that was found to significantly affect  $NO_x$  measurements was the supply of dry air to the ozonator. Daily calibrations of the  $NO_x$  analyzer indicated that the fluctuation in the daily  $NO$  calibrations were subject to the dryness of the analyzer air supply. Desiccant canisters used for drying the input air to the ozonator were set in parallel to provide a longer continuous supply of dry air.

#### Redesigned system

The temperature profiles in the sorbent tube were obtained at 250 °C using an 18-in. type K thermocouple inserted through the air-tight fittings placed temporarily at the bottom of the sorbent tube. Temperature variations from a bed height of 8.5 to 12.5 in.

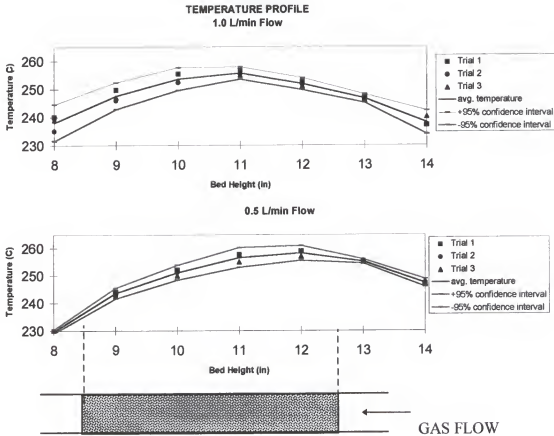
were found to vary from 240 to 265 °C and 249 to 255 °C with no gas flow and at 2 aLpm, respectively. The variations were less at lower temperatures. Cylinder gas N<sub>2</sub> was used for gas flow variation tests.

The mass flow controller added to the system has a full-scale error of 1% when full scale was set at 3.18 Lpm. Thus, the error at the lowest testing flow of 1.5 Lpm (0.5 Lpm x 3 beds) was approximately 2%.

Temperature measures throughout the redesigned triple-bed reactor were sensitive to gas flowrate in the same manner as observed for the original single-sorbent-tube reactor.

Temperature profiles were measured along the length of the reactor beds using thermocouple inserts into each bed. Temperature measures were obtained at 250 °C using a 24-in. type K thermocouple inserted through the air-tight fittings located temporarily at the top of the sorbent tube. The flow rate of gas was varied from 0.5 to 1 Lpm. Cylinder gas N<sub>2</sub> was used for gas flow variation tests. The temperature profiles in the triple bed across the sorbent tube system are shown in Figure 2-3 for these two flows. The bed temperature profiles varied less at lower temperatures. The temperature profiles of each reactor bed indicated that the variation between beds was less than  $\pm 5$  °C during sorption tests. Horizontal variations of the tube temperature were observed to vary less than 2 °C from tube wall to bed center at the maximum sorption testing temperature, 250 °C.

Experimental error in sorption data was evaluated by performing identical tests of NO<sub>x</sub> sorption on untreated alumina. The triple-bed system error may be considered to be of two types. Experimental error tests were performed to include simultaneously tested



**Figure 2-3. Sorbent tube temperature profile of triple fixed-bed reactor system.**

Note: sorbent bed position shown.

samples and consecutively tested samples. Figure 2-4 shows the NO and NO<sub>2</sub> outlet concentrations resulting from experimental reproducibility tests of a) simultaneously run samples of untreated alumina, b) consecutively run samples of untreated alumina, for sorption of 50 ppm NO and 500 ppm NO<sub>2</sub> at 200 °C.

#### General Fixed-Bed Reactor Experimental Procedure

Prepared sorbent material is measured to a specified mass and poured into the reactor tube. The reactor tube is set into the furnace. Gas that has been mixed to the desired concentration is directed to the bypass line. Data collection initially was manually performed. After the system was redesigned, developed in-house software automatically recorded NO and NO<sub>2</sub> measures from the analyzer and temperatures from the thermocouples. The tube furnace temperature controller is set to provide the desired bed temperature. The redesigned system allowed the beds to be flushed (with N<sub>2</sub>) prior to testing. Flushing the beds allowed for adjustments to equalize the outlet rotameter readings and to ensure no gas leakage. Once the bed temperature and gas mixture readings stabilized the gas was directed from the bypass line to the reactor bed line. Adjustments of inlet-gas mixing rotameters was performed during the test to ensure a constant gas mixture input. After the desired time of testing, the input gas is redirected to the bypass line for a post-test check of the inlet gas NO<sub>x</sub> concentrations.

#### Experimental Conditions

Fixed-bed reactor system tests of NO<sub>x</sub> sorption were performed with atypical ratios of NO<sub>2</sub>:NO in gas mixtures. The NO<sub>2</sub>:NO ratios used in laboratory tests were in the range of 1:1 to 50:1, whereas the normal ratio of combustion exhaust NO<sub>2</sub>:NO is 1:20 (Cooper and Alley, 1986). This divergence from the normal ratio is based on

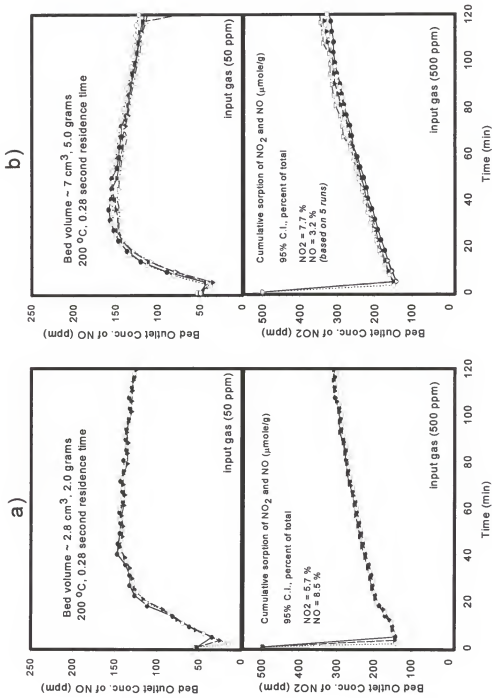


Figure 2-4. Experimental reproducibility tests: a) simultaneously run samples of untreated alumina, b) consecutively run samples of untreated alumina.

an overall NO<sub>x</sub>-removal concept where NO is oxidized to NO<sub>2</sub> prior to NO<sub>x</sub> sorption in flue-gas treatment applications. The mass of material used in the various test series was not constant. Initially the test sample mass was matched to conditions used in previous research (Kimm, 1995). The range of overall flowrates in the reactor beds used in the various test series was 1.0 to 0.5 Lpm. The reactor bed temperature during NO<sub>x</sub> exposure tests varied from ambient (23 °C) to 250 °C.

Some solid materials were thermally decomposed in the fixed-bed reactor system to observe the nature of decomposition species during a substantial ramp in temperature. Only reactor bed #3 was used to study these solid reactant decompositions and product formation. A set flow of N<sub>2</sub> gas was passed through the reactor bed while the temperature was ramped manually at 10 °C/min to a maximum of 750 °C. Exposed samples of reagent-grade nitrate and nitrite salts were decomposed. The salts proved extremely detrimental to the system in that the vaporized and decomposed salts reformed (condensed) along the outlet tube walls that were at lower temperatures. Thorough cleaning of the entire system outlet lines was required following these tests. However, decompositions of NO<sub>x</sub>-exposed sorbent samples did not result in reformation of particulate material along the tube walls. A significant source of error in the results of the decomposition tests was observed following the tests. Reduction of NO<sub>2</sub> to NO by stainless steel is known to occur at temperatures above 500 °C (Sigsby et al., 1973). Tests were performed to observe this effect. The results indicated that measured NO<sub>x</sub> species at or above 500 °C would be only NO due to reactor wall reactions. However, NO<sub>2</sub> was observed above 500 °C. This result is addressed later in the Discussion section.



Reproducibility of similarly NO<sub>x</sub>-exposed samples of untreated alumina exposed for 2 hours to 500 ppm NO<sub>2</sub> and 50 ppm NO at 0.62 sLpm and 150 °C are shown in Figure 2-5. The results from these untreated alumina samples include errors due to NO<sub>x</sub> exposure and, thus, represent a greater error than that expected for decomposition of two similar samples.

Additional gases or vapors tested in conjunction with exposure to NO and NO<sub>2</sub> mixtures include one of the following: water vapor, O<sub>2</sub>, SO<sub>2</sub>, and CO<sub>2</sub>. Water injection was in the range from 1 to 5% of gas volume at temperatures ranging from 25 to 200 °C.

### Sample Preparation

A variety of sorbent materials were studied in this research in which the preparation, if necessary, was varied as well. The materials include magnesium oxide-coated vermiculite (MgO/v), untreated  $\gamma$ -alumina, and  $\gamma$ -alumina treated with one of the following compounds: carbonates (Li, Na, K, Rb, Cs), hydroxides (Li, Na, K, Rb, Cs), or sulfates (Na and K).

#### Magnesium-Oxide Coated Vermiculite (MgO/v)

MgO/v was prepared following the technique used by Kimm (Kimm, 1995). One-kilogram batches were prepared using a 45:55 mass ratio of MgO (Elastomag 170 m<sup>2</sup>/g, Akrochem Inc., Akron, Ohio) and vermiculite (coarse grade, Stronglite Product Inc., Pine Bluff, Arkansas). Each batch was hand-mixed with a 4:1 mass ratio of deionized water/MgO-vermiculite. Batches were baked at 550°C for 30 min. in a muffle furnace and stored in airtight plastic containers. This preparation method is described in more detail in the patent description held by Sorbtech (US patent 4,721,582, 1987). Sorption

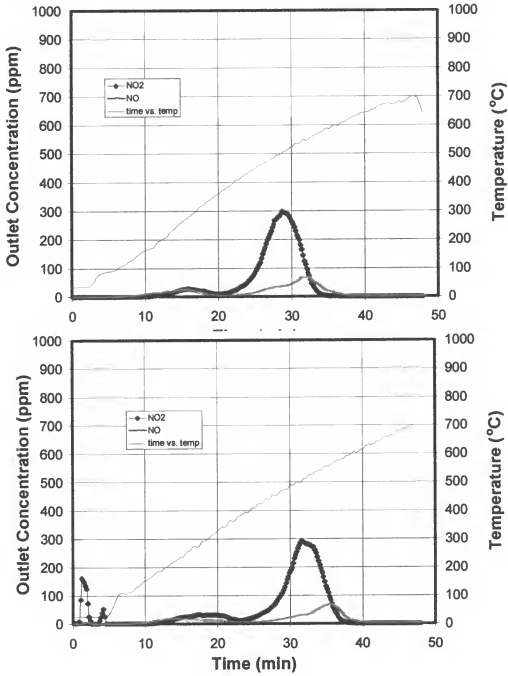


Figure 2-5. Reproducibility of decomposed samples separately sorption tested.

studies of the effects of aging on the MgO/v material stored in airtight containers showed that the stored sorbent performs well without deterioration over a minimum of two years. Storage of MgO/v in ambient air for periods of several weeks also does not appear to alter the NO<sub>x</sub> sorption characteristics.

#### γ-Alumina: Untreated and Treated

Untreated cylindrical pellets (1/8 in O.D. x 1/8 in.) of γ-alumina were obtained commercially (material AL-3438 T, Englehard Corp., Elyria, Ohio) with a nominal surface area of 170 m<sup>2</sup>/g. Pellets were dried at 150°C for a 24-hour period prior to storage in sealed containers. Reagent-grade chemicals (Fisher Scientific, Pittsburgh, Pennsylvania) were used to make aqueous solutions for treating the alumina pellets. Solution concentrations varied from 1.0 to 0.04 *M*. Two types of treatment techniques were used: impregnation and precipitation. Most heated material studies have used the precipitate-prepared treated alumina. Impregnated pellets were prepared by flowing the salt solution through the bed of alumina pellets supported on Whatman 41 filter paper for about two minutes. Precipitated samples were prepared by mixing pellets with the salt solution and evaporating the solution to dryness. Both impregnated and precipitated samples were dried for 24 hours at 150°C. Impregnation treatments were performed only for initial comparative studies of treatment techniques. Table 2-1 provides a listing of the physical properties of treated materials as recorded during preparation.

The nature of the containers (glass or ceramic) used to prepare treated samples does not appear to alter NO<sub>x</sub> sorption behavior. NO<sub>x</sub> sorption tests on precipitated alumina pellets having similar loading of KOH but prepared using different solution

Table 2-1. Physical properties of sorbent materials studied.

| Sorbent material                                  | percent       | bulk density |
|---|---------------|--------------|
| MgO/v   | MgO(45):v(55) | 0.13         |
| untreated $\text{Al}_2\text{O}_3$                 | ----          | 0.70         |
| $\text{LiOH-Al}_2\text{O}_3$                      | 7.3           | 0.59         |
| $\text{NaOH-Al}_2\text{O}_3$                      | 10.6          | 0.77         |
| $\text{KOH-Al}_2\text{O}_3$                       | 13.8          | 0.80         |
| $\text{KOH-Al}_2\text{O}_3$                       | 20            | 0.94         |
| $\text{RbOH-Al}_2\text{O}_3$                      | 21.6          | 0.86         |
| $\text{CsOH-Al}_2\text{O}_3$                      | 33            | 0.98         |
| $\text{Li}_2\text{CO}_3\text{-Al}_2\text{O}_3$    | 7.3           | 0.71         |
| $\text{Na}_2\text{CO}_3\text{-Al}_2\text{O}_3$    | 10.6          | 0.65         |
| $\text{K}_2\text{CO}_3\text{-Al}_2\text{O}_3$     | 13.8          | 0.79         |
| $\text{K}_2\text{CO}_3\text{-Al}_2\text{O}_3$     | 24.7          | 0.85         |
| $\text{Rb}_2\text{CO}_3\text{-Al}_2\text{O}_3$    | 21.6          | 1.01         |
| $\text{Cs}_2\text{CO}_3\text{-Al}_2\text{O}_{3p}$ | 33            | 1.15         |
| $\text{Cs}_2\text{CO}_3\text{-Al}_2\text{O}_{3p}$ | 29            |              |
| $\text{Cs}_2\text{CO}_3\text{-Al}_2\text{O}_{3p}$ | 23            |              |

concentrations demonstrated that they have similar NO<sub>x</sub> removal characteristics as seen in Figure 2-6.

#### Ion-Specific Electrode (ISE) Measurements

ISE methods were developed to measure hydronium ( $H^+$ ), nitrite ( $NO_2^-$ ), and nitrate ( $NO_3^-$ ) ions from extracts of NO<sub>x</sub>-exposed alumina sorbents by David Pocengal (Pocengal, 1999). Separate methods were developed for NO<sub>x</sub>-exposed untreated,  $K_2CO_3$ -treated, and KOH-treated alumina sorbents. NO<sub>x</sub>-exposed sorbent samples were placed in deionized water solution, adjusted for solution *pH* with sulfamic acid, and adding interference suppresser as necessary. Solution concentrations were in the range from  $1 \times 10^{-2}$  to  $10^{-5}$  M. A *pH* electrode (model 13-620-AP50, Accumet, Pittsburgh, Pennsylvania) and portable *pH* meter (model AP-61, Fisher Scientific, Pittsburgh Pennsylvania) were used to measure the *pH* of aqueous-solution extracts. Ion-specific electrodes that measure nitrite (model 93-46, Orion, Beverly, Massachusetts) with a double-junction reference electrode (model 90-02, Orion) and nitrate (model 93-07, Orion) with a double reference electrode (model 09-01, Orion) were used to analyze sample extracts in aqueous solution. A *pH*/mV meter was used for nitrite and nitrate measurements (Model 245, Corning, New York). After NO<sub>x</sub>-exposure, samples of treated or untreated alumina were ISE analyzed or stored in plastic vials (catalog # 14809B, Fisher Scientific, Pittsburgh, Pennsylvania). For certain samples, a portion (~ 0.5 g) was stored so that additional analyses of the sample could be performed if needed.

Measurement error of the developed ISE method was evaluated by splitting individual sorbent samples exposed in the fixed-bed reactor system into three

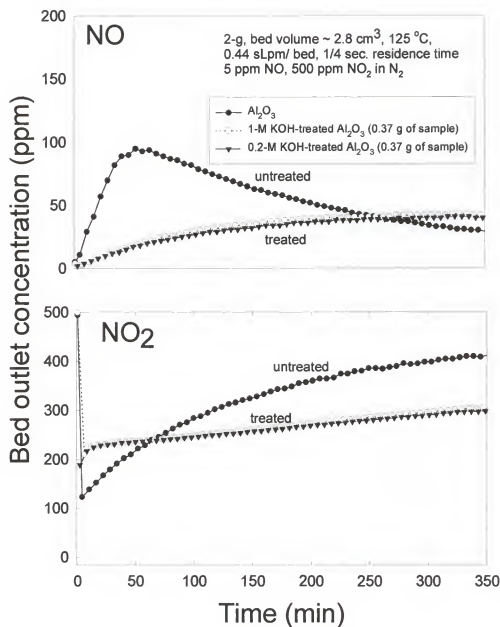


Figure 2-6. Samples prepared by different coating methods with similar mass amounts of coating showing similar  $\text{NO}_x$  sorption characteristics

1-gram samples and performing ISE analyses of each 1-gram sample. Error analysis was performed on NO<sub>x</sub>-exposed untreated, K<sub>2</sub>CO<sub>3</sub>-treated, and KOH-treated alumina samples. The solution concentrations of the 1-gram sample extracts were near the lower concentration range applied in ISE measurements ( $1 \times 10^{-4}$  to  $10^{-5}$  M). Table 2-2 provides results of these tests. Other NO<sub>x</sub>-exposed KOH-treated alumina samples were similarly ISE analyzed and results are shown in Table 2-2. The two additional KOH-treated alumina samples were exposed for varied time periods to evaluate the change in the nitrite-to-nitrate ratio with exposure. These tests are further discussed in the Results And Discussion chapter. The cumulative (NO + NO<sub>2</sub>, and nitrite + nitrate) 95% confidence interval (95% C.I.) is calculated using the Student-t test with a cumulative standard deviation (*Stotal*) as

$$Stotal^2 = Sa^2 + Sb^2$$

where *S* is the standard deviation and *a* and *b* represent NO and NO<sub>2</sub> or nitrite and nitrate.

The ratio of measured ISE nitrogen to measured NO<sub>x</sub> sorbed is used to express a fraction of recovery. Given the calculated 95% C.I. in Table 2-2, the ISE measurements of total nitrite and nitrate are in the range of measured NO<sub>x</sub> sorption for all three sorbent materials. Using the 95% C.I., the fractional amount of error for cumulative nitrite and nitrate by ISE measurement on K<sub>2</sub>CO<sub>3</sub>-treated alumina is (47.2/203.4) 23%. Thus the high fractional NO<sub>x</sub>/NO<sub>x</sub> recovery of 1.19 is within the 95% C.I.. The ISE measurements indicated that recovery for untreated alumina, K<sub>2</sub>CO<sub>3</sub>-treated alumina, and KOH-treated alumina discussed in the Results and Discussion chapter, Gas and Surface Profile for the

Sorption Process section were approximately 70 %, 120%, and 100%, respectively. ISE measurements indicated that recovery of NO<sub>x</sub> sorbed onto untreated alumina decreased with increased time between exposure and ISE analysis. This observed reduction of recovery is further discussed by Pocengal (1999). The reduced recovery affected the average recovery described in the Gas and Surface Profile for the Sorption Process section. Thus, these error-analysis tests, in which ISE analysis was performed immediately after NO<sub>x</sub> exposure, represent a more accurate recovery. In addition to the effects on recovery of time between exposure and ISE analysis, nitrate and nitrite on untreated alumina was found to be difficult to transfer from the solid to liquid phase. Mechanically crushing the untreated alumina pellets and sonication of solution enhanced recovery and was performed. The high recovery of K<sub>2</sub>CO<sub>3</sub>-treated alumina is caused by extract solution ionic activity being greater than that in standard solutions and is further discussed by Pocengal (1999).

Cumulative errors were evaluated for collaborative work of sorbent samples similarly exposed in the fixed-bed reactor system followed by ISE measurement. An evaluation of cumulative errors was performed of NO<sub>x</sub>-exposed untreated, K<sub>2</sub>CO<sub>3</sub>-treated, and KOH-treated alumina samples. The fixed-bed reactor system was used to simultaneously expose three samples using similar conditions used for evaluating the sorption mechanisms discussed later (see Gas and Surface Profile for the Sorption Process section). Three-gram samples of untreated, K<sub>2</sub>CO<sub>3</sub>-treated, and KOH-treated alumina were simultaneously exposed to 1950 ppm NO<sub>2</sub>, residual NO (10 ppm) flowing at 0.885 sLpm per bed at 25 °C. The 30-minute exposures were performed three times and



Table 2-2. ISE measurement error of NO<sub>x</sub>-exposed untreated, K<sub>2</sub>CO<sub>3</sub>-treated and KOH-treated alumina samples.

| Coating material                   | Cumulative NO <sub>x</sub> (μmol/g) |                 |                       | Cumulative nitrite and nitrate (μmol/g) |                              |                                    | Recovery NO <sub>x</sub> /NO <sub>x</sub> |
|------------------------------------|-------------------------------------|-----------------|-----------------------|---|------------------------------|------------------------------------|---|
| fraction error                     | NO                                  | NO <sub>2</sub> | total NO <sub>x</sub> | NO <sub>2</sub> <sup>-</sup>            | NO <sub>3</sub> <sup>-</sup> | total NO <sub>x</sub> <sup>-</sup> |   |
| <b>untreated</b>                   | -97.7                               | 325.4           | 227.7                 | 8.3                                     | 197.0                        |                                    |   |
|                                    |                                     |                 |                       | 13.1                                    | 195.0                        |                                    |   |
|                                    |                                     |                 |                       | 13.4                                    | 185.0                        |                                    |   |
| mean                               |                                     |                 |                       | 11.6                                    | 192.3                        | 203.9                              | 0.90                                      |
| 95% C.I.                           |                                     |                 |                       | 6.48                                    | 14.6                         | 15.9                               |   |
| error fraction                     |                                     |                 |                       |   |                              | 0.08                               |   |
| <b>K<sub>2</sub>CO<sub>3</sub></b> | -5.6                                | 177.1           | 171.5                 | 108.0                                   | 106.0                        |                                    |   |
|                                    |                                     |                 |                       | 84.4                                    | 85.7                         |                                    |   |
|                                    |                                     |                 |                       | 113.0                                   | 113.0                        |                                    |   |
| mean                               |                                     |                 |                       | 101.8                                   | 101.6                        | 203.4                              | 1.19                                      |
| 95% C.I.                           |                                     |                 |                       | 34.6                                    | 32.1                         | 47.2                               |   |
| error fraction                     |                                     |                 |                       |   |                              | 0.23                               |   |
| <b>KOH</b>                         | -5.0                                | 153.0           | 148.0                 | 82.5                                    | 66.3                         |                                    |   |
|                                    |                                     |                 |                       | 80.9                                    | 64.5                         |                                    |   |
|                                    |                                     |                 |                       | 82.8                                    | 72.1                         |                                    |   |
| mean                               |                                     |                 |                       | 82.1                                    | 67.6                         | 149.7                              | 1.01                                      |
| 95% C.I.                           |                                     |                 |                       | 2.3                                     | 9.0                          | 9.3                                |   |
| error fraction                     |                                     |                 |                       |   |                              | 0.07                               |   |
| <b>KOH short exp.</b>              | 46.0                                | 56.7            | 102.7                 | 103.0                                   | 11.5                         |                                    |   |
|                                    |                                     |                 |                       | 82.2                                    | 9.6                          |                                    |   |
|                                    |                                     |                 |                       | 94.6                                    | 9.3                          |                                    |   |
| mean                               |                                     |                 |                       | 93.3                                    | 10.2                         | 103.2                              | 1.01                                      |
| 95% C.I.                           |                                     |                 |                       | 23.7                                    | 2.7                          | 23.8                               |   |
| error fraction                     |                                     |                 |                       |   |                              | 0.23                               |   |
| <b>KOH long exp.</b>               | -363.9                              | 1440            | 1076                  | 134.0                                   | 609                          |                                    |   |
|                                    |                                     |                 |                       | 318.0                                   | 903                          |                                    |   |
|                                    |                                     |                 |                       | 279.0                                   | 801                          |                                    |   |
| mean                               |                                     |                 |                       | 243.0                                   | 771.0                        | 1015                               | 0.94                                      |
| 95% C.I.                           |                                     |                 |                       | 219.4                                   | 337.8                        | 402.8                              |   |
| error fraction                     |                                     |                 |                       |   |                              | 0.40                               |   |

each sample was immediately ISE analyzed. Sorbent samples were not split for ISE analysis but analyzed as one measurement sample each. Based on the triplicate tests Table 2-3 includes results of measured NO<sub>x</sub> sorption and ISE analyses of nitrite and nitrate. Similar results to the ISE measurement error tests (Table 2-2) of K<sub>2</sub>CO<sub>3</sub>-treated alumina are observed in that recovery is high (1.23). The error fraction of the total nitrite and nitrate by ISE measurement for K<sub>2</sub>CO<sub>3</sub>-treated alumina using the 95% C.I. is 14%. The error fraction of the NO and NO<sub>2</sub> sorption measurements for K<sub>2</sub>CO<sub>3</sub>-treated alumina using the 95% C.I. is 8%. Thus, given the combined error fraction of NO<sub>x</sub> sorption measurements and the ISE measurements, a recovery of 123% is possible. The similar error fractions due to NO<sub>x</sub> sorption or ISE measurements in Table 2-3 suggest that errors due to either NO<sub>x</sub>-sorption or ISE measurement were not dominant. Also, comparing the error fraction of the ISE measurements in Table 2-3 and Table 2-2, one observes that ISE measurement fraction error varies from 0.14 to 0.23, respectively. The higher variation of error fraction of ISE measurements, alone (Table 2-2) indicates that ISE measurements are the same if not greater than error of NO<sub>x</sub>-sorption measurements.

#### X-ray Photoelectron Spectroscopy

Certain features of sorbent samples of interest were further studied using X-ray photoelectron spectroscopy (XPS), courtesy of Professor G. Hoflund and his group, Chemical Engineering Department, University of Florida. This ultra-high-vacuum technique uses X-rays to bombard a material that will emit detectable photoelectrons of characteristic energies. Ultra-high vacuum ( $10^{-10}$  torr) is necessary to reduce the interference of gases during X-ray bombardment of the material. Upon bombardment, the

Table 2-3. Cumulative measurement error of fixed-bed reactor testing and subsequent ISE measurement of three samples of NO<sub>x</sub>-exposed untreated, K<sub>2</sub>CO<sub>3</sub>-treated and KOH-treated alumina.

| Coating material                   | Cumulative NO <sub>x</sub> (μmol/g) |                 | total NO <sub>x</sub> | Cumulative nitrite and nitrate μmol/g |                              | total NO <sub>x</sub> | Recovery NO <sub>x</sub> <sup>-</sup> /NO <sub>x</sub> |
|------------------------------------|-------------------------------------|-----------------|-----------------------|---------------------------------------|------------------------------|-----------------------|--|
|                                    | NO                                  | NO <sub>2</sub> |                       | NO <sub>2</sub> <sup>-</sup>          | NO <sub>3</sub> <sup>-</sup> |                       |  |
| <b>untreated</b>                   |                                     |                 |                       |                                       |                              |                       |  |
| mean                               | -114.8                              | 335.0           | 220.2                 | 8.9                                   | 181.3                        | 190.2                 | 0.86   |
| 95% C.I.                           | 4.4                                 | 15.8            | 16.5                  | 0.7                                   | 13.5                         | 13.5                  |  |
| error fraction                     |                                     |                 | 0.09                  |                                       |                              | 0.07                  |  |
| <b>K<sub>2</sub>CO<sub>3</sub></b> |                                     |                 |                       |                                       |                              |                       |  |
| mean                               | -29.7                               | 289.2           | 259.4                 | 143.3                                 | 176.0                        | 319.3                 | 1.23   |
| 95% C.I.                           | 5.1                                 | 20.2            | 20.8                  | 6.9                                   | 43.7                         | 44.2                  |  |
| error fraction                     |                                     |                 | 0.08                  |                                       |                              | 0.14                  |  |
| <b>KOH</b>                         |                                     |                 |                       |                                       |                              |                       |  |
| mean                               | -25.8                               | 284.1           | 258.3                 | 146.0                                 | 144.0                        | 290.0                 | 1.12   |
| 95% C.I.                           | 0.9                                 | 19.4            | 19.4                  | 14.1                                  | 13.6                         | 19.6                  |  |
| error fraction                     |                                     |                 | 0.08                  |                                       |                              | 0.07                  |  |

elemental species will characteristically interact with the X-ray and may emit a photoelectron that is then measured for intensity.

Prior to XPS analysis, alumina pellets are crushed to expose the inner surface, placed in an aluminum cup, pressed into a new pellet, mounted on a stainless steel sample holder, and inserted into the ultra-high-vacuum chamber. This procedure exposes the pore walls for analysis. XPS is performed using a double-pass cylindrical mirror analyzer (CMA) (Perkin-Elmer PHI model 25-270AR, Eden Prairie, Minnesota). Survey spectra are taken in the retarding mode with a pass energy of 50 eV, and high-resolution XPS spectra are taken with a pass energy of 25 eV using Mg K $\alpha$  X-rays (Perkin-Elmer PHI model 04-51 X-ray source). Data collection is accomplished using a computer-interfaced, digital pulse-counting circuit (Gilbert et al., 1982) followed by smoothing using digital filtering techniques (Savitsky and Golay, 1984). Since XPS is performed using a flood source, the XPS data represents an average over the area analyzed (~ 4 mm diameter). The reproducibility of survey spectra was evaluated for several samples. Figure 2-7 shows spectra of two separate samples of untreated alumina and separate samples of KOH-treated  $\gamma$ -alumina that were individually NO<sub>x</sub> saturated. Survey scans of the individually NO<sub>x</sub>-saturated samples include errors from KOH-treatment, and fixed-bed reactor exposure to saturate with NO<sub>x</sub>, as well as sample preparation for XPS analysis.

### BET Analyses

A few samples were tested to determine surface adsorption properties using the Brunauer–Emmett–Teller (BET) technique (Brunauer et al., 1938). The surface

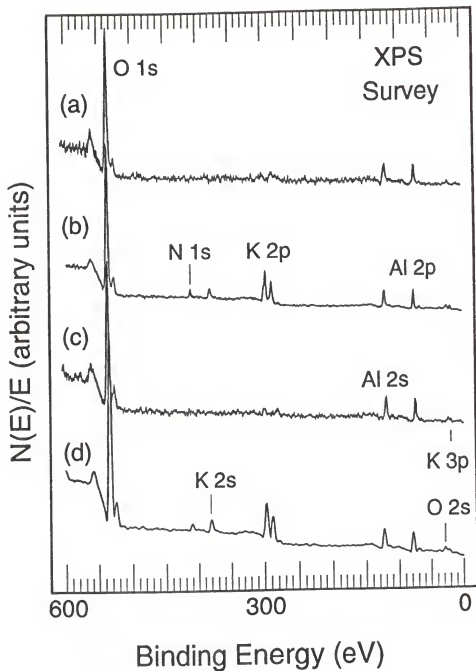


Figure 2-7. XPS survey spectra obtained from (a) untreated  $\gamma$ -alumina, NO<sub>x</sub> saturated (b) untreated  $\gamma$ -alumina after KOH-coating and NO<sub>x</sub>-saturated (c) untreated  $\gamma$ -alumina, NO<sub>x</sub> saturated (d) untreated  $\gamma$ -alumina after KOH coating and NO<sub>x</sub> saturated.

properties are measured by observed changes in pressure upon physical sorption of  $N_2$  to the sorbent. Material surface-area measurements were performed on all supplied samples and pore size distributions were obtained on a few samples. Professor B. Moudgil, Materials Science and Engineering Dept., University of Florida, provided access to a BET analyzer (Model Nova 1200, Quantachrome, Boynton Beach, Florida) using system software.

The BET sample tube is inserted into the analyzer sampling port where a canister of liquid nitrogen is placed around the testing tube. The canister of liquid nitrogen is necessary to maintain the sample near the condensation temperature of  $N_2$  during testing. Certified high-purity  $N_2$  cylinder gas (Grade 5.0, BOC Gases, Riverton, New Jersey) is used to sorb to the analyzed material. A standard set of five pressure point values are collected and converted into surface area measurements by the analyzer. The pressure values are typical for BET analysis from 0.05 to 0.30 fraction of total pressure.

Pore-size distributions were performed by desorbing an  $N_2$ -saturated sample. Twenty pressure points (increments of 5% of total pressure) are collected during desorption. The amount of gas desorbed from the sample is converted by the analyzer to provide an estimate of pore size distribution and pore volume.

Tests were performed to observe possible measurement errors due to variations in the BET analyzer sample preparation procedure. Samples are placed in pre-weighed calibrated glass test tubes, initially vacuum-outgassed for at least 6 hours, and heated to 150 °C to remove trapped gases and vapors within the solid material. The vacuum is set at near 10 Torr. Longer heating time periods do not significantly affect the

reproducibility. After outgassing, the samples were weighed. Reproducibility error is found to be most significant for similarly prepared and NO<sub>x</sub>-sorption-tested treated alumina samples (5% relative std. dev.). Repeated analysis of the same sample indicates insignificant variation (<1% at 95% C.I.).

#### Fourier Transform Infrared (FTIR) Analyses

A Fourier transform infrared spectrometer (FTIR) (Model 5PC, Nicolet, Madison, Wisconsin) was used to perform further analyses of NO<sub>x</sub>-exposed sorbents, courtesy of Professor K. Williams, Department of Chemistry, University of Florida. This technique measures the infrared absorption (4000 to 400 cm<sup>-1</sup> wavenumber) by a material surface in which the absorption is characteristic of that material. The sorbents studied before and after NO<sub>x</sub> exposure were powdered by placing in a container and crushing with a rod made of 316 stainless steel. Powdered samples and reagent-grade materials were stored in plastic vials prior to transport and analysis by FTIR. During FTIR analysis the materials were held in a ZnSe-windowed container. A gas purging system (Model 53-152, Barnstead, Boston, Massachusetts) reduced the amount of gases within the chamber. PC software (Nicolet PC/IR ver 3.2) was used to collect, display and store data from the FTIR. In order to obtain reproducible spectra of a single sample periodic scans (two-minute intervals) were performed until the background CO<sub>2</sub> gas peak (2550 cm<sup>-1</sup>) was constant. Reproducibility testing was performed of the same sample powder that has been mixed between scans. The FTIR reproducibility scans are seen in Figures 2-8.

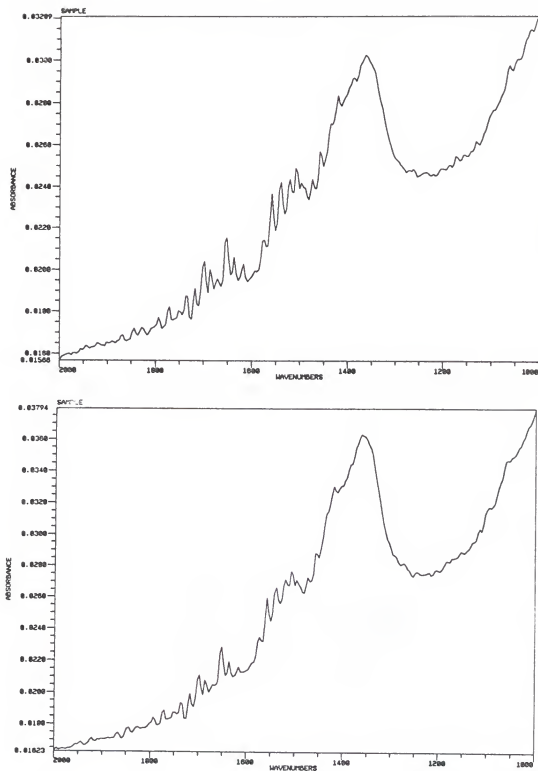


Figure 2-8. FTIR reproducibility of  $\text{Cs}_2\text{CO}_3$ -treated alumina a) initial survey, b) second survey after mixing sample.



### CHAPTER 3

#### RESULTS AND DISCUSSION

Methods of solid sorbent control of nitrogen oxides have been studied by many other research groups (Murphy, 1972; Nelson et al., 1989; Ma et al., 1995; and Nelli and Rochelle, 1998). From this previous research it is apparent that Group-I compounds have been used successfully to sorb NO<sub>x</sub>. Some researchers have proposed mechanisms for the surface reactions occurring during NO<sub>x</sub> sorption. However, an in-depth analysis to quantify the sorption process has not been performed that is crucial to improving sorption properties. Initial studies are described that have led to questions concerning previously proposed mechanisms. Further research is described which identifies multi-step mechanisms of NO<sub>2</sub> sorption and suggests that the process is limited by the formation of nitrate and nitrite that is further converted to nitrate for the Group-I compounds. In addition, Group-I compounds remove both NO and NO<sub>2</sub> in the early stages of sorption.

A fixed-bed dynamic reactor system was constructed to serve as the main experimental method to study NO<sub>x</sub> interactions with solid sorbents. Other analytical methods used to study sorbent exposed to NO<sub>x</sub> include XPS (X-ray photoelectron spectroscopy), FTIR (Fourier-transform infrared spectroscopy), BET (Brunauer et al., 1938) surface analysis, and ion-specific electrodes. Initial experiments were based on the evaluation of magnesium oxide-coated vermiculite (MgO/v) and the effects of other gas constituents on NO<sub>x</sub> sorption. As the research progressed to studies of other sorbents,

the use of alumina pellets and group-I-compound coated  $\gamma$ -alumina were determined to be superior to MgO/v and research became focused on the latter materials. The errors of an analytical technique dictate the quality of experimental data and the resulting conclusions. Therefore, an evaluation of the errors is included in the experimental techniques section of Chapter 2.

Studies of untreated alumina showed that the manufacturer or surface acidity of  $\gamma$ -alumina did not differ in sorption of  $\text{NO}_2$ . XPS analysis of  $\text{NO}_x$ -exposed  $\gamma$ -alumina indicated that potassium impurities interact with  $\text{NO}_2$  sorption. Potassium hydroxide was coated on alumina and found to remove both  $\text{NO}_2$  and  $\text{NO}$ . Given the success of KOH-treated alumina, tests of sulfate, hydroxide, and carbonates in the form of sodium and potassium compounds, were coated in varied amounts onto alumina. Tests showed that potassium compounds improved  $\text{NO}_x$  sorption and carbonate coatings performed better per mole than hydroxide while sulfate compounds performed poorly. Next, group-I, lithium through cesium hydroxides and carbonates showed improved  $\text{NO}_x$  removal with decreasing ionization potential of the alkali metal element. A series of fixed-bed reactor experiments in which the concentrations of  $\text{NO}$  or  $\text{NO}_2$  was varied over temperatures from ambient ( $25^\circ\text{C}$ ) to  $250^\circ\text{C}$ , indicated that  $\text{NO}_x$  sorption improved with temperature. Specifically, increased  $\text{NO}$  removal occurred at higher temperatures.

Proposed mechanisms of sorption of  $\text{NO}_x$  were formulated based on fixed-bed reactor tests and ion-electrode measures of nitrites and nitrates formed. Mass balance estimates for  $\text{NO}_x$  sorbed and surface nitrogen species produced were used to calculate reaction rates of the slowest stage of a multi-step mechanism. Confirmation

of ion-electrode measures of surface nitrite and nitrate was accomplished using FTIR studies. Thermal decomposition of NO<sub>x</sub>-exposed sorbent indicates that differences difference exist in the quantities of surface nitrate and nitrite formed in comparison to bulk salt compounds.

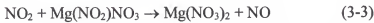
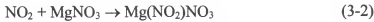
### Initial MgO/v Laboratory Experiments

Initial NO<sub>x</sub>-sorption experiments were conducted on MgO/v in the single fixed-bed reactor system designed by Kimm (1995). The NO<sub>x</sub> sorption potential of magnesium oxide-coated vermiculite (MgO/v) had been shown to be feasible in pilot-scale applications (Nelson et al., 1992, 1993, 1994). Field experiments performed to control NO<sub>x</sub> emissions from a jet engine test cell at Tyndall AFB used MgO/v. Depending on the operational conditions, NO<sub>x</sub> removals were in the range from 40 to 70% (Nelson, 1992). The benefits of MgO/v as a NO<sub>x</sub> sorbent were several. Low cost, easier handling than wet materials, less start-up cost, and ease of scaling to various applications are some of the benefits. The cost of MgO/v is comparable to other high-volume usage sorbents. Kimm performed laboratory experiments on MgO/v (Kimm, 1995). Vermiculite was shown by Kimm to act essentially as a support material with minimal NO<sub>x</sub> interaction. Also, previous flue-gas studies had shown minor NO<sub>x</sub> interaction with vermiculite (Nelson, 1989). The formation of magnesium nitrate through sorption of NO<sub>2</sub> onto MgO/v was proposed by Kimm (1995). As vermiculite is a naturally occurring mineral that is commonly used as plant-potting material, the end product fertilizer consisting of magnesium nitrate and vermiculite was considered a useful product. Alternatively, the

regeneration of MgO/v was found to be possible by heating in a reducing atmosphere (Nelson, 1989).

#### NO<sub>x</sub> Sorption: MgO/v

Laboratory experiments by Kimm showed negligible removal of NO when it is the only NO<sub>x</sub> species present. Kimm's research suggested that only NO<sub>2</sub> removal is possible by MgO/v. Because field experiments indicated that NO is removed by sorption to MgO/v further tests to include the presence of other flue gas constituents were suggested. In addition, Kimm showed that NO<sub>2</sub> sorption resulted in a 1-to-3 ratio of NO production to NO<sub>2</sub> removal. He proposed the following sequential mechanism for the sorption of NO<sub>2</sub> to MgO/v:



Samples of MgO/v that were NO<sub>x</sub> saturated were further tested for nitrates using a nitrate-specific ion electrode. The results showed that saturated MgO/v samples accumulated a 3:2 molar ratio of NO<sub>2</sub> sorbed to nitrate formed. This ratio agrees with the above mechanism proposed by Kimm. In addition, Kimm showed that the saturation capacity of MgO/v utilized less than 2 percent of the magnesium oxide available. If the sorptive characteristics of MgO/v were to be improved additional studies of the material would be necessary. Based on the positive findings of Kimm and the growing interest in this application, additional studies were warranted to improve upon MgO/v as an effective NO<sub>x</sub> sorbent.

Based on research suggested by Kimm (Kimm, 1995) additional MgO/v testing was performed. Laboratory fixed-bed reactor studies were chosen to further describe the removal of NO<sub>x</sub> and the effects of other flue gas constituents. Given that Kimm observed no removal of NO when it was the only NO<sub>x</sub> species present, pre-oxidized NO<sub>x</sub> conditions were selected for experimentation. Experiments were repeated that showed no measurable interaction of gaseous NO with MgO/v.

Preparation procedures and physical properties of the MgO/v material are described by Kimm (1995). A measure of size distribution was performed to confirm Kimm's data. Also, reproducibility testing was performed to compare the data collected using the modified NO<sub>x</sub>-sorption system with the original data collected by Kimm. The reproducibility test results are compared to Kimm's data in Figure 3-1.

#### MgO/v: Internal Diffusion of NO<sub>x</sub>

Kimm notes that the MgO/v material is brittle and MgO powder easily breaks apart from the vermiculite substrate (Kimm, 1995). To test the possible effect of varied particle size on NO<sub>x</sub>, tests were performed at similar conditions on MgO/v samples that were sieved into five size categories. The results displayed in Figure 3-2 indicate that no significant differences in NO<sub>x</sub> removal occurred for the test conditions. Therefore, effects due to particles crumbling to smaller sizes during handling are considered to be insignificant. Problems did occur, however, from small sorbent particles that were carried with the sampled gas into the NO<sub>x</sub> analyzer causing clogging of the capillary tubes. Given the similar results for different particle sizes, a decreased particle size and thus, decreased bed volume for the same mass did not significantly affect NO<sub>x</sub> sorption. Therefore, internal (intra-pellet) mass transfer appeared to be negligible for the particle sizes

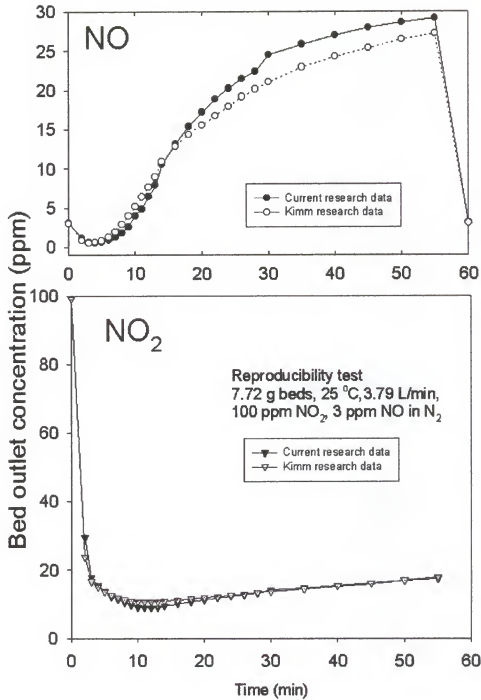


Figure 3-1. NO<sub>x</sub>-sorption test for MgO/v compared with Kimm's (1995) data.

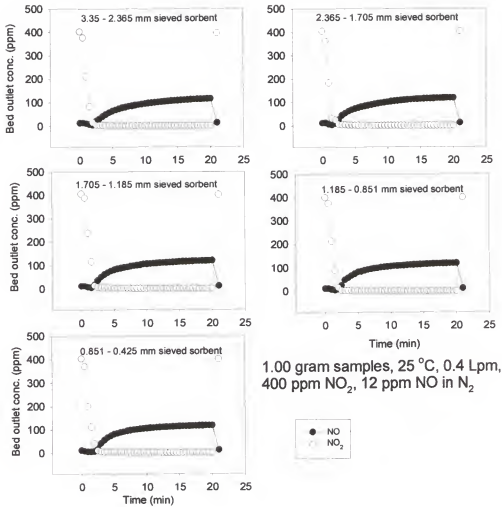


Figure 3-2. NO<sub>x</sub>-sorption tests for sieved MgO/v samples

investigated under these test conditions. In addition, this observation supports Kimm's findings that the sorption process is initially reaction controlled and therefore, diffusion into the particle is not rate limiting.

#### MgO/v: External Diffusion

External (inter-pellet) mass-transfer limitations were evaluated using a method suggested by Ruthven (1968). By varying the face velocity through a sorbent bed while keeping the residence time the same (increasing the volume of sorbent), then similar gas-solid interactions should occur if inter-pellet mass-transfer of the gas is minimized. The data obtained for these tests are presented in Figure 3-3. Kimm's findings for mass-transfer limitations are similar to those reported here (Kimm, 1995).

#### MgO/v: Sorption of NO

MgO/v was tested for the removal of gaseous NO. A gas stream consisting of 400 ppm of NO in nitrogen ( $N_2$ ) did not interact with MgO/v. This test supports those performed by Kimm. Discussions with personnel of companies applying this material (MgO/v) to control of NO<sub>x</sub> emissions suggested that the sorbent must be interacting with other gases to remove NO (Nelson et al., 1992). Field data consistently showed removal of NO (Nelson et al., 1994). Kimm's research had shown that only NO<sub>2</sub> was removed from gas mixtures containing NO, NO<sub>2</sub> and N<sub>2</sub>. NO<sub>x</sub> sorption/catalysts (CuO-alumina) required the presence of other gases, such as SO<sub>2</sub>, to perform reliably (Cooper and Alley, 1986). Other flue gas constituents were, therefore, considered for comparison testing with the NO<sub>x</sub>/MgO/v system.



### MgO/v: Effect of Water on NO<sub>x</sub> Sorption

Kimm suggested (Kimm, 1995) that future research on the effect of water additions to the NO<sub>x</sub>-sorbent system should be performed. A series of tests was performed to evaluate the effect of liquid water added to the sorbent material on NO<sub>x</sub> sorption from 50 to 200 °C over a range of flows measured in bed volumes per second (0.5, 1, and 2 bed vol/sec). The effect on NO<sub>x</sub> sorption was studied by increasing the fraction of deionized water added by spraying onto MgO/v in amounts from 5 to 25% w/w. Improved sorption of combined NO (50 ppm) and NO<sub>2</sub> (500 ppm) was observed at 50 and 200 °C (Figures 3-4, 3-5, 3-6, and 3-7, respectively). No interaction of NO (balance N<sub>2</sub>), when tested alone, was observed over the range of conditions used for these tests.

The maximum amount of added water (25% w/w) to the MgO/v sorbent sample was approximately equal to the amount of sample MgO on a stoichiometric basis. The addition of water was observed to delay NO production, as seen in Figures 3-4, 3-5, 3-6, and 3-7. However, NO<sub>x</sub>-sorption tests that saturated MgO/v at 200 °C indicated an increase in the amount of NO<sub>2</sub> uptake and a decrease in NO production (Figure 3-8). Possible interaction of NO<sub>2</sub> and bulk liquid water would explain additional NO<sub>2</sub> removal at temperatures below the boiling point (100 °C) of water. However, the saturation tests were performed at temperatures near 200 °C and, thus, a mechanism involving bulk liquid water does not seem possible.

Other researchers have studied similar group-II materials in this application, and have proposed that the interaction of NO<sub>2</sub> with these metal oxide surfaces is due to

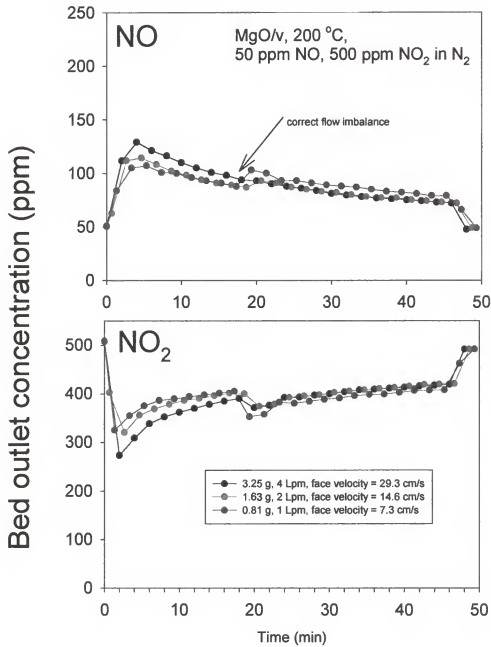


Figure 3-3. External mass transfer test for NO<sub>x</sub> sorption on MgO/v.

adsorbed bulk water (Nelli and Rochelle, 1996). Nelli and Rochelle proposed that nitrous acid formed by  $\text{NO}_2\text{--H}_2\text{O}$  interaction will further interact with additional  $\text{NO}_2$  to form nitric acid and NO. This mechanism is suggested to produce the observed NO. Furthermore, they proposed that  $\text{NO}_2$  interaction with basic surfaces, such as  $\text{Mg}(\text{OH})_2$ , allows the increased surface pH to prevent association of  $\text{H}^+$  and  $\text{NO}_2^-$  and thus delay NO production.

Additions of liquid water to dehydroxylated MgO has been shown to readily form  $\text{Mg}(\text{OH})_2$  species (Fiero, 1990). A monolayer of adsorbed  $\text{H}_2\text{O}$  readily forms when dehydroxylated MgO is exposed to water vapor at 20 °C. Adding water to MgO has been shown to increase hydrogen bonding and hydroxyl reaction. Based on this proposal, water added to a surface increases the surface hydroxyl concentration would increase  $\text{NO}_2$  uptake and increase, but delay, NO production.

Even though the reported dehydration temperature of  $\text{Mg}(\text{OH})_2$  is 350 °C, (CRC, 1992) [above 200 °C]  $\text{Mg}(\text{OH})_2$  should only delay NO production according to the mechanism of Nelli and Rochelle (1996). That no increase in NO production was observed in the latter study suggests that other interactions/mechanisms than those suggested by Nelli and Rochelle (1996) may occur. Given that water added to MgO/v can bind to MgO or vermiculite, speculation on an alternative mechanism seems reasonable. Alternative mechanisms include reactions involving species from sorbed/reacted water/vermiculite.

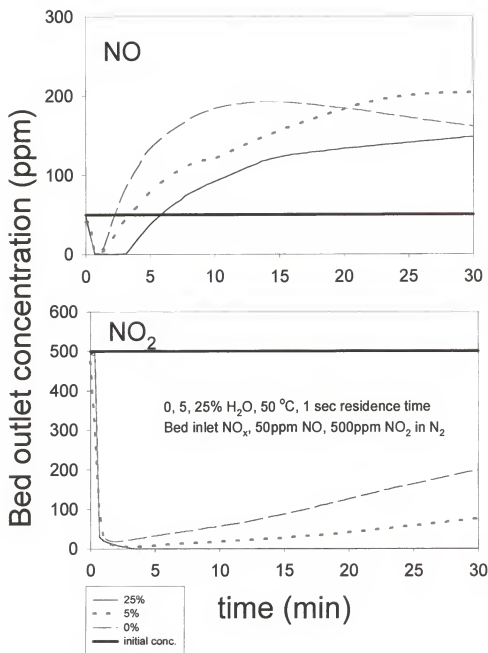


Figure 3-4. Variation of NO<sub>x</sub> sorption at 0, 5 and 25% water additions to MgO/v at 1-second residence time at 50 °C

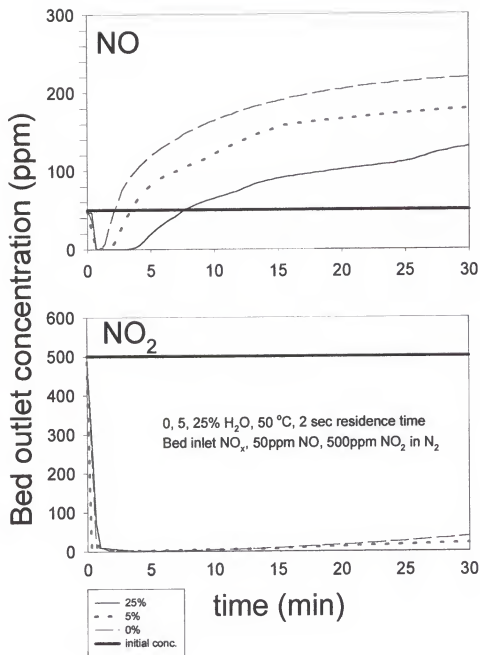


Figure 3-5. Variation of NO<sub>x</sub> sorption at 0, 5 and 25% water additions to MgO/v at 2-second residence time at 50 °C

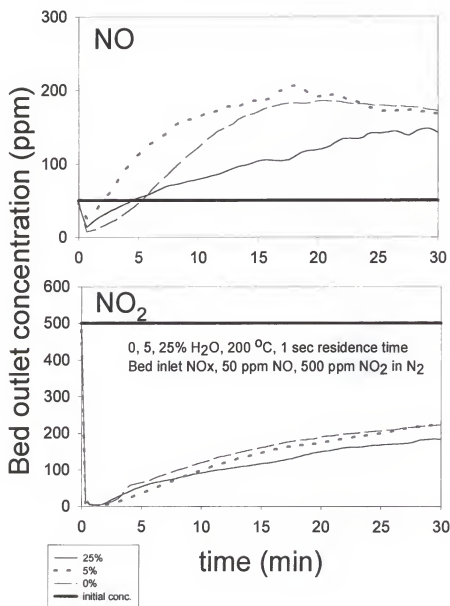


Figure 3-6. Variation of NO<sub>x</sub> sorption at 0, 5 and 25% water additions to MgO/v at 1-second residence time at 200 °C

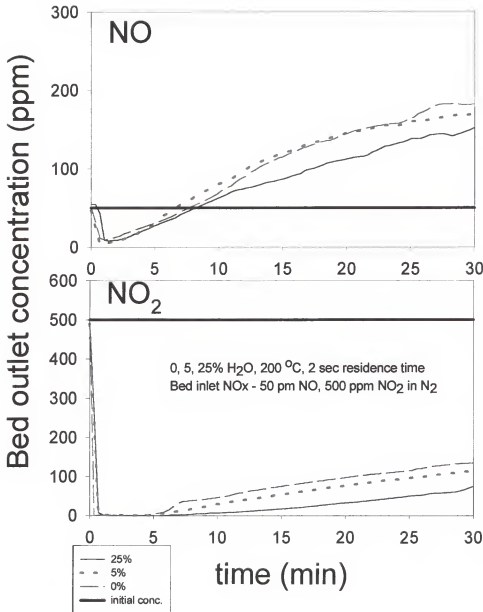


Figure 3-7. Variation of NO<sub>x</sub> sorption at 0, 5 and 25% water additions to MgO/v at 2-second residence time at 200 °C.

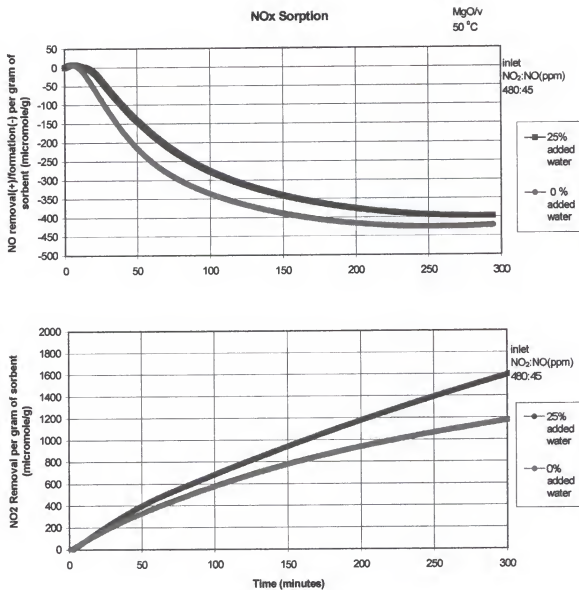


Figure 3-8. NO<sub>x</sub>-saturation study of MgO/v and added water at 200 °C.



### Comparison of MgO/v and Alumina Sorbents

A comparison of MgO/v and alumina ( $\text{Al}_2\text{O}_3$ ) sorbents was performed using the modified fixed-bed reactor system. Alumina was chosen for comparison with MgO/v because it has been extensively studied for similar pollutant gas/vapor control processes (Kirk-Othmer, 1992). Also, it is known to have superior sorption properties, it is a structurally more rigid material, and is widely available at comparable costs (Greenwood and Earnshaw, 1989). Alumina is a common material used for numerous industrial process applications from dehydration to catalysis. The material can be purchased in various structural and physicochemical forms. The gamma ( $\gamma$ ) form of alumina has a high surface area and is commonly used as a support for catalysts. Its high-surface area provides a high activity for reactions. In addition, pressure drop measurement for similar bed volumes showed that pelletized alumina had on average a 20% lower pressure drop than MgO/v (Tyler size 8 (3.35-2.37 mm) particles).

#### MgO/v vs. Alumina: NO<sub>x</sub> Sorption

Initial comparison tests of  $\text{Al}_2\text{O}_3$  and MgO/v were performed on equal-volume beds. The sorbents were sequentially exposed to a gas stream containing 500 ppm  $\text{NO}_2$  and 50 ppm NO in nitrogen at a temperature of 200 °C. The  $\text{NO}_2$  and NO bed outlet concentrations obtained as a function of NO<sub>x</sub>-exposure time are shown in Figure 3-9. Following an initial decrease to zero, the  $\text{NO}_2$  concentration in the stream leaving the MgO/v bed initially increases rapidly and then more slowly, attaining a value of about 430 ppm after 300 min. After initial fluctuations the NO concentration increases rapidly to a maximum of 190 ppm at 20 min and then decreases slowly to about 50 ppm, which is the

NO feed concentration. The fact that the NO concentration rises above 50 ppm indicates that some of the  $\text{NO}_2$  is converted into NO in the bed.

The untreated  $\gamma$ -alumina bed initially removes all  $\text{NO}_2$  from the gas stream and then the outlet  $\text{NO}_2$  concentration increases gradually to a value of 100 ppm at 300 min. Initially, the  $\gamma$ -alumina removes all of the inlet NO. The NO concentration increases fairly rapidly to a level near 200 ppm at about 100 min, indicating that  $\gamma$ -alumina also allows the formation of NO from  $\text{NO}_2$ . Untreated  $\gamma$ -alumina and  $\text{MgO/v}$  actively form significant quantities of NO while removing  $\text{NO}_2$ .

Given the much greater reactivity of the  $\text{Al}_2\text{O}_3$  for  $\text{NO}_x$  for the same bed volume, additional studies of the latter sorbent were warranted. Saturation tests of  $\text{NO}_x$  with alumina showed that overall a 3:1 ratio of  $\text{NO}_2$  uptake to NO production, similar to that for  $\text{MgO/v}$ , occurs on alumina. However, the amount of removal of  $\text{NO}_2$  by  $\text{Al}_2\text{O}_3$  is six times greater than  $\text{MgO/v}$  for similar volumes and exposure times. Measures of the surface area of  $\gamma$ -alumina by BET analyses was  $170 \pm 3 \text{ m}^2/\text{g}$ . Kimm found  $\text{MgO/v}$  to have a BET surface area of  $40 \text{ m}^2/\text{g}$ . Given that the saturated samples masses were 5.0 g of alumina and 1.0 g of  $\text{MgO/v}$ , a comparison by total amount of surface area is  $850 \text{ m}^2$  to  $40 \text{ m}^2$ , respectively. Despite the overall much higher surface area of the alumina used, alumina shows 20 % greater utilization per gram and thus, a smaller bed volume is required to obtain the same reactivity as  $\text{MgO/v}$ . In addition, the much greater structural integrity of alumina proved valuable for gravimetric measurement during initial and subsequent analyses. Also, the homogeneity of alumina proves valuable for preparing sorbents of similar characteristics.

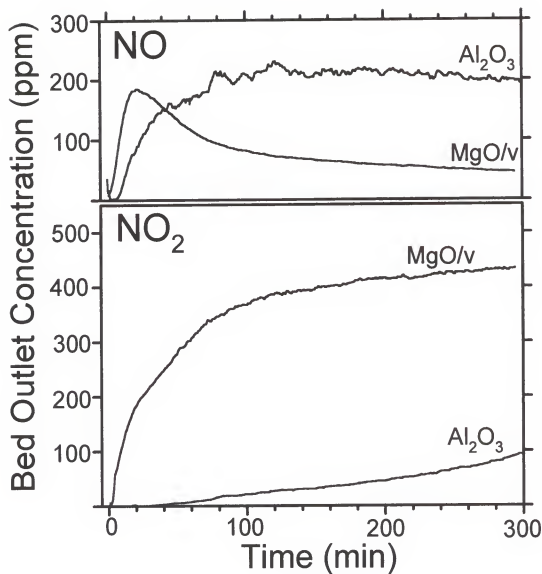


Figure 3-9.  $\text{NO}_x$  sorption by  $\text{MgO/v}$  and untreated  $\gamma$ -alumina ( $\text{Al}_2\text{O}_3$ ) on equal volume beds (Lee et al., 1998b).

### Formation of NO

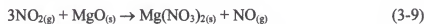
Results shown in Figures 3-9 and MgO/v saturation tests indicate that formation of NO is a by-product of NO<sub>2</sub> sorption on these materials. Nelli and Rochelle (1996) found that 3 mol of NO<sub>2</sub> sorbed to non-alkaline solids and suggested that reaction was with sorbed water to produce 2 mol of nitric acid and 1 mol of NO as follows:



yielding an overall equation



According to Nelli and Rochelle, the rate-limiting step is 3-5. Alkaline solids, such as Ca(OH)<sub>2</sub>, buffer the pH of the sorbent surface and delay the formation of NO. Also, Nelli and Rochelle suggest that alkaline materials [such as Ca(OH)<sub>2</sub>-coated sorbent] prevent HNO<sub>2</sub> and HNO<sub>3</sub> association and, thus, reduce NO production. Kimm et al.(1995) found that NO<sub>2</sub> sorption to MgO in the absence of oxygen formed NO in the same molar ratio of 3:1 (NO<sub>2</sub> uptake: NO production) and suggested that a 3-step process was involved. They suggested that the overall process was



Both mechanisms, which encompass a temperature range of 25 to 200 °C, also state that 3 moles of NO<sub>2</sub> are removed to form 2 moles of nitrate or nitric acid species (depending on pH) and 1 mole of NO. Boehm (1959) has explained the formation of nitrate ions resulting from NO<sub>2</sub> sorption on alumina as a result of a disproportionation of surface OH<sup>-</sup> ions with NO<sub>2</sub>:



The formation of NO via this mechanism agrees with observations of NO<sub>2</sub> sorption on other oxides and with the reported molar ratios for NO<sub>2</sub> removal to NO formation. Other materials such as AgO have been observed to produce NO from NO<sub>2</sub> sorption in a 3:1 molar ratio in a similar manner (Zemlyanov et al., 1998).

The active sites on alumina are described (Sicar, 1980) as basic (hydroxyl and O<sup>2-</sup> anion vacancies) and acidic (unsaturated Al<sup>3+</sup> ions as Lewis and protonated hydroxyl ions as Brönsted acid) sites of various strengths and concentrations. The hygroscopic natures of alumina and MgO have been well documented (Peri, 1965; Knozinger, 1976; Knozinger and Ratnasamy, 1976; Coster and Fripiat, 1995; Sircar et al., 1996) which are known to significantly influence their reactivity. At 50 % relative humidity, activated alumina can adsorb up to 15 % of its own weight of water (CRC, 1980) and a monolayer of surface hydroxyl species can exist on its surface at temperatures of up to 500 °C (Peri, 1965). Thus, the reaction of NO<sub>2</sub> with alumina at the temperatures used in these experiments

(200 °C) could involve sorbed water molecules and may be explained by either reaction (3-8) or (3-10). While these reactions are possible for the sorption of NO<sub>x</sub> on untreated alumina, NO<sub>x</sub> removal by alkali-treated alumina appears to differ substantially in terms of NO<sub>2</sub> sorption rates, saturation capacity and NO production, as discussed previously.

### Initial Studies of Untreated and KOH-Treated $\gamma$ -Alumina

#### Different Sources of $\gamma$ -Alumina

Three different sources of  $\gamma$ -alumina provided sorbent materials for study. The three types of material were obtained from Fisher Scientific Inc. (catal. #, A948 (acid), A941 (basic), and A945(neutral), Pittsburgh, Pennsylvania), Englehard Inc., (catal. # T-3438, Elyria, Ohio), and Edwards High Vacuum Inc., (catal. # H02600055, Liverpool, England).

Fisher Scientific alumina have a Brockman activity of I, meaning the material is heated to have approximately 0% moisture prior to packaging.  $\gamma$ -Aluminas were obtained in three forms described as neutral, acidic, and basic. The manufacturer describes the reactive acidity by suspending the alumina in an 5% w/w aqueous solution and measuring the pH with a hydrogen-ion electrode after 5 minutes. These different acidities are created by adding HCl gas in precise amounts. The three forms (1-gram samples) were tested in this laboratory for the change of the pH of an aqueous solution (50 mL) due to the addition of the alumina. All three materials changed the solution pH as expected (acid, pH 4; neutral, pH 7; base, pH 10). Considering the behavior of the different forms of alumina

as Brönsted acidity, the basic alumina must act in aqueous solution to either extract hydronium ions from solution or release hydroxyl groups.

The materials were individually tested to determine the effect of sorbent acidity on the process of NO<sub>x</sub> sorption. The powdered materials were individually placed inside the sorbent reactor tubes supported on glass fiber wool. A 4-gram portion of each type of powder was exposed to 500 ppm NO<sub>2</sub> and 500 ppm NO at ambient temperature. The amounts of NO<sub>2</sub> and NO accumulated per sample mass obtained as a function of exposure time are shown in Figure 3-10. All materials showed similar results. Complete removal of the input NO<sub>2</sub> is observed during the exposure period. The NO concentration increases indicating a formation of NO. This increase is due to NO<sub>2</sub> sorption followed by its partial conversion to NO. The proposed equation describing the sorption of NO<sub>2</sub> to MgO discussed previously indicates a 1:3 molar ratio of NO produced to NO<sub>2</sub> sorbed. The removal of NO<sub>2</sub> and formation of NO for all Fisher Scientific alumina materials indicates the same 3:1 molar ratio as that observed for MgO/v. The most interesting feature is that the production of NO is not affected by the acidity of the alumina. The bonding structure of the three forms of alumina is designed to alter the *pH* in aqueous solution. Alumina normally contains some bound hydroxyl groups and bulk water at ambient conditions.

According to Nelli and Rochelle, the formation of NO is based on the surface pH such that a “basic” surface will prevent the association of surface nitrites and nitrates and therefore delay NO production. However, the basic form of alumina did not delay the production of NO. The latter test was performed at ambient conditions and thus the solid alumina should contain some sorbed water and related hydroxyl groups. As no delay in NO production was observed, either the production of NO from the surface is not based

on its acidity or basicity alumina does not interact with  $\text{NO}_2$  in a similar manner as alkaline materials. Alumina samples from the different manufacturers were tested to determine if significant differences in the sorption of  $\text{NO}_x$  are apparent. Preliminary tests showed inefficient  $\text{NO}_2$  sorption by the Edwards High Vacuum spherical pellets. The Fisher Scientific alumina sample was shown to remove all  $\text{NO}_2$ , produced NO in the proposed stoichiometry, and provided evidence supporting the proposed mechanism of reaction. A comparison of the three different manufacturer's materials was made by exposing all three materials to completely remove input  $\text{NO}_2$  for a known period of time. If the production of NO is observed to be similar then additional evidence for the proposed stoichiometry would be obtained. To provide complete removal of  $\text{NO}_2$  by the three different alumina samples the Englehard and Edwards High Vacuum materials were crushed to fine powders using a marble pestle and mortar. The material was crushed and passed through a Tyler size 200 sieve to remove larger particles. Additional  $\text{NO}_x$ -sorption testing showed that the 4-gram portion of Edwards crushed powder would not provide complete removal of  $\text{NO}_2$ . Therefore, the  $\text{NO}_x$  sorption of the three materials was performed with different material masses to ensure complete  $\text{NO}_2$  removal. The accumulated removals of  $\text{NO}_2$  and NO by the three different materials are shown in Figure 3-11. All three materials show a similar 3:1 molar ratio of  $\text{NO}_2$  sorbed to the NO formed.



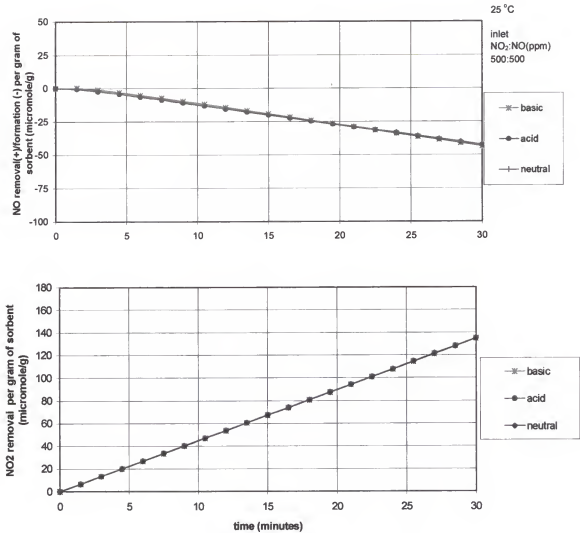


Figure 3-10. Sorption of NO<sub>x</sub> to Fisher Scientific<sup>®</sup>, acid, basic and neutral “pH” forms of alumina.

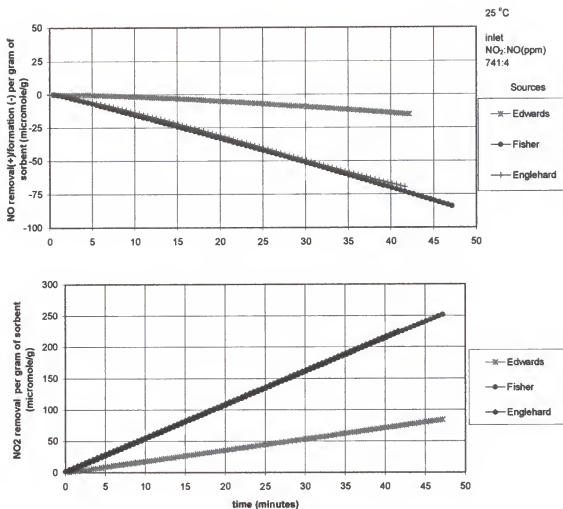


Figure 3-11.  $\gamma$ -Alumina from different sources exposed to NO<sub>2</sub>.

### Alumina: Removal of Gaseous NO

Tests on alumina similar to those for MgO/v were performed for the sorption of gaseous NO (400 ppm) alone at 25 and 250 °C. No interaction of gaseous NO with alumina was observed. As discussed in the experimental section, simulated preoxidized NOx conditions (high NO<sub>2</sub>, low NO) were used for all sorption tests. The molar ratio of input NO<sub>2</sub>:NO for testing was varied for certain tests. However, the general premise behind effective NOx sorption remains that initial conversion of NO into NO<sub>2</sub> is essential. A series of tests was performed which altered the ratio of NO<sub>2</sub>:NO and the effect on NOx sorption studied. These tests are discussed later.

### X-ray Photoelectron Spectroscopy (XPS) Analysis of Untreated $\gamma$ -Alumina

Unexposed alumina and a NOx-saturated alumina sample were analyzed by X-ray photoelectron spectroscopy (XPS). Survey spectra are shown in Figures 3-12 a and b. Peak assignments pertain to both spectra. The spectra show Al (2s and 2p), C (1s), and O (1s and 2s) peaks. The C (1s) peaks in both spectra are probably due to the presence of about a 2% graphite component from the manufacturing process. The N-(1s) peak is apparent only after NOx exposure in Figure 3-12 b. The small K (2p) peak in Figure 3-12 a is enhanced after exposure to NOx in Figure 3-12 b. Potassium has been identified as a common contaminant in aluminum foils (Jimenez-Gonzalez, 1991). Observation of this significant increase in the K-(2p) peak after chemical interaction between a surface K compound and NOx, provides justification for examining the effects of pretreating  $\gamma$ -alumina with a potassium compound.

Krizek (1966) evaluated absorption of  $\text{NO}_2$  by aqueous KOH and found that potassium nitrite is formed. Also, he found that aqueous KOH more efficiently absorbs  $\text{NO}_2$  than aqueous NaOH, although the latter has been used for ambient  $\text{NO}_2$  measurement in past EPA reference methods (Jacobs and Hochheiser, 1965), and for  $\text{NO}_x$  flue-gas measurements (Himi and Muramatsu, 1969). Furthermore, Nelli and Rochelle suggested that an alkaline solid, such as  $\text{Ca}(\text{OH})_2$ , moderates the surface acidity. The surface of the  $\text{Ca}(\text{OH})_2$ -buffered sorbent has enough alkaline sites to keep  $\text{HNO}_2$  and  $\text{HNO}_3$  dissociated, thereby minimizing the production of gaseous NO. Since this previous research has shown that hydroxide compounds can reduce the production of NO, and XPS studies suggest that K compounds and  $\text{NO}_x$  interact, KOH was chosen for treatment of  $\gamma$ -alumina.

#### KOH-Treated $\gamma$ -Alumina: Initial Testing

Given the observed interaction of potassium species with  $\text{NO}_x$ , potassium hydroxide (KOH) was coated onto alumina from solution of various concentrations by methods of impregnation and of precipitation. KOH-treated  $\gamma$ -alumina was tested for  $\text{NO}_x$  removal under conditions similar to those used for comparing  $\text{MgO}/\text{v}$  and untreated alumina. The  $\text{NO}_x$  exposure data obtained for untreated  $\gamma$ -alumina, KOH-impregnated  $\gamma$ -alumina, and KOH-precipitated  $\gamma$ -alumina are shown in Figure 3-13. All three sorbent beds yield very low outlet  $\text{NO}_2$  concentrations for the first 40 min of  $\text{NO}_x$  exposure. After 40 min the outlet  $\text{NO}_2$  concentrations are minimal and the same, within experimental error, for KOH-impregnated and -precipitated  $\gamma$ -alumina, and gradually increase to 50 ppm at 300 min. The KOH-impregnated  $\gamma$ -alumina NO outlet concentration

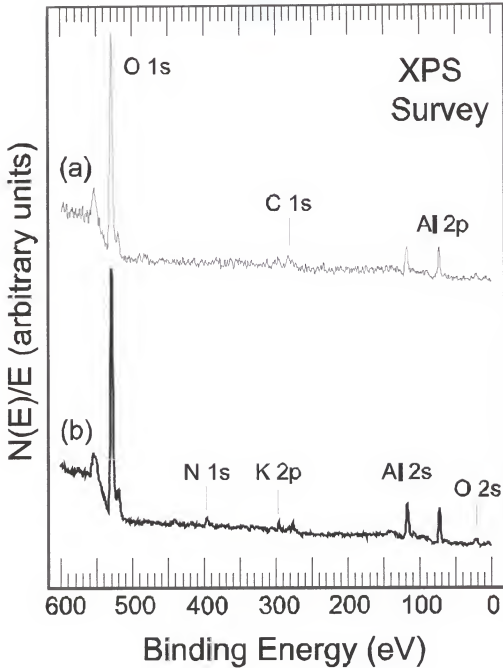


Figure 3-12. XPS survey spectra obtained from (a) fresh and (b)  $\text{NO}_x$ -saturated  $\gamma$ -alumina pressed powder samples (Lee et al., 1998b). Assignments made pertain to both spectra.

indicates removal of NO for the first 140-min exposure period but increases to about 150 ppm at 300 min, which is lower than that for untreated  $\gamma$ -alumina. KOH-precipitated  $\gamma$ -alumina removes nearly all the input NO over the time period examined. KOH-precipitated  $\gamma$ -alumina exhibits a 90% removal of both NO and NO<sub>2</sub> at 300 min, at which time approximately 12 mol (300 L) of NO<sub>x</sub>-containing gas has been treated.

XPS survey spectra obtained from the unexposed KOH-impregnated and NO<sub>x</sub>-saturated KOH-impregnated  $\gamma$ -Al<sub>2</sub>O<sub>3</sub> are shown in Figures 3-14 (a) and (b) respectively. Peak assignments in Figure 3-14 pertain to both spectra. The Al-(2s and 2p), C-(1s), O-(1s and 2s), and K-(2p) peaks are apparent in these spectra. The surface carbon content of this sample is large since the C-(1s) peak is similar in size to the aluminum peaks and carbon has a low XPS sensitivity.

The K (2p) peak is enhanced after exposure to NO<sub>x</sub>, as observed in Figure 3-14 (b). This is consistent with the XPS data obtained from untreated alumina (Figure 3-12). The N (1s) peak is barely apparent after the NO<sub>x</sub> exposure. XPS survey spectra obtained for the unexposed 1-M KOH-precipitated and NO<sub>x</sub>-saturated KOH-precipitated  $\gamma$ -Al<sub>2</sub>O<sub>3</sub> are shown in Figure 3-15 (a) and (b) respectively. Before NO<sub>x</sub> exposure the survey spectrum is quite similar to that obtained from the unexposed KOH-impregnated  $\gamma$ -alumina except that this surface appears to contain less carbon. After NO<sub>x</sub> exposure, very prominent K (2p and 2s) and N (1s) peaks are apparent, and the C (1s) peak height also is increased.

High-resolution N (1s) spectra obtained from unexposed KOH-precipitated and KOH-precipitated, NO<sub>x</sub>-saturated  $\gamma$ -Al<sub>2</sub>O<sub>3</sub> samples are shown in Figure 3-16 (a) and (b),

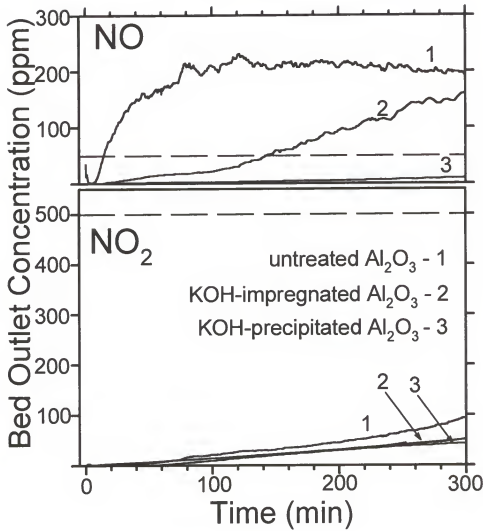


Figure 3-13. Bed outlet NO and  $\text{NO}_2$  concentrations as a function of time for untreated and KOH-treated  $\gamma$ -alumina (Lee et al., 1998b).

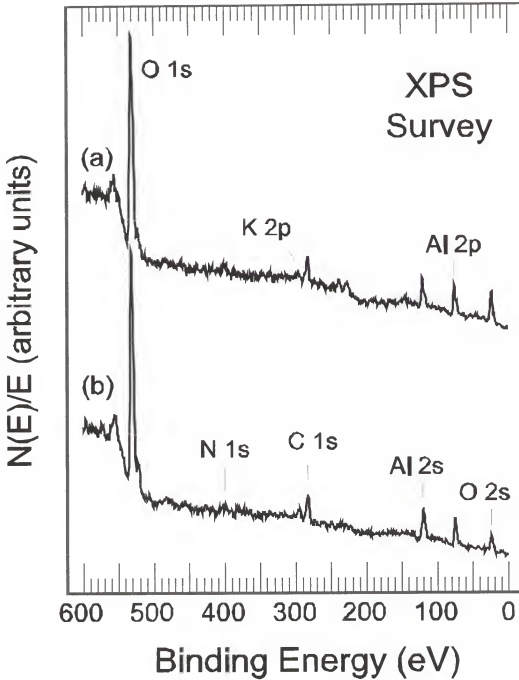


Figure 3-14. XPS survey spectra obtained from (a) KOH-impregnated and (b) NO<sub>x</sub>-saturated KOH alumina pressed powder samples (Lee et al., 1998b). Assignments made pertain to both spectra.



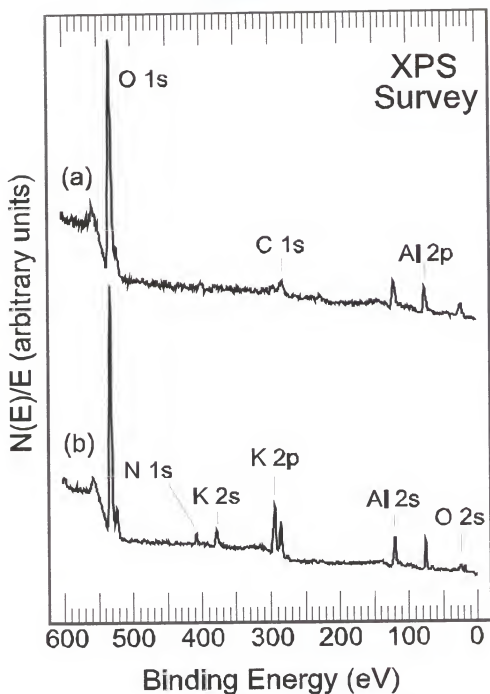


Figure 3-15. Unexposed (a) and  $\text{NO}_x$ -saturated (b) KOH-precipitated  $\gamma\text{-Al}_2\text{O}_3$  pressed powder samples (Lee et al., 1998b). Assignments made pertain to both spectra.

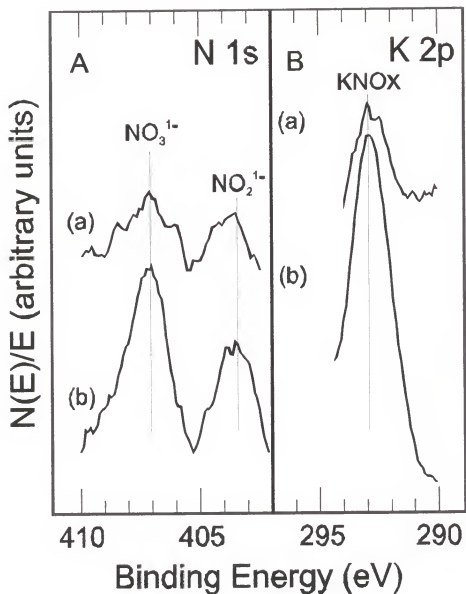


Figure 3-16. XPS (A) N 1s and (B) K 2p spectra obtained from (a) KOH-precipitated and (b) NOx-saturated KOH-precipitated alumina pressed powder samples (Lee et al., 1998b).

respectively. The presence of nitrate and nitrite chemical states are clearly observed. The  $\text{NO}_3^-:\text{NO}_2^-$  ratios are approximately 1.5:1 and 2.0:1, respectively, in (a) and (b), indicating that more nitrate forms during the  $\text{NO}_x$  adsorption. The K (2p) feature is significantly increased in size after  $\text{NO}_x$  exposure similar to the N (1s) features. The K (2p) peaks suggest that it is present as nitrate and/or nitrite before and after the  $\text{NO}_x$  exposure, but it may be present as hydroxide before exposure.

As stated previously, Nelli and Rochelle (1996) proposed that a  $\text{Ca}(\text{OH})_2$ -buffered sorbent is basic enough to keep  $\text{HNO}_2$  and  $\text{HNO}_3$  dissociated. They assume that decompositions of  $\text{HNO}_2$  and  $\text{HNO}_3$  are rate limiting in the mechanism for the overall reaction. Even though buffering compounds such as  $\text{Ca}(\text{OH})_2$  or KOH keep  $\text{HNO}_2$  and  $\text{HNO}_3$  dissociated, results of Nelli and Rochelle demonstrate that NO is eventually formed with continued exposure to  $\text{NO}_2$ .

Results of saturation testing in the fixed-bed reactor system containing  $\gamma$ -alumina, in both untreated and treated forms, are shown in Table 3-1. The saturation capacity is defined as that exposure condition at which the bed  $\text{NO}_x$  outlet concentration does not differ by more than 5% from the inlet concentration. These tests were conducted at the same temperature and  $\text{NO}_x$  concentration used in previous tests. However, to conserve cylinder gas resources, smaller sorbent sample masses (5 grams) were used. Preliminary tests indicate that the ratio of  $\text{NO}_2$  removed per unit sample mass does not vary for different sample masses of untreated alumina saturated with  $\text{NO}_x$ . The amount of  $\text{NO}_2$  removed per unit amount of added KOH is reduced with increased KOH added. BET surface area measurements indicate that the surface area is reduced as the KOH added is

Table 3-1. NO<sub>x</sub> saturation capacity of untreated and KOH-treated  $\gamma$ -alumina (Lee et al., 1998b).

| $\gamma$ -alumina | sorbed NO <sub>2</sub><br>per NO<br>formed<br>(mmol/mmol) | mass of KOH<br>(w/w% of<br>sample) | mol of sorbed<br>NO <sub>2</sub> /mol of<br>KOH | BET surface<br>area (m <sup>2</sup> /g)<br>nonexposed | BET surface<br>area (m <sup>2</sup> /g)<br>NO <sub>x</sub> sat. |
|-------------------|---|------------------------------------|---|---|---|
| untreated         | 1.5/0.54  | 0                                  | ---   | 170   | 170   |
| KOH-impreg        | 1.96/0.65   | 0.1 g (2%)                         | 1.1   | 163   | 154   |
| KOH-precipitat    | 7.8/2.4   | 0.96 g (20%)                       | 0.44  | 98  | 39  |

increased and that NO<sub>x</sub> exposure further reduces the surface area, which explains the reduction in efficiency. The increased molar volume of nitrate species formed by NO<sub>x</sub> sorption has also been suggested as a reason for reduced efficiency (Kimm, 1995).

#### KOH Treatment Parameters: NO<sub>x</sub>-Sorption Effects

The maximum KOH solution concentration that could be applied homogeneously to  $\gamma$ -alumina was found to be 1 g-mol/L (1 *M*). Alumina precipitated in a 2-*M* KOH solution showed a significant decrease in NO<sub>x</sub> removal when compared to using a 1-*M* solution. From tests of NO<sub>x</sub> sorption on treated Al<sub>2</sub>O<sub>3</sub>, a trend was observed of increased NO<sub>x</sub> removal with increased solution concentrations up to 1 *M* KOH. However, KOH-coated alumina that was prepared using lower-concentration solutions but more solution volume and acquired equal added KOH mass from the treatment. These KOH-treated sorbents performed similarly in NO<sub>x</sub>-sorption testing as shown in Figure 2-6. In addition, if the method of treatment [impregnation or precipitation] resulted in similar mass additions, no significant difference of sorption characteristics for NO<sub>x</sub> is observed. Therefore, the change in NO<sub>x</sub> sorption by KOH treatment proved to be a simple factor of KOH coating mass. An effective maximum addition of KOH to Al<sub>2</sub>O<sub>3</sub> was found to be near 20% w/w alumina and was limited by macroscopic surface deterioration and decreased NO<sub>x</sub> sorption at higher levels. Further addition of KOH produced a weakly bound coating layer that flaked off when handled (i.e., mechanically unstable). This observation was visible to the naked eye and was studied with a microscope (Bausch and Lomb, Rochester, NY). Concern was raised over the effect of hydration on the sorbent as KOH is a highly hygroscopic material. Samples of treated alumina were exposed to

ambient conditions and observed through a microscope over a period of one month. Samples of  $\gamma$ -alumina coated with greater than 1-M KOH solution immediately after coating were observed to be brittle and cracks covered the pellets in comparison to untreated samples. During the month of observations the samples coated with 20% w/w (or less) appeared to maintain a consistent surface integrity.

Preparation variables in the drying atmosphere employed for KOH coatings were varied to evaluate their effect on NO<sub>x</sub> sorption. In order to test the effect of the drying atmosphere an inert gas, argon, was chosen. A cylinder of research-grade argon (Bi-Tec Southeast, Inc., Tampa, Florida) was used to supply a 10-mL/min flow into a Griffin beaker containing a preparation slurry of the alumina pellets and KOH solution during the baking process. The flow of argon was assumed to replace the lighter ambient air in the void space above the slurry. After baking, the samples were tested similarly for NO<sub>x</sub> sorption. No measurable difference in NO<sub>x</sub> sorption was observed due to preparation in an argon atmosphere when compared to ambient air.

The effect of baking temperature was compared from 100 to 300 °C. Samples of prepared slurry were dried at different temperatures for 24 hours and subsequently NO<sub>x</sub>-sorption tested. Preparing the sorbent at drying temperatures between 100 and 300 °C did not appear to affect NO<sub>x</sub> sorption characteristics. Drying the sorbent at temperatures above 400 °C showed that the alumina pellets became white. Loss of carbon, is suspected to cause the color to change from black to white, which occurred at the temperatures tested from 400 to 800 °C. Alumina manufactured without binder material is white. In addition, the time of drying at these elevated temperatures was a factor in the degree of

change in color. Literature on the properties of  $\gamma$ -alumina suggest that the form of  $\gamma$ -alumina will change to a lower surface-area material such as  $\alpha$  (alpha)-alumina upon heating to temperatures above about 500 °C.

The time of baking at 150 °C was tested for KOH-treated alumina at 12, 24, 48, and 316 hours. Portions of one batch of KOH-treated alumina were removed at the selected time intervals and stored in air-tight containers prior to testing. Portions of samples from each time interval were divided and thrice NO<sub>x</sub>-sorption tested. After all of the material was prepared, samples were tested in random order of bed placement within the triple-bed reactor to examine possible testing errors. The results indicate that NO<sub>2</sub> sorption is unaffected by the time of drying but that NO sorption is enhanced for the samples dried 12 hr. The observed increased removal of NO for the 12-hr preparation sample may be due to changes in surface properties during treatment. Even though a specific reason to explain this effect has not been found, at longer drying times the material appears to stabilize and become more reproducible.

Given that the method of treatment and the time of drying (> 24 hrs.) were found to be inconsequential, preparations of varied coating amounts onto alumina using the latter reproducible conditions were selected in further studies.

#### Studies of Group-I Treated $\gamma$ -Alumina

Although previous researchers have studied NO<sub>x</sub> removal by  $\gamma$ -alumina treated with various chemicals (Haslbeck et al., 1985; Nelli and Rochelle, 1989; Ma et al., 1995) and NO<sub>x</sub> sorption has been achieved using aqueous solutions of alkaline materials (American Public Health Association, 1939-40; Jacobs and Hochheiser, 1958; Krizek,

1966), it seemed that further evaluation of potential coating treatments was warranted. Carbonates, sulfates, and hydroxides of sodium and potassium were studied as potential coating treatments for alumina. Two types of treatment techniques, impregnation and precipitation, were evaluated for consistency in providing stable added mass and observations were made of adhesion and physical changes resulting from the treatment process used. Treatment by impregnation showed that the added mass varied with solution concentration. However, volumes of solution greater than four times the bulk volume of alumina pellets did not appear to further increase the added mass in impregnation treatments. For precipitated samples, the added mass was a simple function of the volume of solution used to treat the pellets. Observation of precipitation-treated alumina samples showed carbonate- and sulfate-treated samples were limited due to shedding and flaking at high loading, whereas solutions more dilute than 0.04 *M* deposited so little material that the weight difference was obscured by gravimetric measurement error. Tests were performed to study NO<sub>x</sub> sorption by alumina, when treated with one of the treatment chemicals listed above either by precipitation or impregnation and producing an equal amount of added coating mass but from solutions of different concentrations.

Tests of alumina samples treated with different added masses of coating material under similar conditions for the sorption of NO<sub>x</sub> are shown in Figures 3-17 to 3-20. Data for sulfate-treated alumina samples are not included because the tests showed very low NO<sub>x</sub> removal capacity in comparison with other coatings. Each treatment material was tested using three different amounts of coating material. Typical reproducibility data for this study are included for the KOH-treated alumina in Figure 3-17. Also, in Figure 3-17,



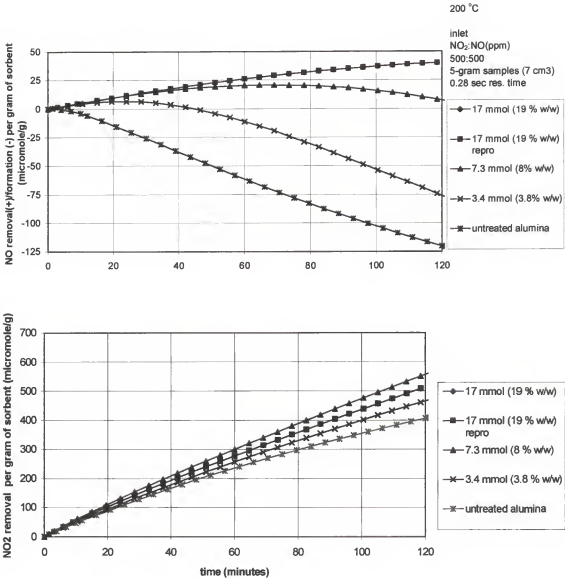


Figure 3-17. NO<sub>x</sub> sorption by KOH-treated and untreated alumina samples at 200 °C.

Note mmol (millimole) refers to the amount of treatment material on  $\gamma$ -alumina, “% w/w” indicates the percent of the total sample mass.

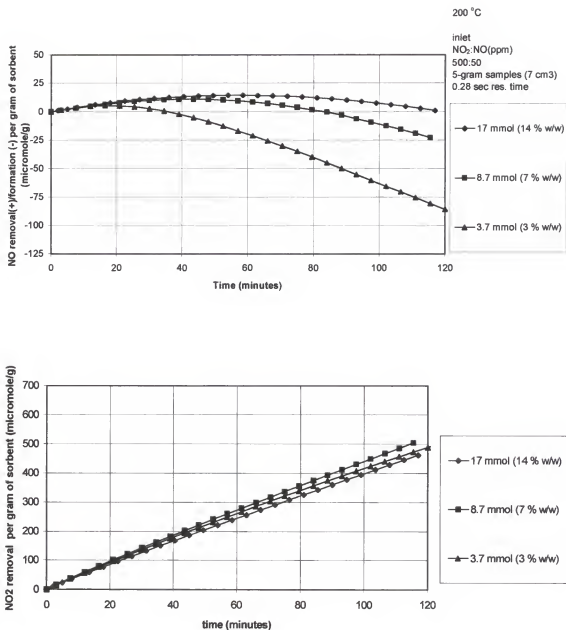


Figure 3-18.  $\text{NO}_x$  sorption by NaOH-treated alumina samples at 200 °C.

Note mmol (millimole) refers to the amount of treatment material on  $\gamma$ -alumina, “% w/w” indicates the percent of the total sample mass.

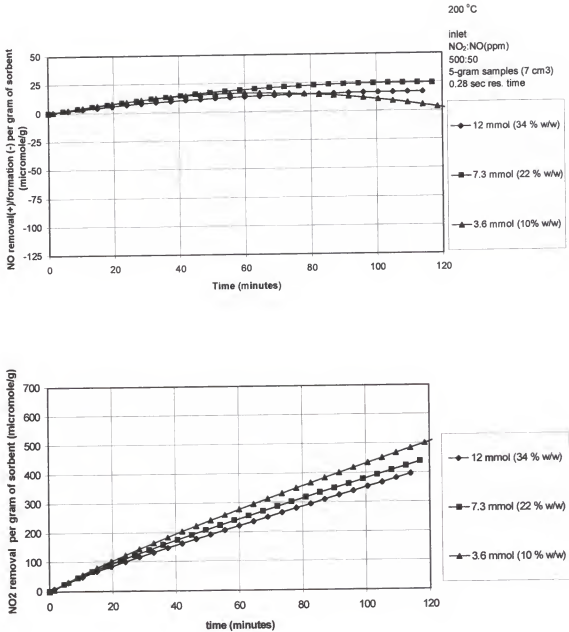


Figure 3-19. NO<sub>x</sub> sorption by K<sub>2</sub>CO<sub>3</sub>-treated alumina samples at 200 °C.

Note mmol (millimole) refers to the amount of treatment material on  $\gamma$ -alumina, “% w/w” indicates the percent of the total sample mass.

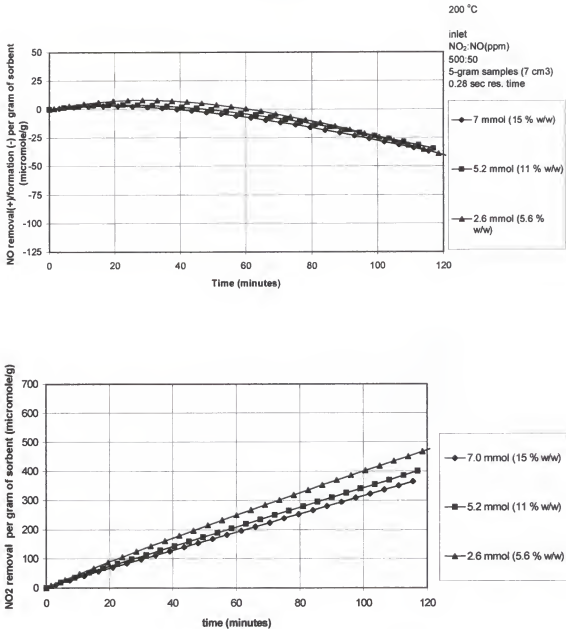


Figure 3-20. NO<sub>x</sub> sorption by Na<sub>2</sub>CO<sub>3</sub>-treated alumina samples at 200 °C.

Note mmol (millimole) refers to the amount of treatment material on  $\gamma$ -alumina, “% w/w” indicates the percent of the total sample mass.

KOH treatment data includes the sorption behavior of untreated alumina. Each treatment material includes the response for the maximum amount of added mass that provided for best binding to alumina. Best binding for each treatment was defined by shaking the tested pellets in a sieve and observing a minimum percent weight loss of the pellets per mass of coating. The minimum weight loss was about 5–1% depending on the coating examined. In addition, pellets were initially visually observed after preparation for the quality of coating to alumina.

For hydroxide treatments (Figures 3-17 and 3-18), the removal of NO is maximized for the highest quantity of coating but NO<sub>2</sub> removal is a maximum for the intermediate coating. Carbonate-treated alumina (Figures 3-19 and 3-20) shows increasing NO<sub>2</sub> removal with decreasing quantity of coating, yet the lowest coating mass shows increasing NO formation. This suggests that the formation of NO by carbonate-treated alumina is directly proportional to the removal of NO<sub>2</sub>. However, studies of initial sorption rates show that the fraction of NO<sub>2</sub> removed is not proportional to the percent of coating increase for both hydroxides and carbonates. In comparing NO<sub>x</sub> sorption by potassium hydroxide and carbonate for treatment using equimolar amounts (7 mmol), removal of NO by K<sub>2</sub>CO<sub>3</sub> is significantly better, while superior NO<sub>2</sub> removal is provided by KOH. On a per-mole basis, potassium compounds generally show better NO removal than sodium compounds under the testing conditions. Variation of NO removal per added amount of hydroxide coating is greater than for carbonate coatings. In comparing NO<sub>x</sub> sorption by untreated and treated alumina, decreasing the mass treatments for all chemicals show a gradual trend toward the behavior of untreated alumina. The trend in

NO formation for different coating materials relative to that of untreated alumina is greatest for hydroxides. The greatest combined removal of NO and NO<sub>2</sub> (NO<sub>x</sub>) was achieved by KOH-treated (17 mmol) alumina.

#### NO<sub>x</sub> Sorption: Temperature Effects

The temperature of the sorbent bed was varied from 100 to 200 °C to evaluate changes in the rates of NO<sub>x</sub> sorption as a function of temperature (Figures 3-21 through 3-24). Two effects are seen from the data shown in these figures, the small overall change in NO<sub>2</sub> sorption rate with temperature and the difference in the rates of NO<sub>2</sub> removal for sodium and potassium-compound treatments. The decreases in the rates of NO<sub>2</sub> removal with an increase in temperature from 100 to 200 °C are small and consistent for all coating materials. This suggests that the process may have a small negative or zero activation energy or that the end product is not thermally stable, as indicated by the production of NO.

#### NO<sub>x</sub> Sorption: Concentration Effects

Tests performed to evaluate the effects of treatment mass and temperature were carried out with different concentrations of NO. Operating conditions for these evaluations were the same except for NO concentration. Comparisons of concentration effects on the sorption of NO<sub>x</sub> are shown in Figures 3-25 and 3-26. The amount of treatment in the temperature-evaluation (Figures 3-21 through 3-24) was similar for all materials at 20% by mass. These treatment masses of KOH and K<sub>2</sub>CO<sub>3</sub> are within the range of treatments used in the mass evaluation shown in Figures 3-17 through 3-20. Therefore, the effect of lowering inlet NO concentration in the NO<sub>x</sub> sorption process for KOH and K<sub>2</sub>CO<sub>3</sub> treatments can be observed from the data in Figures 3-17 and 3-21, and

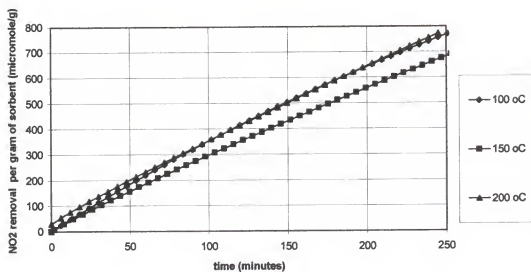
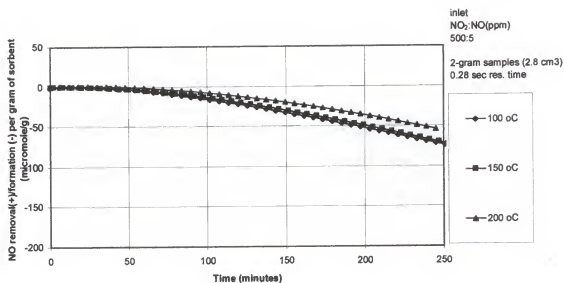


Figure 3-21. Effect of temperature on NO<sub>x</sub> sorption by KOH-treated alumina.

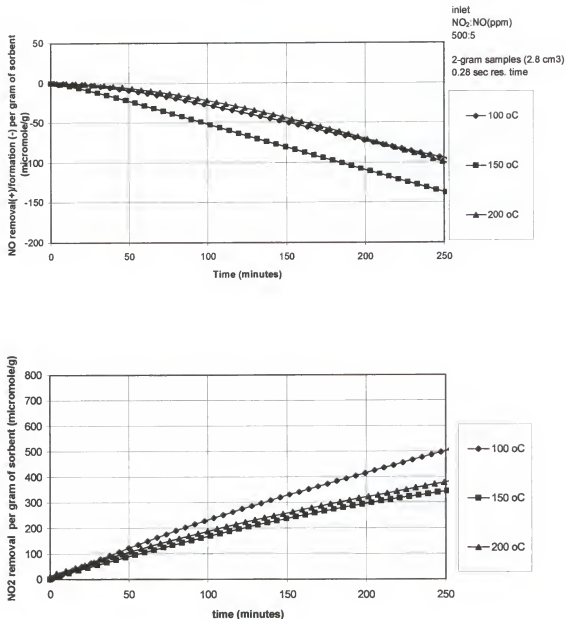


Figure 3-22. Effect of temperature on NO<sub>x</sub> sorption by NaOH-treated alumina.



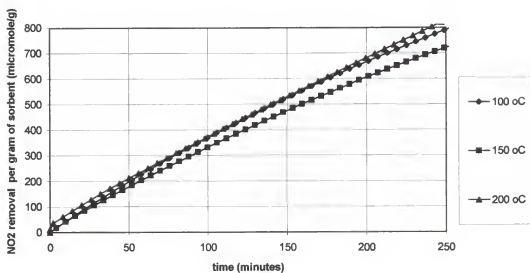
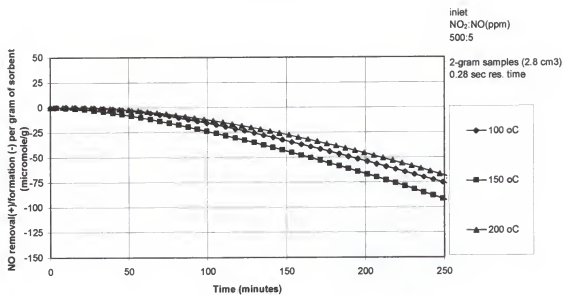


Figure 3-23. Effect of temperature on NO<sub>x</sub> sorption by K<sub>2</sub>CO<sub>3</sub>-treated alumina.

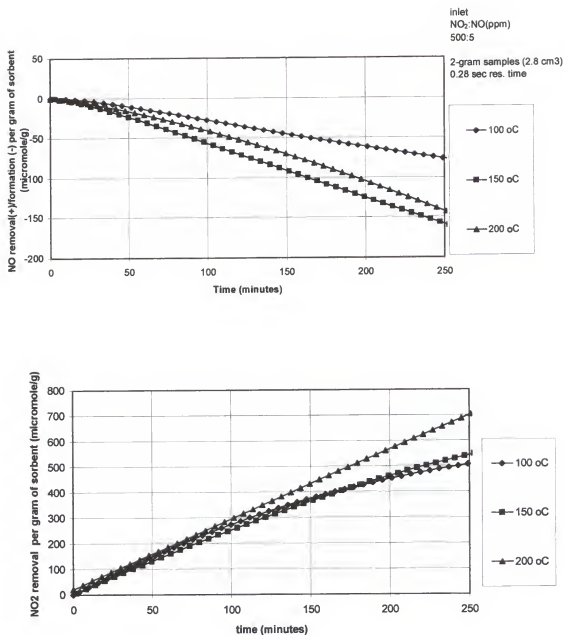


Figure 3-24. Effect of temperature on NO<sub>x</sub> sorption by Na<sub>2</sub>CO<sub>3</sub>-treated alumina.

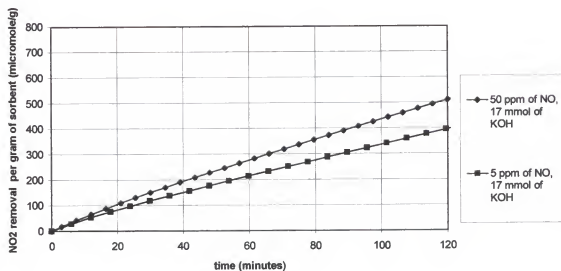
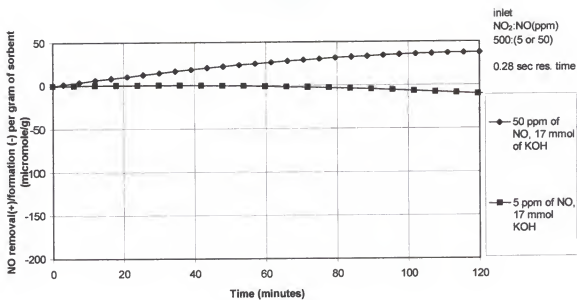


Figure 3-25. Effect of varied NO concentration on the sorption of NO<sub>x</sub> by KOH-treated alumina.

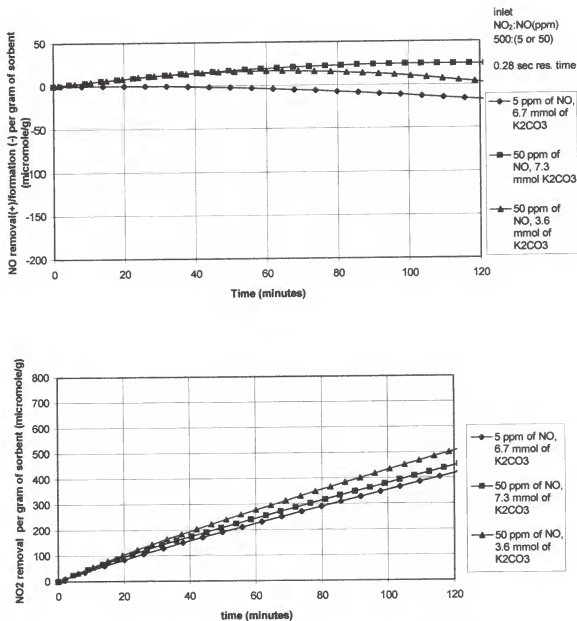


Figure 3-26. Effect of varied NO concentration on the sorption of NO<sub>x</sub> by K<sub>2</sub>CO<sub>3</sub>-treated alumina.

3-19 and 3-23, respectively. The relevant data from these figures are summarized in Figures 3-25 and 3-26. For the KOH-treated (19% by mass) sample in Figure 3-25, removal of NO is small if the NO concentration is 5 ppm but increases at 50 ppm. Furthermore, the removal of NO<sub>2</sub> is significantly less for 5 ppm than for 50 ppm of NO in the inlet gas stream. This observation suggests that the rates of removal of NO and NO<sub>2</sub> by KOH-treated alumina are not independent.

It should be noted that 5-gram samples of sorbent were used in the treatment-mass evaluations but 2-gram samples were used in the temperature evaluations to conserve cylinder gas. However, preliminary testing of NO<sub>x</sub> sorption by 2-gram and 5-gram samples using similar residence times showed no significant difference. Tests of 2- and 5-gram samples of untreated alumina under similar conditions are shown in Figure 2-4a) and 2-4b), respectively. Similar observations were made for treated alumina.

Additional sorption tests using a pure gas stream of NO showed no measurable removal by untreated, KOH-treated, and K<sub>2</sub>CO<sub>3</sub>-treated alumina during a 5-hour period. However, after the 5-hour exposure period, additions of NO<sub>2</sub> to the input-gas showed that treated KOH and K<sub>2</sub>CO<sub>3</sub> removed both NO<sub>2</sub> and NO. This observation supports the suggestion that combined gas-solid interaction of NO and NO<sub>2</sub> on alumina is a major factor in the sorption of the two gases. Additional work is necessary to understand this phenomenon and it is important to the detailed understanding of the mechanism of NO<sub>x</sub> removal on sorbents.

### NO<sub>x</sub> Sorption: Saturation

Two-gram treated (20% by mass) alumina samples were saturated with NO<sub>x</sub> (500 ppm NO<sub>2</sub> and 5 ppm NO). The results are displayed in Table 3-2. The reproducibility for triple runs of potassium hydroxide-treated alumina samples was low ( $\pm 15\%$ ). However, general trends are observable from the results. Carbonate and hydroxide compounds showed that potassium compounds removed greater amounts of NO<sub>x</sub> than sodium compounds. Potassium hydroxide and carbonate performed equally well for similar amounts of treatment mass while sodium hydroxide and carbonate varied greatly. On a molar basis potassium carbonate exhibited the highest efficiency of NO<sub>2</sub> removal. All treatments reduced the amount of NO formed per unit amount of NO<sub>2</sub> removed. Sulfate treatments actually reduced the overall uptake of NO<sub>x</sub> compared to untreated alumina, which could be an important feature if sulfur dioxide is a copollutant in the gas stream being treated by a solid sorbent.

### Comparison of Alkali Compounds: NO<sub>x</sub> Sorption

The alkali elements of Li, Na, K, Rb, and Cs, as hydroxides and carbonates were precipitated onto  $\gamma$ -alumina pellets in equimolar amounts for each element. Laboratory sorption studies of NO and NO<sub>2</sub> were performed in the fixed-bed reactor system followed by either surface area measurement by the BET method or X-ray photoelectron spectroscopy (XPS) analysis.

Sorbent samples were prepared by mixing pellets with solution and evaporating to dryness at 150 °C. Repeated preparations were performed to obtain sorbent samples with equimolar amounts of group-I elements. Thus, a 3-g sorbent sample consists of either

0.14 g of LiOH (6 mmol of lithium) or 1.00 g of  $\text{Cs}_2\text{CO}_3$  (6 mmol of Cs). The amount of treatment to alumina (6mmol) was based on previous tests that indicated a limiting range of treatment with Na and K hydroxides and carbonates (see Figures 3-17 through 3-20 and discussion thereof).

#### Alkali-Hydroxide Treatments

The adsorption of NO and  $\text{NO}_2$  by alkali hydroxide-treated  $\gamma$ -alumina is shown in Figure 3-27. A clear trend can be observed, increased  $\text{NO}_2$  removal with increasing group-I alkali metal atomic weight. While equal molar amounts of hydroxides are present on these sorbents, alkali elements of lower ionization potential show improved  $\text{NO}_2$  removal. CsOH is observed to improve removal of  $\text{NO}_2$  by 30 % when compared to LiOH.

#### Alkali-Carbonate Treatments

A similar test series of group-I carbonate-treated alumina samples exposed to  $\text{NO}_x$  is shown in Figure 3-28. Each of the sorbent samples tested contained 6 mmol of the group-I element. The  $\text{NO}_x$  sorbent of highest activity is  $\text{Cs}_2\text{CO}_3$ -treated alumina while  $\text{Li}_2\text{CO}_3$  is the lowest.

#### Cesium Treatments

Cesium compounds showed the highest activity of  $\text{NO}_x$  sorption and were further studied. An initial test was performed to show that sorption of NO alone does not occur for CsOH and  $\text{Cs}_2\text{CO}_3$ -treated alumina. Figure 3-29 shows the bed outlet concentration of NO during the test. The slight uptake of NO that is observed during the first 15 minutes

Table 3-2. Saturation capacity of treated alumina samples.

| Coating material                | Time to saturation (hours) | Total NO <sub>x</sub> removed (mmol) <sup>a</sup> | mol NO <sub>2</sub> removed /mol NO formed | Coating amount (% by mass) | mol NO <sub>2</sub> removed/mol of coating |
|---------------------------------|----------------------------|---|--|----------------------------|--|
| untreated                       | 13                         | 0.36  | 3.0  | 0                          | 0  |
| KOH                             | 47                         | 2.09  | 3.9  | 20                         | 0.38                                       |
| NaOH                            | 28                         | 0.59  | 4.0  | 20                         | 0.08                                       |
| K <sub>2</sub> CO <sub>3</sub>  | 48                         | 2.12  | 4.0  | 20                         | 0.97                                       |
| Na <sub>2</sub> CO <sub>3</sub> | 37                         | 1.71  | 3.8  | 20                         | 0.61                                       |
| K <sub>2</sub> SO <sub>4</sub>  | 10                         | 0.15  | 3.6  | 20                         | 0.09                                       |
| Na <sub>2</sub> SO <sub>4</sub> | 10                         | 0.10  | 3.7  | 20                         | 0.05                                       |

Based on an average of 3 tests of KOH-treated  $\gamma$ -alumina, the molar ratio of NO<sub>2</sub> removed/NO formed is 3.9 (  $\pm 0.5$  @ 2 std. dev.). Test conditions: 200 °C, 0.28 sec. residence time, gas input 500 ppm NO<sub>2</sub>, 5 ppm NO, 2.8 cm<sup>3</sup> bed volume

<sup>a</sup> Total NO<sub>x</sub> removed = mole of NO<sub>2</sub> removed - mole of NO formed



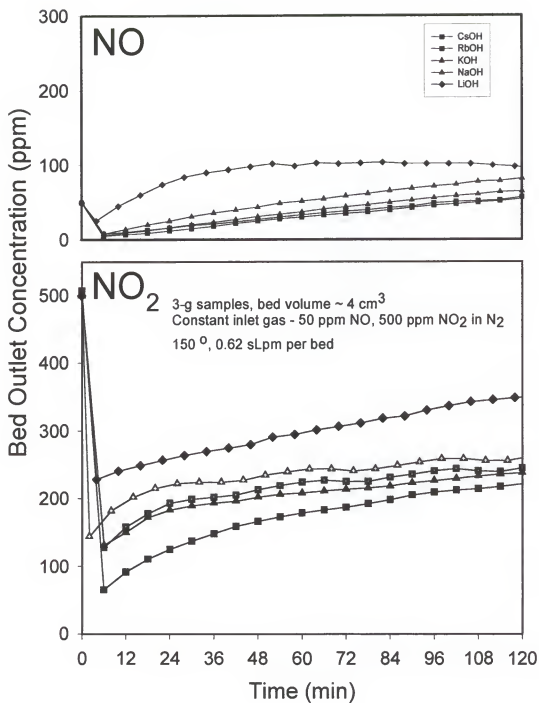


Figure 3-27. Group-I hydroxide equimolar-treated  $\gamma$ -alumina sorption of NOx.

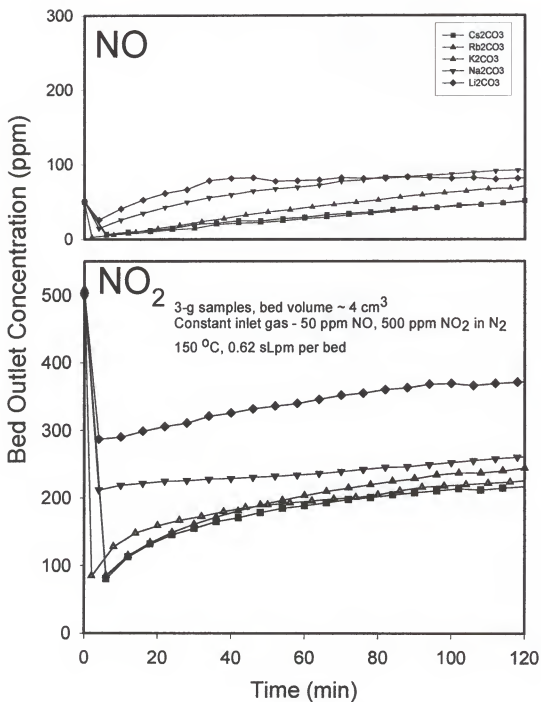


Figure 3-28. Group-I carbonate equimolar-treated  $\gamma$ -alumina sorption of NO<sub>x</sub>.

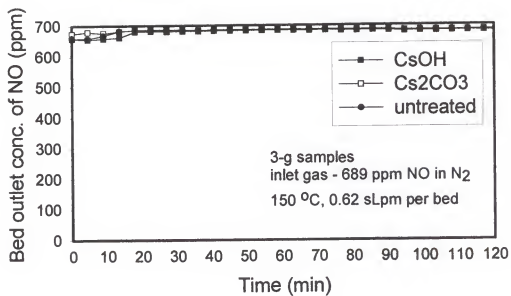


Figure 3-29. Sorption of NO (balance N<sub>2</sub>) by untreated and CsOH-treated and Cs<sub>2</sub>CO<sub>3</sub>-treated alumina.

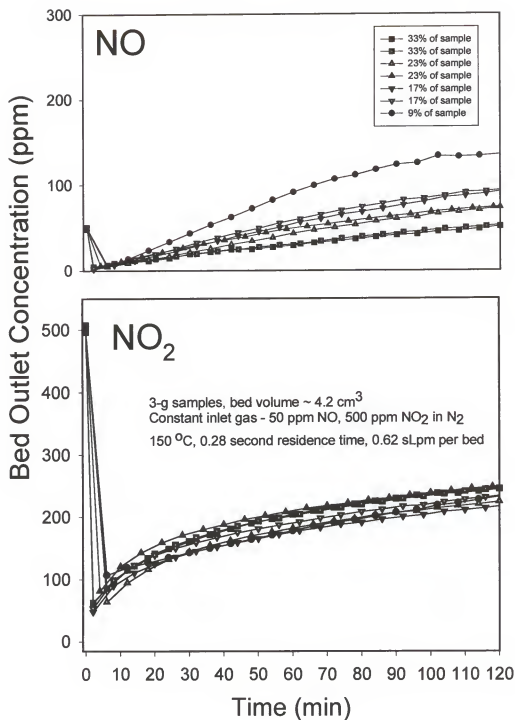


Figure 3-30. Effect of varied amount of cesium carbonate treated onto  $\gamma$ -alumina on the sorption of NO<sub>x</sub>.

of the tests is less than 1% of the input NO and within the expected range of experimental error. Previous tests have shown that the uptake of NO by untreated alumina was negligible. Given that in this test the sorption of NO by untreated alumina is observed to perform similarly to the Cs-treated alumina samples it appears that all of these tested materials do not react with NO alone. Varied treatment masses of  $\text{Cs}_2\text{CO}_3$  were prepared onto alumina and tested for NO<sub>x</sub>-sorption. All of these treatments indicate similar NO<sub>2</sub> uptake yet varied NO uptake/production. Based on the rate of NO<sub>2</sub> uptake for all levels of treatment the interaction of  $\text{Cs}_2\text{CO}_3$  with NO<sub>2</sub> appears to dominate over the uptake of NO<sub>2</sub> by alumina (Figure 3-30). Thus, the production of NO could indicate a faster overall saturation of the surface with production of a stable intermediate presumably  $\text{CsNO}_2$ . Build up of nitrites on the surface presumably establish a path to form nitrate and NO.

The  $\text{Cs}_2\text{CO}_3$ -treated alumina (33 % w/w) sample was XPS analyzed before and after NO<sub>x</sub>-exposure. After NO<sub>x</sub> exposure no significant peak is observed for nitrogen. This unexpected result was further studied to determine why nitrogen was not observed on the surface.

In the preparation process for XPS analysis the weak bonding force of sorbed gases to Cs was revealed. During the outgassing process to reach  $10^{-10}$  torr, the  $\text{Cs}_2\text{CO}_3$ -treated sample evolved a large amount of gas. Furthermore, during analysis the x-ray bombardment heated the sample from 25 °C to approximately 50 °C. During this heating an additional amount of gas evolved.

To determine if the outgassing process did in fact remove sorbed nitrogen a subsequent test was performed. A portion of the  $\text{Cs}_2\text{CO}_3$ -treated sample was placed in the

outgassing chamber and the pressure reduced to  $10^{-8}$  torr. The sample was then removed and stored for further testing. The sample was transported and placed in the fixed-bed reactor. A decomposition test was performed on the sample to determine if any NO or NO<sub>2</sub> species would evolve. The sample was flushed with a constant flow of 1 sLpm N<sub>2</sub>. The furnace heating rate was 10 °C /min. The temperature was increased until it was observed that a significant amount of NO was released from the surface. From the decomposition test it was clear that the outgassing process did not remove sorbed NO<sub>x</sub> species. Therefore, another explanation for not observing nitrogen species through XPS analysis is necessary. The relative scale of the information collected from the XPS system is a function of the greatest intensity peak. The Cs (3d) peak has an intensity factor of approximately 10 times that of nitrogen. Therefore, detection of the N (1s) peak is presumably decreased due to the large intensity of the Cs (3d) peak.

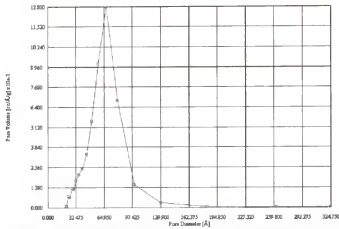
#### Alkali-Treated Alumina: Surface Area Measurements

Surface area measurement data for the equimolar treated alumina materials are shown in Table 3-3. A trend in decreasing surface area with increasing group-I atomic radius is apparent. Given that these materials have equimolar treatments of each alkali element the differences in the surface area measurement are believed to be primarily caused by the change in the alkali metal atomic radius. Having observed that lithium compounds performed relatively poorly compared to cesium, the surface areas of these materials indicates that the relative activity of cesium is even greater per surface area.

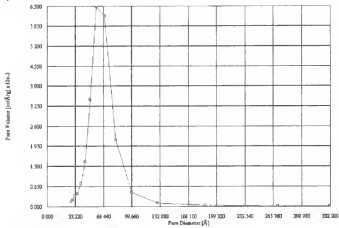
Figures 3-31 a), b), and c) show the pore size distribution for untreated  $\gamma$ -alumina, Cs<sub>2</sub>CO<sub>3</sub>-treated (33% w/w)  $\gamma$ -alumina, and NO<sub>x</sub>-saturated Cs<sub>2</sub>CO<sub>3</sub>-treated (33% w/w)

Table 3-3. BET surface area measurement of treated  $\gamma$ -alumina sorbents.

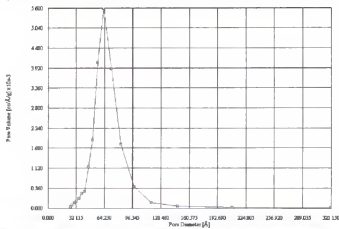
| Treatment Compound              | coating millimoles per sample | NOx exposure NO <sub>2</sub> /NO | Surface Area (m <sup>2</sup> /g) | Atomic Radius (Å) |
|---------------------------------|-------------------------------|----------------------------------|----------------------------------|-------------------|
| Li <sub>2</sub> CO <sub>3</sub> | 3.0                           | ----                             | 157                              | 0.53              |
| LiOH                            | 3.0                           | ----                             | 122                              | 0.53              |
| Na <sub>2</sub> CO <sub>3</sub> | 2.85                          | ----                             | 142                              | 0.67              |
| NaOH                            | 3.0                           | ----                             | 126                              | 0.67              |
| K <sub>2</sub> CO <sub>3</sub>  | 3.0                           | ----                             | 120                              | 0.86              |
| KOH                             | 3.0                           |                                  | 114                              | 0.86              |
| Rb <sub>2</sub> CO <sub>3</sub> | 2.8                           | ----                             | 85                               | 1.53              |
| RbOH                            | 3.0                           |                                  | 83                               | 1.53              |
| Cs <sub>2</sub> CO <sub>3</sub> | 2.95                          | ----                             | 71                               | 1.90              |
| CsOH                            | 3.0                           | ----                             | 71                               | 1.90              |
| Cs <sub>2</sub> CO <sub>3</sub> | 2.95(33% w/w)                 | saturated                        | 58                               |                   |
| Cs <sub>2</sub> CO <sub>3</sub> | 2.95(33%)                     | 1.2:0.12                         | 61                               |                   |
| Cs <sub>2</sub> CO <sub>3</sub> | 1.40(17%)                     | ----                             | 122                              |                   |
| Cs <sub>2</sub> CO <sub>3</sub> | 1.40(17%)                     | 1.2:0.12                         | 116                              |                   |
| Cs <sub>2</sub> CO <sub>3</sub> | 0.80 (9%)                     | ---                              | 144                              |                   |



a) Pore size distribution of untreated  $\gamma$ -alumina.



b) Pore size distribution of  $\text{Cs}_2\text{CO}_3$ -treated (33% w/w)  $\gamma$ -alumina.



c) Pore size distribution of  $\text{NO}_x$ -saturated  $\text{Cs}_2\text{CO}_3$  (33% w/w)-treated  $\gamma$ -alumina

**Figure 3-31.** Pore size distribution of a) untreated  $\gamma$ -alumina, b)  $\text{Cs}_2\text{CO}_3$ -treated alumina, and c)  $\text{NO}_x$ -saturated  $\text{Cs}_2\text{CO}_3$ -treated alumina.



$\gamma$ -alumina, respectively. Pore size distribution measures of the  $\text{Cs}_2\text{CO}_3$ -treated alumina (33% w/w) before and after  $\text{NO}_x$ -exposure compared to untreated alumina indicate that the average pore size is not significantly altered but that overall surface area and pore volume is decreased by treatment and  $\text{NO}_x$ -exposure. The pore radius increases from 90 to 94 Ångstroms upon coating treatment with  $\text{Cs}_2\text{CO}_3$  and further increases to 97 Ångstroms after  $\text{NO}_x$  saturation. The surface area decreases from 172 to 75  $\text{m}^2/\text{g}$  after coating treatment and reduces to 58  $\text{m}^2/\text{g}$  after  $\text{NO}_x$  saturation. The pore volume decreases from 0.388 to 0.176  $\text{cc/g}$  upon treatment and reduces to 0.142  $\text{cc/g}$  after  $\text{NO}_x$  saturation. Because there is little change in the average pore diameter yet a decrease in the available pore volume possibly indicates that the pore channels are simply closed by surface treatment and  $\text{NO}_x$  exposure. The pore closure effect suggests an inefficient use of the total material surface. The molecular size of sorbed particles has been suggested for observed pore closure of  $\text{Ca}_2\text{O}$  when used as a sorbent for  $\text{SO}_2$  (Borgwardt and Harvey, 1972). The molecular sizes of group-I nitrate compounds are greater than the corresponding carbonates and this may explain the decreased surface area after  $\text{NO}_x$  saturation.

A small sample (0.8 g) of  $\text{Cs}_2\text{CO}_3$ -treated alumina (33% w/w) was set in the sorbent tube such that it formed a one-pellet thick layer of sorbent. This material was to be  $\text{NO}_x$ -exposed for further study by either XPS, FTIR or ion-selective-electrode. A small sample was used to achieve quick saturation. Also, the thin layer should minimize any secondary effects of  $\text{NO}$  gas produced by sorbed  $\text{NO}_2$ . The tests performed involved exposing the sorbent to a stream containing 1950 ppm  $\text{NO}_2$  at 150 °C. The sorbent was

exposed until the  $\text{NO}_2$  outlet concentration was 85% of the  $\text{NO}_2$  inlet concentration. Only trace amounts of  $\text{NO}$  were present in the  $\text{NO}_2$  gas stream. Unexpectedly, the single-pellet layer bed of  $\text{Cs}_2\text{CO}_3$ -treated alumina immediately produced  $\text{NO}$  as a result of  $\text{NO}_2$  sorption. During 4 hours of exposure the ratio of  $\text{NO}$  produced approached approximately a 3:1 ratio. This trend is shown in Figure 3-32.

#### Relation of Alkali Element Ionization Potential to $\text{NOx}$ Sorption

The activities of the group-I alkali metal compounds with  $\text{NOx}$  appear to correlate with their ionization potentials. Similar trends are observed for hydroxide and carbonate materials. Table 3-4 lists the ionization potential of each element and the average fraction of  $\text{NO}_2$  removed during the  $\text{NOx}$ -sorption tests shown in Figures 3-27 and 3-28. Lithium has the highest ionization potential and is least reactive to  $\text{NOx}$ , while cesium has the lowest ionization potential and highest reactivity per mole with  $\text{NOx}$ .

#### Sorption Studies of the Effect of Varying $\text{NO}$ and $\text{NO}_2$ Concentrations

A series of experiments was performed on untreated,  $\text{K}_2\text{CO}_3$ -treated and  $\text{KOH}$ -treated  $\gamma$ -alumina to characterize the effect on  $\text{NOx}$  sorption of varying the concentrations of  $\text{NO}$  or  $\text{NO}_2$  in the presence of both reactive gases. Previous tests had shown an unexpected increase in  $\text{NO}$  sorption in the presence of  $\text{NO}_2$  for alkaline-coated aluminas. Gaseous  $\text{NO}$  alone is not removed by any of the sorbent materials studied. Tests in which the  $\text{NO}_2$  concentration was held constant while the  $\text{NO}$  concentration was increased showed an increase in  $\text{NO}$  sorption (Figures 3-25 and 3-26). Knowing that  $\text{NO}$  alone is not removed, the observation of increased removal of  $\text{NO}$  with concentration suggested that  $\text{NO}_2$  reacted in coordination with  $\text{NO}$  at the sorbent surface. This should also be

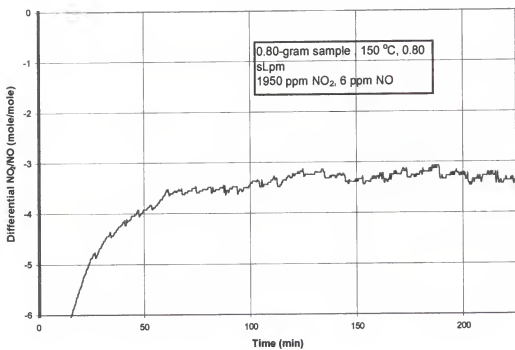


Figure 3-32. Incremental molar ratio of NO<sub>2</sub>/NO for Cs<sub>2</sub>CO<sub>3</sub>-treated alumina sorption of NO<sub>2</sub>.

Table 3-4. Fractional NO<sub>2</sub> removal of group-I treated compound alumina and element ionization potential.

| Treatment Compound              | Fraction of NO <sub>2</sub> Removed | group-I element<br>Ionization Potential (eV) |
|---------------------------------|-------------------------------------|--|
| LiOH                            | 0.299                               | 5.392  |
| NaOH                            | 0.497                               | 5.139  |
| KOH                             | 0.538                               | 4.341  |
| RbOH                            | 0.541                               | 4.177  |
| CsOH                            | 0.625                               | 3.894  |
| Li <sub>2</sub> CO <sub>3</sub> | 0.287                               |  |
| Na <sub>2</sub> CO <sub>3</sub> | 0.498                               |  |
| K <sub>2</sub> CO <sub>3</sub>  | 0.585                               |  |
| Rb <sub>2</sub> CO <sub>3</sub> | 0.595                               |  |
| Cs <sub>2</sub> CO <sub>3</sub> | 0.600                               |  |

confirmed by an increased  $\text{NO}_2$  uptake with increased NO as well as increased  $\text{NO}_2$ -formation.

#### Initial Tests on Sorption of Gaseous NO

A preliminary test was made to confirm that NO sorption alone did not occur but when combined with  $\text{NO}_2$ , NO is sorbed. Figure 3-33 shows the  $\text{NO}_x$  outlet concentrations of  $\text{K}_2\text{CO}_3$ -treated and KOH-treated  $\gamma$ -alumina. The test consists of two segments of a specific inlet feed of  $\text{NO}_2$  and NO. Initially NO, alone is directed through the bypass line which is indicated by 50 ppm NO. The feed gas, which is absent of  $\text{NO}_2$ , is then directed to the sorbent beds. As seen in the figure, the outlet NO concentration during this exposure was the same as the inlet concentration (50 ppm NO). After exposure of the bed to NO for 40 minutes the NO gas was redirected to the bypass and the  $\text{NO}_2$  gas (50 ppm) is added to the NO flow. Upon redirection of the gas mixture flow to the beds, the sorption of NO in the presence of  $\text{NO}_2$  is immediately apparent.

#### Interaction of NO with Sorbents following $\text{NO}_2$ Sorption

Other tests were performed to further identify the process of NO- $\text{NO}_2$  sorption. One question arises as to whether NO sorption is due to a species formed from sorbed  $\text{NO}_2$  or by another process. An experiment to answer this question was performed. A fixed-bed reactor test was performed in which the  $\text{K}_2\text{CO}_3$ - and KOH-treated materials were first exposed to  $\text{NO}_2$  (689 ppm) at 25 °C. Following  $\text{NO}_2$  exposure the bed was flushed with  $\text{N}_2$  to remove residual  $\text{NO}_2$  gas. The bed was then exposed to NO. Two tests were performed to observe effects of lengthened  $\text{NO}_2$  exposures. In Figure 3-34 time-resolved outlet NO and  $\text{NO}_2$  concentrations for  $\text{K}_2\text{CO}_3/\gamma$ -alumina are plotted. The test procedure during the time intervals is described below numerically (1–8).

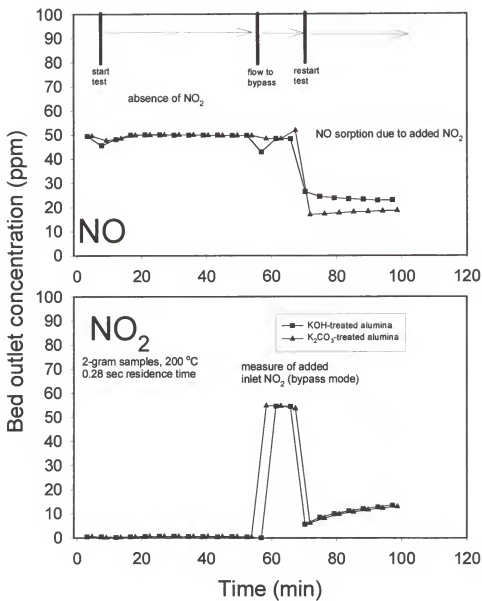


Figure 3-33. Effect of presence of NO<sub>2</sub> on sorption of NO for KOH-treated and K<sub>2</sub>CO<sub>3</sub>-treated alumina.

1. Certified cylinder-gas NO (680 ppm @ 1 sLpm) is measured in the bypass line.
2. Certified cylinder-gas NO<sub>2</sub> (689 ppm @ 1 sLpm) is measured in the bypass line.
3. NO concentration is measured in the empty reactor tube.
4. NO<sub>2</sub> concentration is measured in the empty reactor tube.
5. The empty reactor tube is removed and filled with 2-g of K<sub>2</sub>CO<sub>3</sub>-treated (24.7 % w/w) alumina. The filled reactor tube is replaced in the system.
6. The bed is exposed to NO<sub>2</sub> (689 ppm @ 1 sLpm) for 20 minutes (Figure 3-34 a)) or 5 minutes (Figure 3-34 b)).
7. The flow of NO<sub>2</sub> is stopped and the bed is flushed with N<sub>2</sub> (1 sLpm).
8. The reactor bed is exposed to NO until the outlet concentration reaches <1% of empty-tube NO concentration.

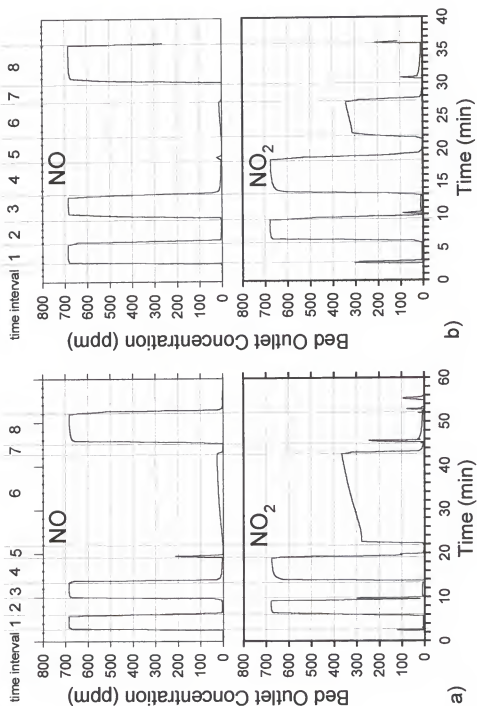


Figure 3-34. Surface interaction of NO following exposure of  $K_2CO_3$ -treated alumina to  $NO_2$  at 25 °C.



The test revealed several interesting features. First, after  $\text{NO}_2$  exposure to the  $\text{K}_2\text{CO}_3$ -treated alumina, a small fraction of  $\text{NO}$  flowing through the sorbent bed is observed to be sorbed (Figures 3-34 a) and b), time interval 8.). Comparing Figures 3-34 a) and b), increased amounts of  $\text{NO}$  sorption occurs that corresponds to increased  $\text{NO}_2$  exposure time. The ratio of  $\text{NO}_2$  initially sorbed (time interval 6, (41.1 and 143.5  $\mu\text{mole/g}$  sorbent) to the amount of  $\text{NO}$  subsequently sorbed (time interval 8, (0.78 and 6.89  $\mu\text{mole/g}$  sorbent)) are 2.6 and 4.8 % for the 20 and 5 minute exposures, respectively. Thus, the amount of  $\text{NO}$  subsequently sorbed is a small fraction of the  $\text{NO}_2$  sorbed and does not increase proportionally to the amount of  $\text{NO}_2$  sorbed.

Second, an unexpected phenomenon can be observed.  $\text{NO}$  sorption simultaneously occurs to a production of  $\text{NO}_2$  (time interval 8). This corresponding production of  $\text{NO}_2$  during  $\text{NO}$  sorption is proportional to the amount of  $\text{NO}$  sorbed (time interval 8). The ratio of  $\text{NO}$  sorbed/ $\text{NO}_2$  produced during time interval 8) is 0.88 (20 min (Figure 3-34 a)) and 0.73 (5 min (Figure 3-34 b)). A reason for this observed simultaneous  $\text{NO}_{\text{sorption}}\text{-NO}_2\text{ production}$  is that the increased concentration of inlet  $\text{NO}$  (680 ppm) and the absence of  $\text{NO}_2$  causes a reversal of a reaction with surface species formed during  $\text{NO}_2$  exposure (time interval 6). The surface species formed may then reversibly react to convert  $\text{NO}$  to  $\text{NO}_2$ . Similar results were observed for untreated and  $\text{KOH}$ -treated  $\gamma$ -alumina. Again, untreated,  $\text{K}_2\text{CO}_3$ -treated, and  $\text{KOH}$ -treated alumina are observed to sorb  $\text{NO}$  and produce  $\text{NO}_2$  in similar tests after  $\text{NO}_2$  exposure.

According to the proposed reactions of others (Kimm, 1995; Nelli and Rochelle, 1996),  $\text{NO}_2$  can convert to nitrite, nitrate, and  $\text{NO}$ . This study may indicate a reversal of

a reaction, similar to reaction 3-3 or 3-8, that is a reaction of NO with an intermediate complex nitrate. Thus, it is suggested that the phenomenon described above is the reversal of nitrite to nitrate conversion. However, the small fraction amounts of NO sorbed (time interval 8) suggest a high barrier to reversing the suggested reaction.

To test the proposed reaction, pure  $\text{KNO}_3$  was exposed to NO to determine if  $\text{NO}_2$  could be produced in a similar manner to that observed in the above study. This test was performed by placing pure  $\text{KNO}_3$  within the fixed-bed reactor system and exposing to NO at 25 °C. Production of  $\text{NO}_2$  was not observed. In addition, tests with  $\text{KNO}_3$ -treated alumina exposed to NO did not produce  $\text{NO}_2$  in the fixed-bed reactor. Assuming the reaction proposed above is correct, this result suggests that nitrate species formed by  $\text{NO}_2$  sorption may have very different properties from bulk-phase nitrate. Thus, these tests may not be indicative of the proposed reaction. Decomposition tests, that are discussed later (see section entitled Thermal Decomposition Studies), of pure samples of potassium nitrite and nitrate did not similarly decompose as NOx-exposed sorbents and alumina treated with  $\text{KNO}_3$  or  $\text{KNO}_2$  solutions.

#### Effect of Varying the Inlet NO Concentration

A series of fixed-bed reactor experiments was performed on untreated  $\gamma$ -alumina,  $\text{K}_2\text{CO}_3$ -treated and KOH-treated  $\gamma$ -alumina to measure the effects of increasing NO in the presence of a constant  $\text{NO}_2$  concentration. Experiments were performed with the concentration of  $\text{NO}_2$  held constant at 500 ppm and varied NO concentrations (10, 50, 200, and 500 ppm) with a constant gas bed residence time at temperatures of 25, 50, 100, 200, and 250 °C. Gas residence time in the sorbent bed has been discussed to significantly

effect the sorption behavior of these materials and thus was kept constant during these tests (see Figure 3-3). Therefore, at different temperatures (25, 50, 100, 200, and 250 °C) the gas flow was varied to provide a similar bed residence time of approximately 0.25 sec. The bed masses were held constant at 3 grams for consistency of comparison by mass. The experimental results are shown as cumulative sorption of NO and NO<sub>2</sub> in micromole/g of sorbent in Appendix A.

Reproducibility tests of three samples each of untreated, K<sub>2</sub>CO<sub>3</sub>-treated, and KOH-treated alumina show 95% confidence intervals to be 7.6, 8.7, and 7.6 percent, respectively, of the accumulated NO<sub>2</sub> sorbed after 2 hours of NO<sub>x</sub> exposure. These tests were performed at 250 °C that have greater errors than lower-temperature tests due to lower flowrates and higher temperature variations. Thus, lower-temperature tests should have greater reproducibility.

The efficiency of NO<sub>2</sub> removal is constant with temperature. However, the reduced molar flow rate of NO<sub>x</sub> applied at higher temperatures reduces the amount of cumulative NO<sub>2</sub> sorbed. Treated materials show a significant increase in cumulative NO sorbed with increased temperature. As well, the rate of NO sorption for treated materials becomes more linear at higher temperature. At lower temperature, NO sorption decreases rapidly and production of NO is observed eventually for the treated materials.

Over the tested temperature range, increased NO input appears to increase NO<sub>2</sub> sorption to treated alumina yet is not significant given the 95 % confidence intervals. Based on previously described tests (see Figure 3-25 and 3-26) this result was not expected. Previous tests indicated that the sorption of NO corresponded to additional

NO<sub>2</sub> sorption. One may propose that NO and NO<sub>2</sub> interact to provide sorption of both gases. Another sorption process observed may be sorption of NO<sub>2</sub> alone. Given that these tests did not show increased NO<sub>2</sub> sorption and the extensive coverage of conditions of these tests, sorption of NO with NO<sub>2</sub> may be competitive with sorption of NO<sub>2</sub> alone.

#### Effect of Varying Inlet NO<sub>2</sub> Concentrations

A similar series of experiments was performed to study the effect of varying NO<sub>2</sub> concentration (10, 50, 200, and 500 ppm) in the presence of constant NO concentration (500 ppm). Tests were performed at the same temperature and flow used for the previously discussed series. Cumulative sorption of NO and NO<sub>2</sub> in  $\mu\text{mole/g}$  are shown in Appendix B for this series of tests.

Results from the test indicate the sorption of NO<sub>2</sub> is first order with respect to itself over the range of temperatures. NO sorption trends to a first order relation at higher temperature with respect to input NO<sub>2</sub>.

A significant finding is that higher temperature increases cumulative NO sorbed. However, at lower temperatures a maximum cumulative amount of NO sorbed is observed. Also, at lower temperature less cumulative NO sorption is observed for an NO<sub>2</sub> inlet concentration of 500 ppm than 200 ppm. Thus, having observed at lower temperature that increased NO<sub>2</sub> inlet concentration decreases the cumulative amount of NO sorbed suggests a competitive sorption process may occur where sorption of NO<sub>2</sub> is preferred. This preferred sorption may be the sorption of NO<sub>2</sub> alone. Thus, if two sorption processes are proposed to be sorption of NO<sub>2</sub> and NO or sorption of NO<sub>2</sub> alone, a preference is observed for NO<sub>2</sub> alone in tests of 500 rather than 200 ppm NO<sub>2</sub> inlet

concentration. Tests with lower  $\text{NO}_2$  inlet concentration (200 ppm) increase the cumulative NO sorption because the ratio of  $\text{NO}:\text{NO}_2$  inlet concentration is higher.

#### Gas and Surface Profile for the Sorption Process

Preliminary studies of KOH-treated  $\gamma$ -alumina showed both NO and  $\text{NO}_2$  sorption for an initial period of  $\text{NO}_x$  exposure (see Figure 3-7). Thus, a mechanism that includes treated sorbent removal of NO is necessary. Having observed an interaction of NO in the presence of  $\text{NO}_2$  by alkali-treated  $\gamma$ -alumina (Figure 3-33), a series of fixed-bed reactor experiments was designed to measure the outlet gas concentrations and surface species formed by  $\text{NO}_x$  sorption within a sorbent bed of untreated,  $\text{K}_2\text{CO}_3$ -treated, and KOH-treated alumina. These data could give indications of possible reactions that occur on the sorbent surface.

The fixed-bed reactor system was used to expose untreated,  $\text{K}_2\text{CO}_3$  and KOH-treated alumina (15-gram samples) to a 0.885 sLpm (per bed) flow of  $\text{NO}_2$  (1950 ppm) at 25 °C. NO was present in the feed gas as a trace impurity in the  $\text{NO}_2$  gas cylinder. After  $\text{NO}_x$  exposure for a maximum of 2 hours, the 15-gram samples were removed from the reactor and sectioned into 3-gram portions. These 3-gram sections were dissolved in aqueous solution and analyzed by ion-specific electrode (ISE) for nitrite and nitrate concentrations. An in-depth discussion of the data collected and analysis is provided elsewhere (Pocengal, 1999). The total sample mass of 15 grams was chosen to ensure that the individual samples would contain sufficient surface nitrogen species for measurement by ISE analysis. Other 15-gram sorbent samples were exposed to  $\text{NO}_x$  for shorter time periods of 30, 60 and 90 minutes and were similarly analyzed for nitrite and

nitrate concentrations. The ISE analyses can provide the concentration of the formed surface nitrite and nitrate species for the four different exposure times. Nitrite and nitrate concentrations found at each bed layer for 30, 60, 90, and 120 minute-exposure times are presented in Figures 3-35, 3-36, and 3-37 for the three materials.

Estimated gaseous concentrations of NO and NO<sub>2</sub> within the sorbent bed were obtained by testing sorbent masses of 3, 6, 9, and 12 grams under similar conditions as the 15-gram samples. These measurements of the gas-phase NO and NO<sub>2</sub> concentration profiles throughout the sorbent beds for the three materials are shown in Figures 3-38, 3-39, and 3-40. During the first 30-min exposure period it is seen that essentially no NO<sub>2</sub> or NO gas is emitted from the treated alumina beds. After the 30-min exposure the first layer of all treated materials studied shows a low nitrite-to-nitrate ratio, which corresponds to a high production of NO. Thus, the first layer of all materials appears to be sorbing NO<sub>2</sub> and also converting nitrite to nitrate and NO. For untreated alumina, at longer times of exposure it was observed that continual conversion of a proportional amount of NO<sub>2</sub> into NO occurred throughout the bed (Figure 3-38). As the treated sorbents convert NO<sub>2</sub> into NO in the first and second layers, the NO produced appears to be sorbed within the successive (3rd, 4th or 5th) layers. In Figures 3-36 and 3-37 it is seen that an increased amount of nitrite is formed throughout the bed that corresponds to the subsequent sorption of produced NO. As the beds become saturated over time, the nitrite-to-nitrate ratio in the lower bed layers gradually decreases.

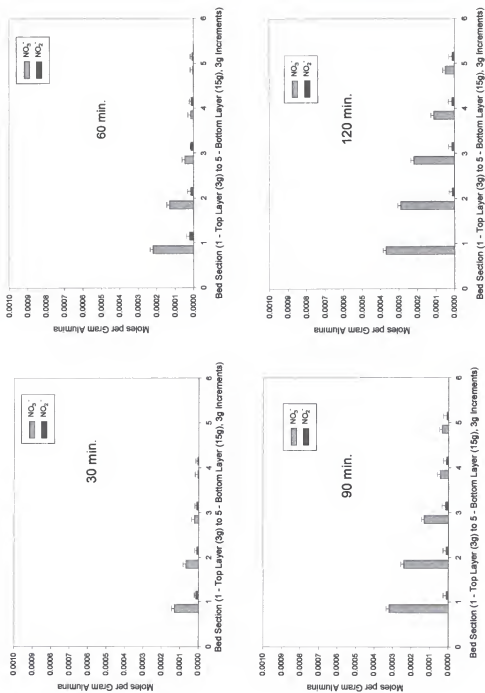


Figure 3-35. Nitrite and nitrate measured on incremental layers of a sorbent bed of untreated alumina.

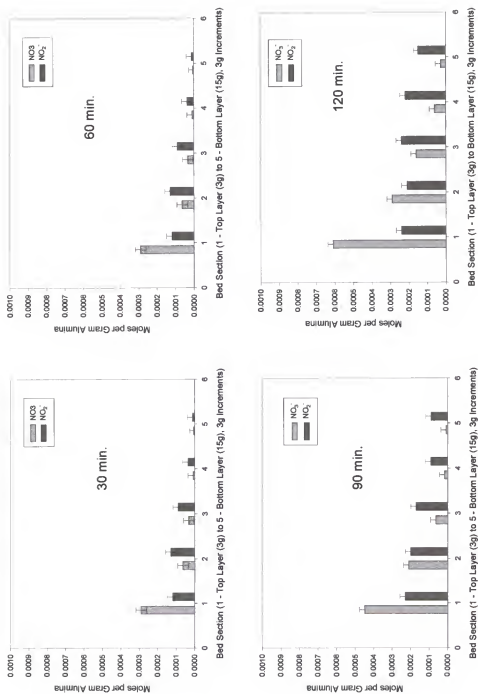


Figure 3-36. Nitrite and nitrate measured on incremental layers of a sorbent bed of  $\text{K}_2\text{CO}_3$ -treated alumina.



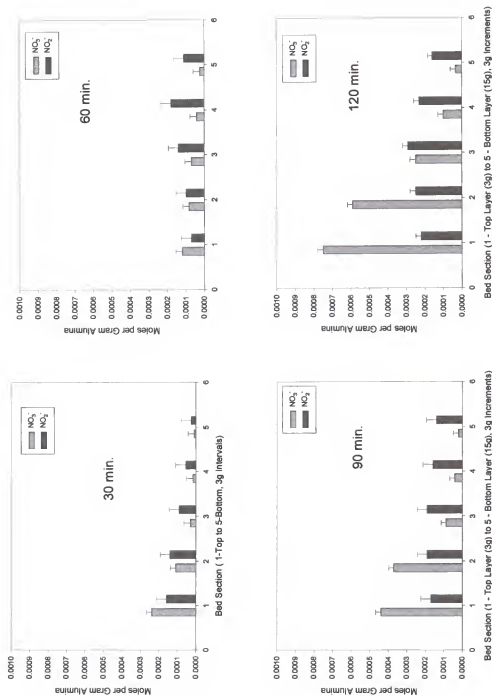


Figure 3-37. Nitrite and nitrate measured on incremental layers of a sorbent bed of KOH-treated alumina.

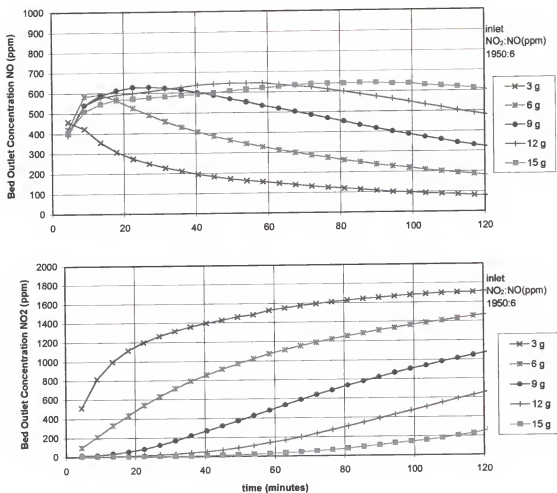
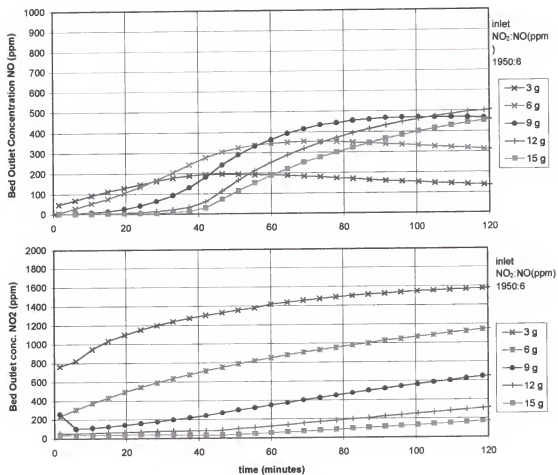


Figure 3-38. Change of NO and NO<sub>2</sub> gas concentrations throughout a bed of untreated  $\gamma$ -alumina.



**Figure 3-39.** Change of NO and NO<sub>2</sub> gas concentration throughout a bed of K<sub>2</sub>CO<sub>3</sub>-treated  $\gamma$ -alumina.

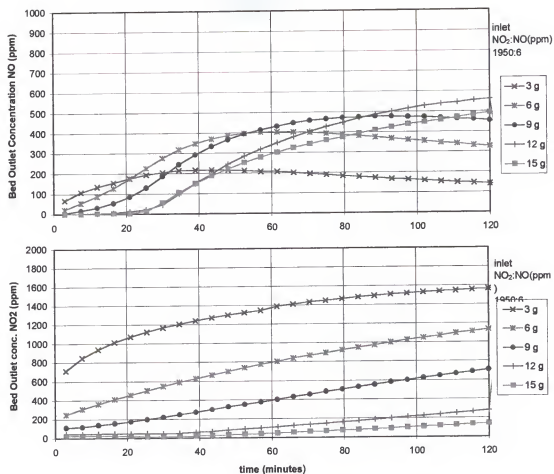


Figure 3-40. Change of NO and NO<sub>2</sub> gas concentrations throughout a bed of KOH-treated  $\gamma$ -alumina.

### Molar Ratio of Nitrite to Nitrate

For the treated materials, the reactions that create NO may occur at a slower rate than the process of NO sorption. By observing the ratio of nitrite to nitrate, one may evaluate the rates of NO removal throughout the bed. The molar amounts of nitrite to nitrate throughout the bed for 30, 60, 90, and 120-minute exposure times for the three materials are plotted in Figures 3-35 to 3-37. For the treated materials, one can observe that at the top of the bed nitrate concentrations are greater than nitrite, suggesting that the sorption mechanism at the top of the bed is dominated by reaction with  $\text{NO}_2$ . However, progressing down the bed, the ratio of nitrite to nitrate increases. As NO is sorbed in these lower layers this suggests that the reaction with NO becomes more active. Also, as the time of  $\text{NO}_x$  exposure progresses the nitrite to nitrate ratio becomes smaller in the top layers and greater in the bottom layers suggesting that reaction with  $\text{NO}_2$  increases the amount of nitrate formed in the top layers. With further exposure the nitrite to nitrate ratio will decrease to where essentially all nitrite becomes constant.

A comparison of the recovery of nitrite and nitrate (moles) to the sorbed  $\text{NO}_x$  (moles) is presented in Table 3-5. The average molar amounts of nitrite and nitrate are approximately 62, 122, and 100 percent of the sorbed  $\text{NO}_x$  ( $\text{NO}_{2 \text{ sorbed}} - \text{NO}_{\text{produced}}$ ) for untreated,  $\text{K}_2\text{CO}_3$ -treated, and KOH-treated  $\gamma$ -alumina, respectively. Reproducibility of these data is given in the Experimental section (Tables 2-2 and 2-3). A molar balance can be performed throughout the bed given the input  $\text{NO}_2$ , the accumulated nitrate and nitrate, and the NO produced. In Table 3-5 it can be seen that the molar balance is consistent throughout the bed except for the case of KOH (at 60 min exposure). The data for the latter may be erroneous as ISE analyses are suspect.

Table 3-5. Fractional recovery of surface nitrogen species ( $\text{NO}_2^-$  and  $\text{NO}_3^-$ ) to sorbed  $\text{NO}_x$  gas.

column 1-3. Ratio cumulative moles (sum of  $\text{NO}_3^- + \text{NO}_2^-$ ) per sum of ( $\text{NO}_2$  sorbed -  $\text{NO}_{\text{produced}}$ ).

column 4-6. Ratio cumulative moles (sum of  $\text{NO}_3^- + \text{NO}_2^- + \text{NO}$ ) per sum of ( $\text{NO}_2$  sorbed).

| layer & exposure time | 1<br>Untreat | 2<br>$\text{K}_2\text{CO}_3$ | 3<br>KOH | 4<br>Untreat | 5<br>$\text{K}_2\text{CO}_3$ | 6<br>KOH |
|-----------------------|--------------|------------------------------|----------|--------------|------------------------------|----------|
| 1 - 30 min            | 0.64         | 1.25                         | 1.37     | 0.76         | 1.41                         | 1.32     |
| 1 - 60 min            | 0.72         | 1.30                         | 0.42     | 0.82         | 1.42                         | 0.54     |
| 1 - 90 min            | 0.78         | 1.37                         | 1.08     | 0.86         | 1.40                         | 1.06     |
| 1 - 120 min           | 0.76         | 1.46                         | 1.35     | 0.85         | 1.38                         | 1.25     |
| 2 - 30 min            | 0.58         | 1.23                         | 1.28     | 0.72         | 1.22                         | 1.26     |
| 2 - 60 min            | 0.58         | 1.30                         | 0.44     | 0.77         | 1.26                         | 0.55     |
| 2 - 90 min            | 0.65         | 1.25                         | 1.10     | 0.84         | 1.20                         | 1.07     |
| 2 - 120 min           | 0.75         | 1.43                         | 1.19     | 0.84         | 1.33                         | 1.14     |
| 3 - 30 min            | 0.54         | 1.17                         | 1.24     | 0.68         | 1.16                         | 1.23     |
| 3 - 60 min            | 0.53         | 1.14                         | 0.53     | 0.69         | 1.13                         | 0.58     |
| 3 - 90 min            | 0.64         | 1.13                         | 1.01     | 0.76         | 1.11                         | 1.00     |
| 3 - 120 min           | 0.66         | 1.26                         | 1.15     | 0.78         | 1.21                         | 1.12     |
| 4 - 30 min            | 0.51         | 1.17                         | 1.23     | 0.65         | 1.18                         | 1.23     |
| 4 - 60 min            | 0.51         | 1.09                         | 0.62     | 0.66         | 1.09                         | 0.64     |
| 4 - 90 min            | 0.58         | 1.10                         | 0.93     | 0.72         | 1.09                         | 0.94     |
| 4 - 120 min           | 0.62         | 1.19                         | 1.03     | 0.75         | 1.16                         | 1.03     |
| 5 - 30 min            | 0.48         | 1.17                         | 1.26     | 0.62         | 1.17                         | 1.26     |
| 5 - 60 min            | 0.48         | 1.13                         | 0.71     | 0.63         | 1.12                         | 0.72     |
| 5 - 90 min            | 0.56         | 1.14                         | 0.97     | 0.70         | 1.13                         | 0.98     |
| 5 - 120 min           | 0.58         | 1.18                         | 1.04     | 0.71         | 1.17                         | 1.03     |
| avg.                  | 0.62         | 1.22                         | 1.00     | 0.74         | 1.22                         | 1.00     |
| std. dev.             | 0.10         | 0.11                         | 0.30     | 0.07         | 0.11                         | 0.26     |

### Trends in $\Delta\text{NO}_2_{\text{ sorbed}}/\Delta\text{NO}_{\text{ formed}}$ : Untreated and Treated Alumina

Trends in the ratio of sorbed  $\text{NO}_2$  to NO produced over time for the three types of materials are shown in Figures 3-41, 3-42 and 3-43. Untreated alumina trends to a value near three, which correlates to the overall general reactions expressed for  $\text{NO}_x$  with metal oxides (Kimm, 1995; Kimm et al., 1995; Knozinger, 1976; Nelli and Rochelle, 1996; Boehm, 1965; Zemlyanov et al., 1998).  $\text{K}_2\text{CO}_3$ -treated alumina also shows a trend to a value near 3 but the trend is less clear and shows a point of inflection in the ratio that occurs at increased time for increased bed depth. A similar trend in the ratio is seen for KOH-treated alumina. These trends indicate that all of the materials over time show that the amount of  $\text{NO}_2$  sorbed becomes proportional to three times the NO produced.

### Proposed Reaction Mechanisms of $\text{NO}_x$ with Alkali-Treated or Untreated Alumina

Based on the results of this study the delayed production of NO is a function of sorbent surface material. Production of NO from sorption of  $\text{NO}_2$  by various metal oxides has been observed (Kimm, 1995; Kimm et al., 1995; Knozinger, 1976; Nelli and Rochelle, 1996; Boehm, 1965; Zemlyanov et al., 1998). A general overall reaction has been proposed for alkaline-earth compounds (Kimm, 1995; Kimm et al., 1995; Nelli and Rochelle, 1996):



where M is an alkaline-earth element, i.e., Ca, Mg.

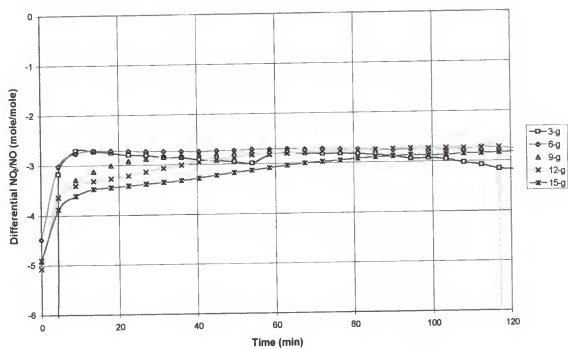


Figure 3-41. Incremental ratio of  $\text{NO}_2$  sorbed /  $\text{NO}$  formed for successive bed layers of untreated alumina.



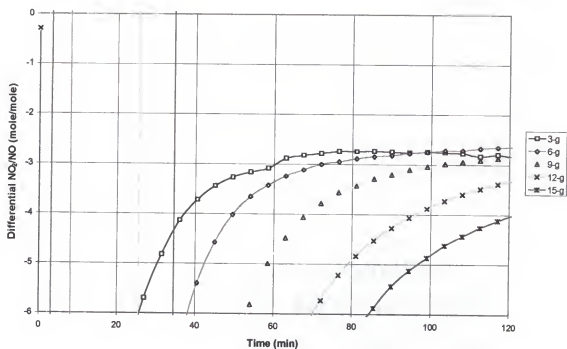


Figure 3-42. Incremental ratio of  $\text{NO}_2$  sorbed/ $\text{NO}$  formed for successive bed layers of layers of  $\text{K}_2\text{CO}_3$ -treated alumina.

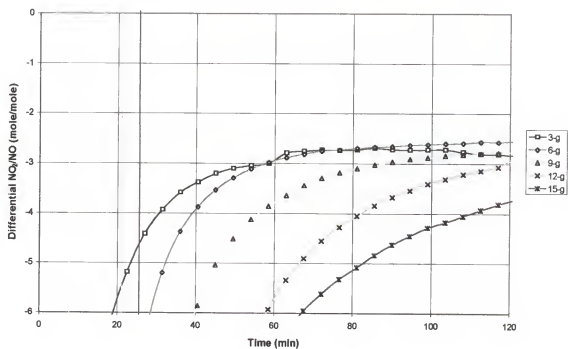


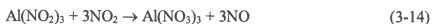
Figure 3-43. Incremental ratio of  $\text{NO}_2$  sorbed/ $\text{NO}$  formed for successive bed layers of layers of KOH-treated alumina.

### Untreated $\gamma$ -Alumina

In saturation tests the overall stoichiometry ( $3\text{NO}_2$  removed per NO formed) has held true for untreated alumina (Lee et al., 1998b). A reaction mechanism is proposed for untreated alumina based on this observation and other properties of exposed  $\gamma$ -alumina. There is no reaction of NO with untreated alumina. The reaction of  $\text{NO}_2$  with untreated  $\gamma$ -alumina may proceed as follows because nitrate is a major product. Nitrite achieves a very low steady state concentration and apparently is highly unstable. The equations suggest specific forms of nitrite and nitrate structures which is arbitrary. However, ISE measures and gas-phase data suggests trends of the proposed stoichiometry.



The nitrite formed in (3-12) may react as follows:



Combining reactions (3-12), and (3-13) or (3-14) provides the following overall reaction:

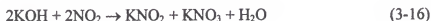


The steady-state nitrite concentration should be small due to the instability of aluminum nitrite. Thus, decomposition reaction (3-13) is proposed to form  $\text{NO}_2$  and NO. The overall reaction stoichiometry is the same applying reaction (3-14). The proposed overall reaction predicts a molar ratio  $\text{NO}_2$  sorbed to NO formed of 3:1. Aluminum nitrite is not commonly produced like other nitrite salts due to its instability. NO is sorbed by  $\gamma$ -alumina in minimal amounts in the presence of  $\text{NO}_2$  and only for a high concentration ratio

of NO:NO<sub>2</sub> feed gas. Sorption of NO by untreated alumina was only observed for an input NO<sub>2</sub>:NO ratio of 500:50 and 500:10 with very low efficiencies of less than 5 percent sorption of NO input.

#### KOH-Treated $\gamma$ -Alumina

In the case of KOH-coated alumina, experimental data suggest that NO<sub>x</sub> interacts strongly with the KOH coating but minimally with the alumina support due to the strong sorption of NO<sub>2</sub> with treated alumina. If this is the case then the following mechanism is possible



These two reactions are proposed because although NO does not react alone, it does react in the presence of NO<sub>2</sub>, and in the presence of NO, NO<sub>2</sub> sorption is enhanced. NO production is delayed, which suggests that an intermediate is necessary for production since potassium nitrite is stable. Nitrite formation also is a function of NO<sub>2</sub> and NO concentrations. Reaction with NO<sub>2</sub> is proposed as a source of NO and nitrate in the later stages of reaction.



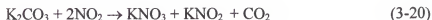
Based on these reactions the overall reaction can be represented by



This overall reaction indicates that in the later stages of reaction, when nitrite is at steady state, a 3:1 molar ratio of NO<sub>2</sub> sorbed to NO produced should be observed.

### K<sub>2</sub>CO<sub>3</sub>-Treated $\gamma$ -Alumina

A similar mechanism is proposed for the reactions of K<sub>2</sub>CO<sub>3</sub>-coated alumina with NOx:



and

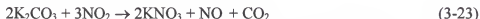


As nitrite builds, reaction (3-20) becomes more important for NO<sub>2</sub> reaction.

Eventually, nitrite will reach steady state.



When nitrite has achieved steady state the overall reaction can be represented by (3-23):



The overall reaction for potassium carbonate coated material predicts a 3:1 molar ratio of NO<sub>2</sub> sorbed to NO formed. In the early stages of exposure reaction (3-21) can remove NO and NO<sub>2</sub> in addition to (3-20) removing NO<sub>2</sub>. The question arises as to the extent of these reactions and the reaction rates prior to and at equilibrium. In heterogeneous processes the reaction rate can be affected by the gas-solid transport mechanism. Presumably in this case the sorption is reaction controlled rather than diffusion controlled as discussed previously.

### Confirmation of NO Production from Nitrite-NO<sub>2</sub> Interaction

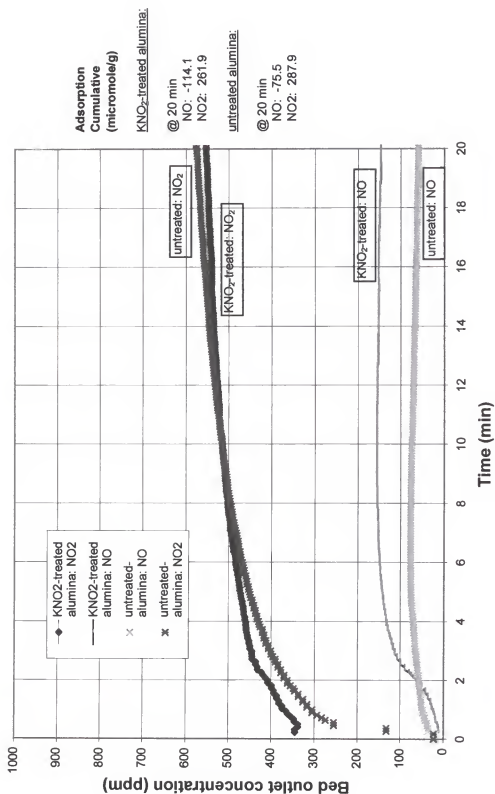
Based on experimental observations, reactions (3-12) through (3-23) were formulated to account for the observed sorption of NOx by the three sorbents. Two tests

were performed to evaluate the final step in all three mechanisms in which  $\text{NO}_2$  reacts with surface nitrite to form NO and surface nitrate. The first test evaluated the differences in  $\text{NO}_2$  sorption for untreated and  $\text{KNO}_2$ -treated alumina. Similar (mass) samples were exposed to  $\text{NO}_2$  gas (741 ppm) at a flow of 0.75 sLpm at 25 °C. The bed outlet concentrations of NO and  $\text{NO}_2$  as a function exposure time are shown in Figure 3-44. From this figure it is seen that the amount of  $\text{NO}_2$  sorbed is similar for both sorbents. However, the production of NO is much greater for the  $\text{KNO}_2$ -treated alumina sample. Also shown in Figure 3-44 are the accumulated amounts of  $\text{NO}_2$  sorbed and NO produced by the two sorbents. This test indicated that, indeed,  $\text{KNO}_2$  treatment more readily converts  $\text{NO}_2$  into NO than does untreated alumina. Another test was performed to measure the concentrations of nitrite and nitrate on  $\text{KNO}_2$ -treated alumina at different times of exposure to  $\text{NO}_2$ .

Two 5-gram samples of  $\text{KNO}_2$ -treated alumina were exposed to a mixture of certified 4750 ppm  $\text{NO}_2$  in  $\text{N}_2$  gas at a flow of 0.75 sLpm at 25 °C. The  $\text{NO}_x$  exposure results and data for the measures of nitrite and nitrate on the two samples are shown in Figure 3-45. The results indicate that the nitrite does react to form nitrate and that the nitrite-to-nitrate conversion is proportional to  $\text{NO}_2$  sorption.

#### Fourier Transform Infrared (FTIR) Spectroscopy Confirmation of ISE Measurements

Analysis of samples for surface nitrite and nitrate species was carried out using ion-specific electrode (ISE) methods. The ISE methods require that the sorbent samples be in the form of aqueous extracts and adjusted for pH. The ISE procedure is subject

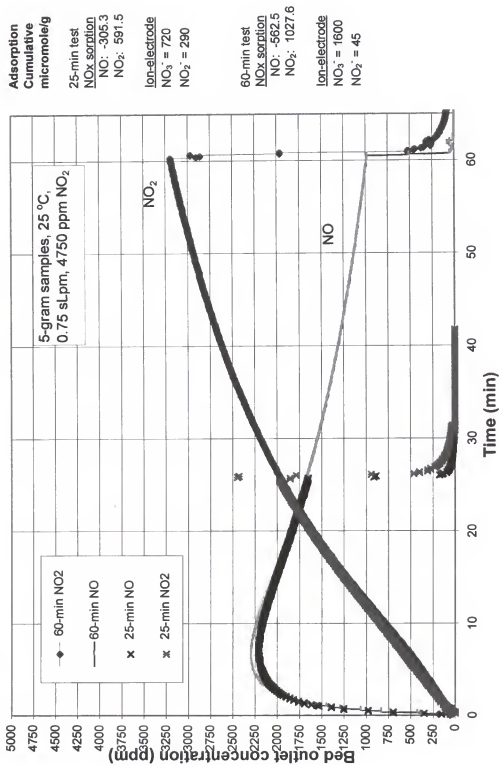
Figure 3-44. NO<sub>2</sub> sorption activity of KNO<sub>2</sub>-treated and untreated alumina.

to error due to the possible effects resulting from solution analysis of sorbed ions from a dry or solid material. Therefore, another analytical method that does not require dissolution of the sorbent prior to analysis for surface species was chosen to confirm that the ISE measurements were not affected by the preparation and measurement procedures.

FTIR is a spectroscopic technique that can measure the absorbance of reflected infrared light that is characteristic of the material from which it is reflected. Reference materials included ACS reagent grade  $\text{KNO}_3$ ,  $\text{KNO}_2$ , and  $\text{K}_2\text{CO}_3$ . Reference literature was used to determine the regions of frequency or wave number that have been established as being characteristic of specific function groups or indicative of a given compound (Nyquist and Kagel, 1971). Sorbent samples before and after treatment and  $\text{NO}_x$  exposure were analyzed against specific references to determine the changes due to treatment and  $\text{NO}_x$  exposure. Separate portions of two samples of  $\text{K}_2\text{CO}_3$ -treated alumina tested in the gas profile study and tested by ISE were analyzed by FTIR for comparison.

First, the reference materials  $\text{KNO}_2$ ,  $\text{KNO}_3$ , and  $\text{K}_2\text{CO}_3$  were analyzed. FTIR spectra scans of these materials are shown in Figures 3-46, 3-47 and 3-48, respectively. Pure samples of  $\text{KNO}_3$  and  $\text{KNO}_2$  show low absorbancies for peaks at  $1320\text{ cm}^{-1}$  [0.010 absorbance units (au)] and  $1210\text{ cm}^{-1}$  [0.0794 au]. These spectra indicate the low sensitivity of the FTIR method for these compounds. Note that absorption peaks for gaseous  $\text{CO}_2$  are typically present in all spectra as background. The gas purge system attached to the FTIR analysis chamber was not able to remove all of the air within the chamber. However absorptions of the common gases  $\text{H}_2\text{O}$  vapor and  $\text{CO}_2$  do not occur in the regions of interest. Specific peaks for  $\text{KNO}_3$  and  $\text{KNO}_2$  are found at  $810$  and  $790\text{ cm}^{-1}$ ,



Figure 3-45. Sorption of NO<sub>2</sub> to KNO<sub>2</sub>-treated alumina with subsequent ISE analysis.

respectively. The  $K_2CO_3$  spectrum has a broad absorbance region near  $1330\text{ cm}^{-1}$  and a more specific peak at  $890\text{ cm}^{-1}$ .

The spectrum for untreated alumina is shown in Figure 3-49. No specific peaks are identifiable. This spectrum is also used for comparison to  $K_2CO_3$ -treated alumina, see Figure 3-50. The spectrum of  $K_2CO_3$ -treated alumina indicates a shift in the broad peak for pure  $K_2CO_3$  at  $1330\text{ cm}^{-1}$  to a maximum peak position of  $1400\text{ cm}^{-1}$ . This shift suggests that the coating treatment of  $K_2CO_3$  results in a different binding energy than bulk  $K_2CO_3$ . Also observable are specific peaks at  $1000\text{ cm}^{-1}$  and  $810\text{ cm}^{-1}$ . The reference literature indicates a strong broad absorption at  $1320\text{--}1530\text{ cm}^{-1}$ , and weak absorptions near  $1040\text{--}1100$ ,  $800\text{--}890$ , and  $670\text{--}745\text{ cm}^{-1}$  occur.

Two samples of  $K_2CO_3$ -treated alumina that were exposed to  $NO_x$  in the gas profile study were analyzed by FTIR (Figures 3-51 and 3-52). The first sample was the same as that from the top layer in the gas profile study (see Figure 3-36, 120 minute exposure, layer 1). The FTIR spectrum of the sample shows increased absorbance in regions near  $1350\text{ cm}^{-1}$  and  $1220\text{ cm}^{-1}$ . Also, a peak near  $750\text{ cm}^{-1}$  is observed. Reference literature indicates nitrite broad strong absorption near  $1170\text{--}1320\text{ cm}^{-1}$  and a weak bond near  $820\text{--}850\text{ cm}^{-1}$ . Also published literature indicates that nitrate has a strong, broad absorption near  $1280\text{--}1520\text{ cm}^{-1}$  and weak absorptions near  $1020\text{--}1060$ ,  $800\text{--}850$ , and  $715\text{--}770\text{ cm}^{-1}$ . Measurements of nitrate and nitrite ions on this sample by ISE indicate that nitrate and nitrite concentrations were  $0.75\text{ mmol/g}$  and  $0.22\text{ mmol/g}$ , respectively. The second  $NO_x$ -exposed  $K_2CO_3$ -treated alumina sample analyzed by FTIR was that from the fourth layer in the gas profile study. The FTIR spectrum of the sample showed

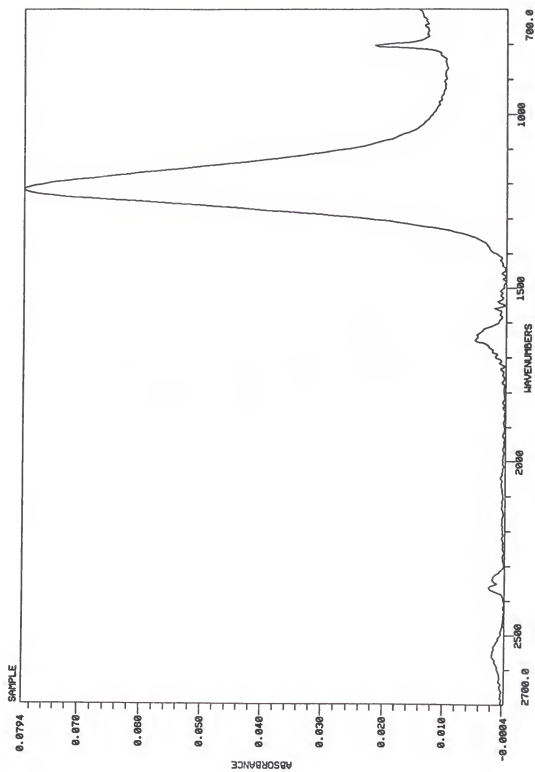
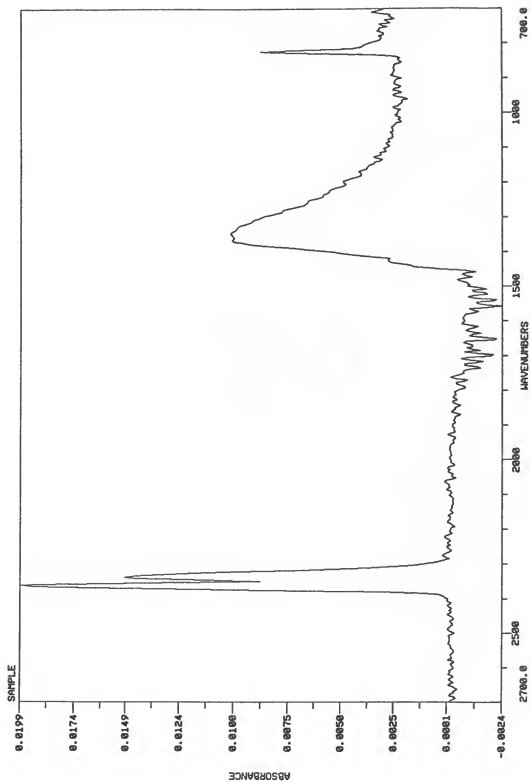


Figure 3-46. FTIR spectrum of reagent-grade KNO<sub>3</sub>.

Figure 3-47. FTIR spectrum of reagent-grade  $\text{KNO}_3$ .

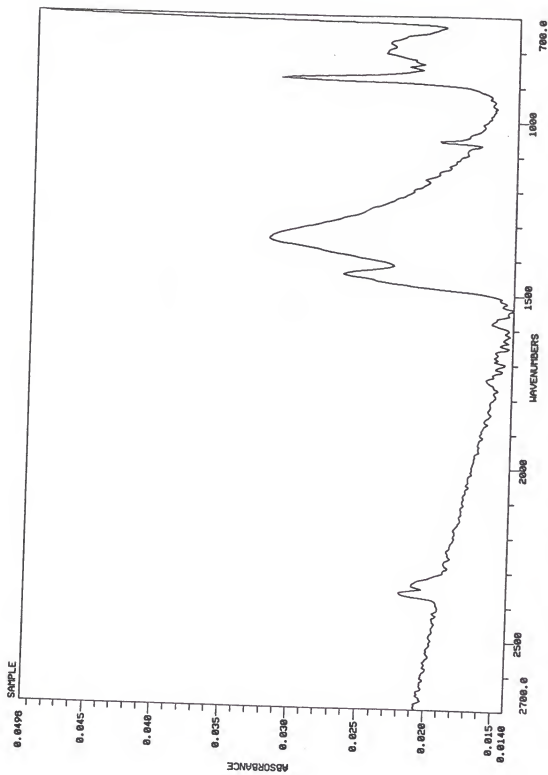


Figure 3-48. FTIR spectrum of reagent-grade  $K_2CO_3$ .

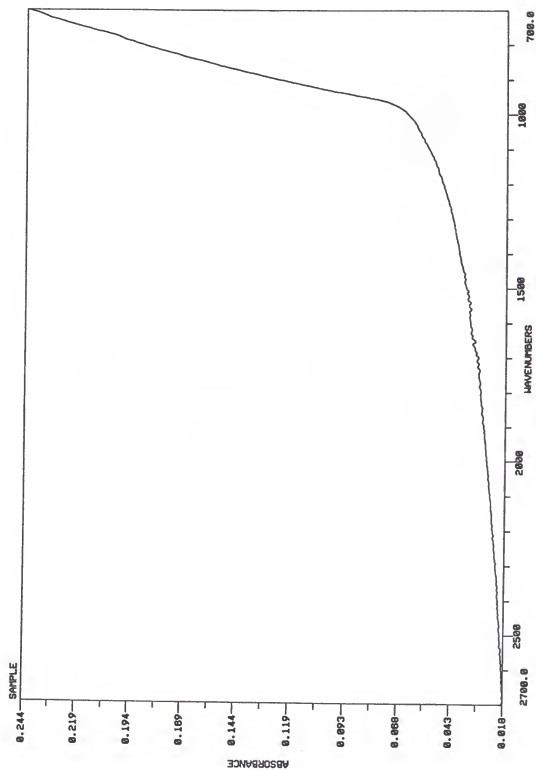


Figure 3-49. FTIR spectrum of untreated alumina.

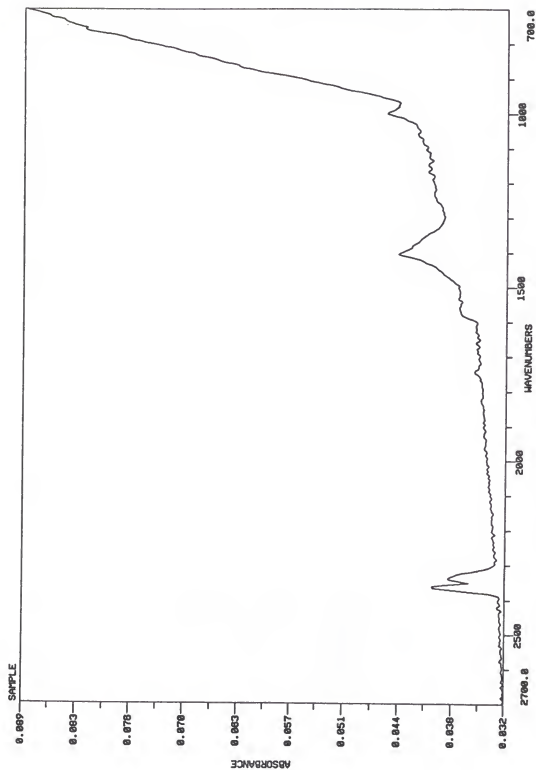


Figure 3-50. FTIR spectrum of  $K_2CO_3$ -treated alumina.

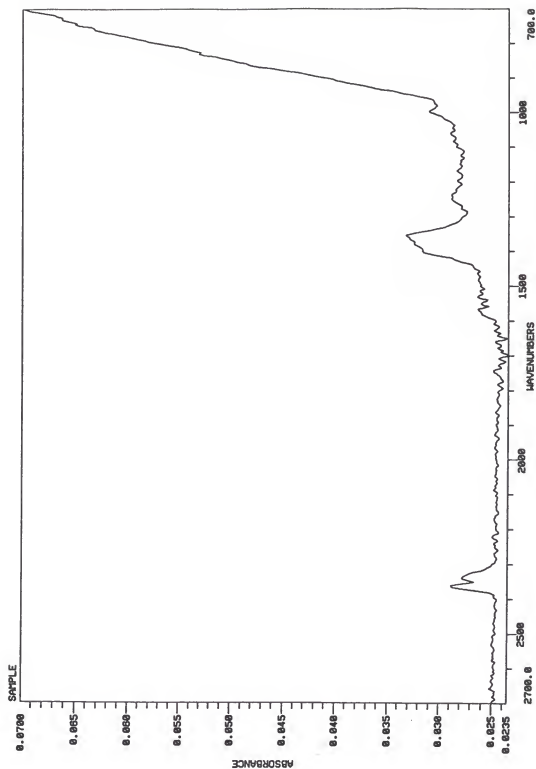


Figure 3-51. FTIR spectrum of  $K_2CO_3$ -treated alumina after exposure to  $NO_x$  (1st layer)



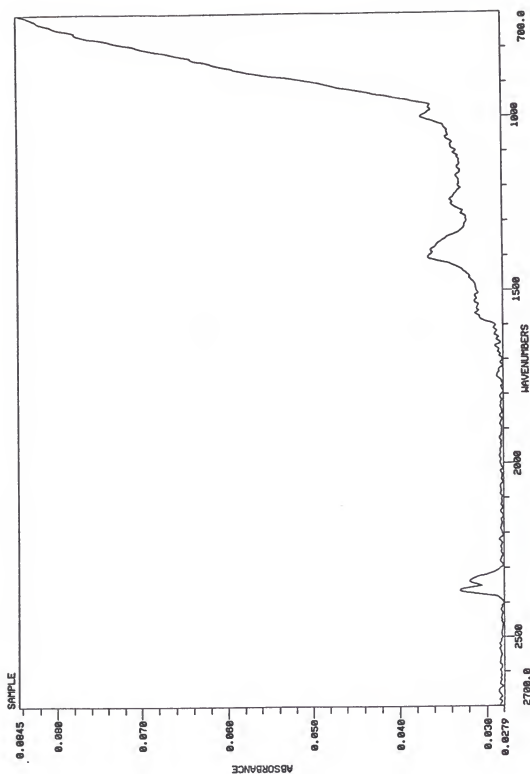


Figure 3-52. FTIR spectrum of  $K_2CO_3$ -treated alumina after exposure to  $NO_x$  (4th layer)

decreased absorbance in the region near  $1350\text{ cm}^{-1}$  relative to the first sample and that the peak near  $1220\text{ cm}^{-1}$  has a similar absorbance. Also, the peak at  $750\text{ cm}^{-1}$  on the first sample was not observed on this sample. The ISE measurements for this sample showed nitrate and nitrite accumulations to be 0.01 and 0.23 mmol/g, respectively.

The FTIR results qualitatively indicate that the measurements of nitrate and nitrite by ISE analyses to correspond with the FTIR data. However, quantitation of FTIR data is not reliable due to low sensitivity.

#### Thermal Decomposition Studies

A method to possibly examine surface materials and changes in their properties can be performed by thermally decomposing samples. Specific instruments such as differential thermal analyzers (DTA) based on this principle have been designed solely for this purpose and can be obtained commercially. However, the fixed-bed reactor system can also be used to simulate this method. Samples can be placed in the reactor tubes and gradually heated in a flow of inert gas to carry the gaseous decomposition products to the NO<sub>x</sub> analyzer. The decomposition gases can be analyzed for emissions of NO and NO<sub>2</sub>. This information may allow for evaluation of changes in properties of sorbed materials during and after NO<sub>x</sub> exposure. The decomposition temperature at which NO<sub>x</sub>-exposed sorbents release sorbed NO<sub>x</sub> should provide knowledge of the limiting temperature at which these sorbent can effectively perform as NO<sub>x</sub> sorbents. Reference materials, such as nitrite and nitrate salts can be decomposed and their decomposition properties compared with NO<sub>x</sub>-exposed sorbents. Samples of sorbents that have been analyzed by ISE for nitrite and nitrate can be thermally decomposed to allow for comparative analyses of the sample.

A crucial point should be made prior to discussion of the results of these decomposition tests. After completing the series of decomposition tests indicated that stainless steel reacts with  $\text{NO}_2$  at temperatures above  $550^\circ\text{C}$ . Sigsby et al. (1973) observed this phenomenon and this property is used in the chemiluminescent detection of  $\text{NO}_2$ . Thus, it is expected that decomposition data obtained at temperatures above  $550^\circ\text{C}$  maybe affected by this phenomenon and could be invalid. However, in these decomposition tests it is observed that  $\text{NO}_2$  is emitted at temperatures above  $550^\circ\text{C}$ . The reason for this is probably due to several factors including the physical design of the fixed-bed reactor and flow of gas within the reactor.

During the decomposition of a sample in the reactor bed, the gas decomposes from the sample in the sorbent tube and flows downward into a region of the stainless steel tube where the temperature decreases substantially over a space of several inches. Depending on the flowrate of the  $\text{N}_2$  carrier gas, the decomposition products may not have sufficient exposure time at high temperatures to react with the stainless steel walls and convert  $\text{NO}_2$  into  $\text{NO}$ . A test was carried out to observe conversion of  $\text{NO}_2$  into  $\text{NO}$  in the fixed-bed reactor system. It was found that by flowing  $\text{NO}_2$ -laden gas through an empty reactor tube, the conversion of  $\text{NO}_2$  to  $\text{NO}$  can occur more extensively as the gas experiences higher temperatures in regions above the sorbent bed and longer residence times in the reactor bed region.

#### Decomposition of $\text{NO}_2$ -Exposed Sorbents: Varied Exposure Time

Three types of materials: untreated,  $\text{K}_2\text{CO}_3$ -treated, and  $\text{KOH}$ -treated  $\gamma$ -alumina were exposed to  $\text{NO}_2$  (500 ppm) for varied lengths of time to observe changes in thermal

decomposition products from the sorbents. Three-gram samples were placed in the fixed-bed reactor and simultaneously exposed to  $\text{NO}_2$  at a molar flow of  $0.098 \text{ mol NO}_2/\text{min}$  for 10, 15 (only untreated alumina), 30 and 120 minutes. For the shorter time exposure data were not collected during the sorption process as the amount of gas used during the initial exposure was less than that required for the  $\text{NO}_x$  analyzer. However, the sorption for these short-time exposures can be followed by observing the sorption process at the beginning of exposure for the longer time exposures, during which data were collected. After  $\text{NO}_2$  exposure the samples were either stored or immediately decomposed *in situ* by flowing  $\text{N}_2$  carrier gas through the bed and ramping the bed temperature. The sorption processes for 120-minute exposure of the three sorbents are shown in Figure 3-53. Corresponding thermal decomposition profiles of samples for the three materials at 10, 30 and 120 minutes  $\text{NO}_x$ -exposure are presented in Figures 3-54 to 3-62. The decomposition profiles provide the temperature of the bed and corresponding  $\text{NO}_2$  and  $\text{NO}$  concentration over time. It was necessary to control and keep consistent the rate of temperature increase for a comparison of data. All subsequent decomposition tests used a constant temperature ramp of  $10^\circ\text{C}/\text{min}$  and  $\text{N}_2$  flowrate of  $1 \text{ sLpm}$ .

As the quantity of decomposition products increased with  $\text{NO}_2$  exposure time it was necessary to either decrease the sample size, increase the  $\text{N}_2$  flowrate, or decrease the temperature ramping rate. Thus it was decided to well-mix the sample and decompose only a portion of the sample at an increased flowrate of  $\text{N}_2$ . An added benefit is that increasing the flow rate improves the resolution of emission peaks. The 120-minute exposure samples were decomposed using 1-gram portions of the total 3-gram sample.

Also, the flowrate was increased from 1 to 3 Lpm. The tests had to be predicted for the emission rates of decomposed gas in order to either adjust the sample mass for decomposition or the flowrate of  $N_2$ . Thus, several sample had to be repeatedly decomposed in order to obtain a decomposition profile where the gas emitted remained on the NO<sub>x</sub> analyzer measuring range.

Decomposition of the NO<sub>x</sub>-exposed untreated alumina samples show three significant regions at 150, 325, and 550 °C for NO emissions and one peak for NO<sub>2</sub> emissions at 500 °C. With greater time of exposure to NO<sub>x</sub> the NO<sub>2</sub> peak increases relative to the NO peaks.

Decomposition of K<sub>2</sub>CO<sub>3</sub>-treated alumina showed a distinctive peak pattern at 600 to 650 °C that remains consistent with irregardless of NO<sub>x</sub> exposure. The peak is forward tailed and may be composed of several unresolved peaks.

Decomposition of the 10 and 30 minute NO<sub>2</sub>-exposed sample of KOH-treated alumina shows a more symmetrical peak pattern than NO<sub>x</sub>-exposed K<sub>2</sub>CO<sub>3</sub>-treated alumina. The temperature of decomposition is about 600 °C. The 120 minute NO<sub>x</sub> exposure with an increased flow provides an emission peak pattern composed of several unresolved peaks major peak.

#### Decomposition of Pure Compounds Treated onto $\gamma$ -Alumina

ACS reagent-grade KNO<sub>3</sub>, KNO<sub>2</sub>, and Al(NO<sub>3</sub>)<sub>3</sub>·9H<sub>2</sub>O were dissolved in individual portions of N<sub>2</sub>-flushed DI water to provide solutions for coating alumina pellets. The alumina in the treating solution was dried at 150 °C for 24 hours. During drying a slow flow of N<sub>2</sub> gas was maintained over the solution to prevent oxidation or contamination.

These dried synthetic materials supported on alumina were then decomposed to provide the emissions vs. temperature data seen in Figures 3-63 to 3-65. The similarities between  $\text{KNO}_3$ -treated alumina decomposition pattern (Figure 3-63) and that of  $\text{NO}_2$ -exposed untreated alumina (Figure 3-56) are noteworthy. A symmetrical  $\text{NO}_2$  peak occurs near  $500^\circ\text{C}$  followed by a smaller  $\text{NO}$  peak at higher temperature ( $\sim 600^\circ\text{C}$ ). The  $\text{KNO}_2$ -treated alumina shows two  $\text{NO}$  peaks at  $300$  and  $600^\circ\text{C}$ . The  $\text{NO}$  peak at  $300^\circ\text{C}$  is accompanied by a broad  $\text{NO}_2$  peak of much lower magnitude. Also, the low-temperature  $\text{NO}$  peak ( $300^\circ\text{C}$ ) and accompanying  $\text{NO}_2$  peak are similar to the peaks observed for untreated alumina exposed to very small quantities of  $\text{NO}_2$  (see Figure 3-54, 10 min.  $\text{NOx}$ -exposed untreated alumina). Decomposition of aluminum nitrate-treated alumina shows a peak near  $300^\circ\text{C}$  but its decomposition pattern does not appear to be similar to  $\text{NOx}$ -exposed untreated alumina. The only similarity appears to be the  $\text{NO}$  peak at  $300^\circ\text{C}$ .

#### Decomposition of Pure Salts

Pure  $\text{KNO}_3$  and  $\text{KNO}_2$  salts were decomposed in the fixed-bed reactor.  $\text{KNO}_2$  did not decompose at temperatures less than  $500^\circ\text{C}$ . Two peaks appeared near  $625$  and  $700^\circ\text{C}$ . Pure  $\text{KNO}_3$  decomposed producing  $\text{NO}_2$  at  $275^\circ\text{C}$  followed by a  $\text{NO}$  peak at  $350^\circ\text{C}$ . The major fraction of these nitrogen salts did not decompose below  $600^\circ\text{C}$ . Decomposition of pure nitrite and nitrate salts resulted in a melt that solidified at lower temperatures. The material that condensed throughout the system was very reactive with  $\text{NOx}$ . Thus, the results are not reliable. No further tests of pure salts were carried out. The effect of coating the pure salts onto high-surface area  $\gamma$ -alumina appears to reduce the

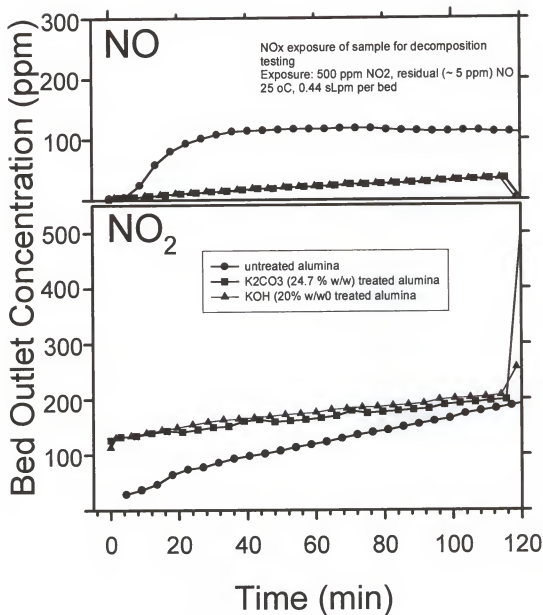


Figure 3-53. Representative NO<sub>x</sub>-exposure test for samples decomposed after varied NO<sub>x</sub>-exposure times.

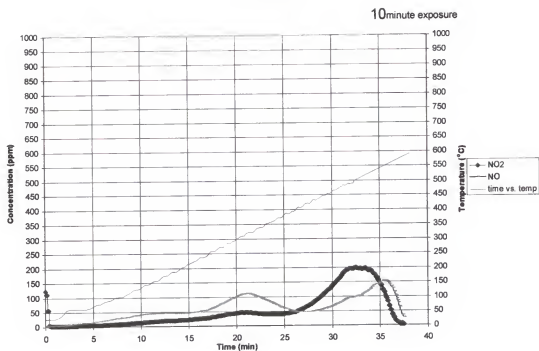


Figure 3-54. Thermal decomposition of untreated alumina after 10-min exposure to NO<sub>x</sub>.

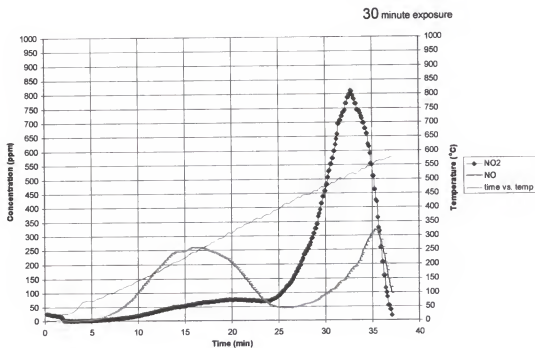


Figure 3-55. Thermal decomposition of untreated alumina after 30-min exposure to NO<sub>x</sub>.



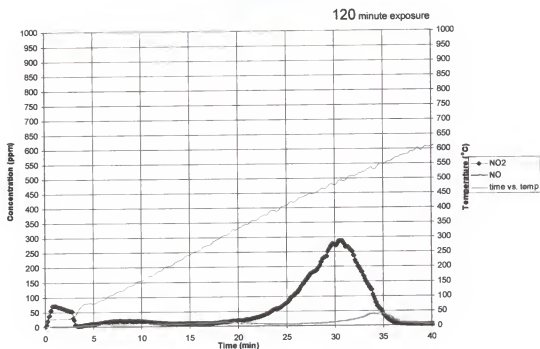


Figure 3-56. Thermal decomposition of untreated alumina after 120-min exposure to NOx.

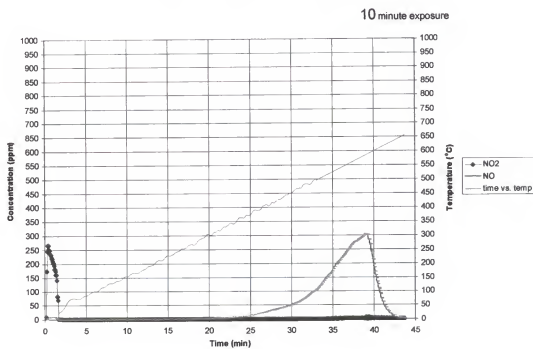


Figure 3-57. Thermal decomposition of K<sub>2</sub>CO<sub>3</sub>-treated alumina after 10-min exposure to NOx.

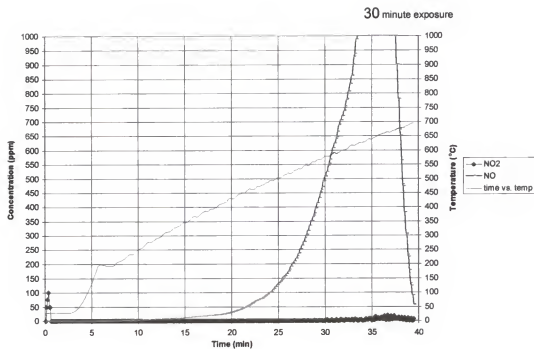


Figure 3-58. Thermal decomposition of  $K_2CO_3$ -treated alumina after 30-min exposure to  $NO_x$ .

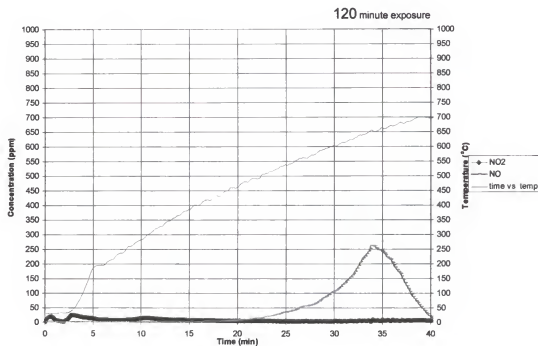


Figure 3-59. Thermal decomposition of  $K_2CO_3$ -treated alumina after 120-min exposure to  $NO_x$ .

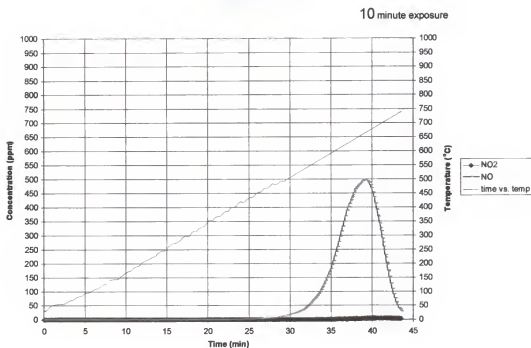


Figure 3-60. Thermal decomposition of KOH-treated alumina after 10-min exposure to NO<sub>x</sub>.

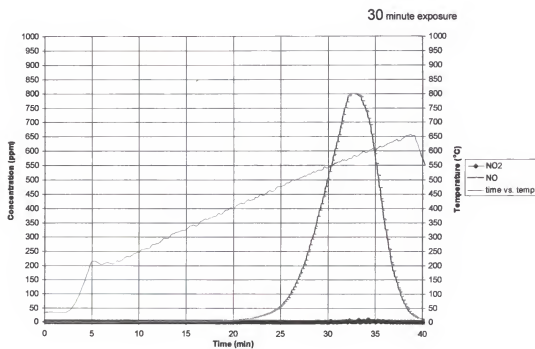


Figure 3-61. Thermal decomposition of KOH-treated alumina after 30-min exposure to NO<sub>x</sub>.

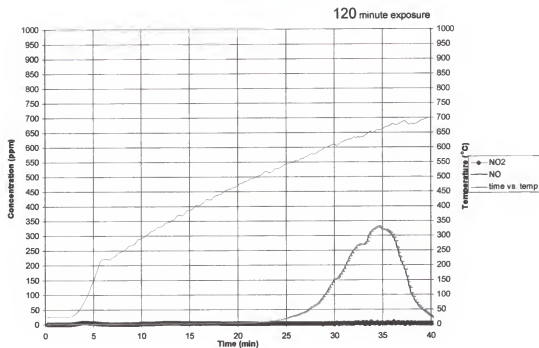


Figure 3-62. Thermal decomposition of KOH-treated alumina after 120-min exposure to NO<sub>x</sub>.

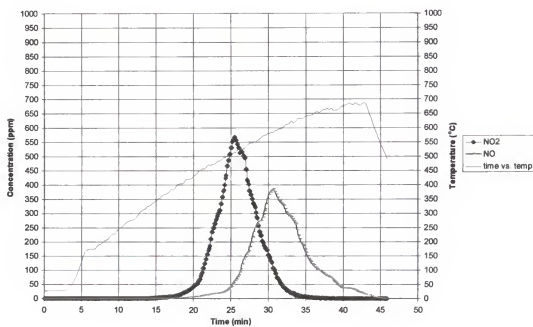


Figure 3-63. Thermal decomposition of KNO<sub>3</sub>-treated alumina.

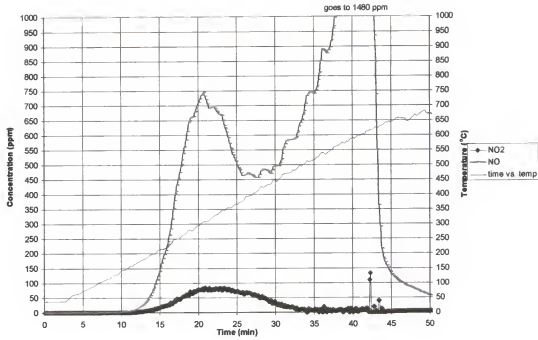


Figure 3-64. Thermal decomposition of KNO<sub>2</sub>-treated alumina.

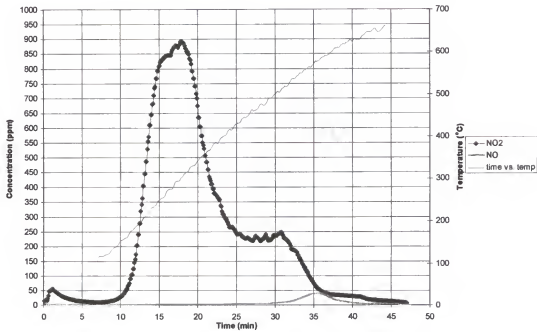


Figure 3-65. Thermal decomposition of aluminum nitrate-treated alumina.

bonding energy as observed by the decreased decomposition temperatures for  $\text{KNO}_2$ - and  $\text{KNO}_3$ -treated alumina.

#### Effect of Additional Gases on $\text{NO}_x$ Sorption

Three types of materials: untreated,  $\text{K}_2\text{CO}_3$ -treated, and  $\text{KOH}$ -treated alumina were exposed to  $\text{NO}_x$  (500 ppm  $\text{NO}_2$  and 500 ppm  $\text{NO}$ ) and other gases:  $\text{H}_2\text{O}$  vapor,  $\text{O}_2$ ,  $\text{CO}_2$ , and  $\text{SO}_2$  in the fixed-bed reactor system at 25 and 250 °C. Certified cylinder gases of  $\text{O}_2$  (1% in  $\text{N}_2$ ),  $\text{SO}_2$  (100 ppm in  $\text{N}_2$ ), and  $\text{CO}_2$  (100% industrial grade) were used to supply the added gases.  $\text{H}_2\text{O}$  vapor was supplied using  $\text{N}_2$  flow through water and assuming the saturation vapor pressure of water at a specific temperature. A thermocouple was used to measure the temperature of the water. The temperature was used to find the saturation vapor pressure of  $\text{H}_2\text{O}$  and this vapor pressure was used to calculate the concentration of input  $\text{H}_2\text{O}$  vapor. The saturated gas is mixed with a other gases to produce a gas mixture with the desired  $\text{NO}_x$  concentrations. Concentrations of added gases are estimated by flow rate measurements. The effect on  $\text{NO}_x$  sorption is determined by the  $\text{NO}_x$  analyzer measurements.

#### Added $\text{H}_2\text{O}$ vapor

Water vapor was added at a concentration of approximately 23000 ppm. The data from these experiments were compared to similar samples without  $\text{H}_2\text{O}$  vapor. Measurements were also made using an empty sorbent reactor tube at 250 °C. Approximately 5% reduction of  $\text{NO}_2$  uptake was observed when the  $\text{H}_2\text{O}$  vapor is present. A correction factor was used in the calculations for the measured  $\text{NO}_x$  sorption in the added water tests due to changes in empty bed residence times at effluent temperatures.

Reproducibility tests for each run were carried out. The results in cumulative sorption of NO and NO<sub>2</sub>  $\mu\text{mole/g}$  for the three tested materials can be found in Appendix C. The tests were performed at 25, 100, and 250 °C. In the case of untreated alumina, added H<sub>2</sub>O vapor significantly increases the sorption of both NO and NO<sub>2</sub> at 25 °C when the partial pressure of H<sub>2</sub>O vapor in the gas is constant. The effect of added water to the sorption of NO<sub>2</sub> and NO is similar at 25 and 250 °C for untreated alumina. The sorption of NO<sub>2</sub> is increased 25% at 25 °C and 250 °C. An unexpected result was observed at 100 °C. The effect of H<sub>2</sub>O vapor on NO<sub>x</sub> sorption was significantly less than at 25 °C or 250 °C. Given the excellent reproducibility of the data this anomalous effect defies explanation.

For the K<sub>2</sub>CO<sub>3</sub>-treated (24.7% w/w) and KOH-treated (20 % w/w) alumina the effect at 25 °C of H<sub>2</sub>O vapor is most significant in increasing NO sorption. The effect of H<sub>2</sub>O vapor is less at 100 °C and further reduced at 250 °C. There is no effect on NO<sub>x</sub> sorption at 250 °C for K<sub>2</sub>CO<sub>3</sub>-treated alumina. NO<sub>x</sub> sorption on KOH-treated alumina appears to be more affected than K<sub>2</sub>CO<sub>3</sub>-treated alumina by the presence of water at higher temperatures.

#### Added O<sub>2</sub> gas

The effect of added O<sub>2</sub> (8800 ppm) on NO<sub>x</sub> sorption was studied for all three materials under the conditions of 500 ppm NO<sub>2</sub> and 500 ppm NO and found to be negligible at both 25 and 250 °C. Multiple runs were performed to confirm the results.

### Added CO<sub>2</sub> gas

The effect of added CO<sub>2</sub> on NO<sub>x</sub> sorption was studied for all three materials (10% v/v) using 500 ppm NO<sub>2</sub> and 500 ppm NO and found to be negligible at both 25 and 250 °C. Multiple runs were performed to confirm the results.

### Added SO<sub>2</sub> gas

The effect of added SO<sub>2</sub> gas (83 ppm) on NO<sub>x</sub> sorption was studied using 500 ppm NO<sub>2</sub> and 500 ppm NO. SO<sub>2</sub> concentrations were limited to the certified cylinder gas concentration. The results in cumulative sorption of NO and NO<sub>2</sub> μmole/g for the three tested materials are appended.

At 25 °C SO<sub>2</sub> causes an increase in NO production by untreated alumina. This increase may be due to SO<sub>2</sub> competitively sorbing to available sites to NO<sub>x</sub>. Thus, the surface saturation and conversion of formed surface nitrite to nitrate occurs more readily. Results for K<sub>2</sub>CO<sub>3</sub>-treated alumina indicate NO<sub>2</sub> removal is decreased while NO removal is slightly increased at 25 °C. While the reduction of NO<sub>2</sub> removal may be expected as seen for untreated alumina, the increased removal of NO is curious. This observed increase in NO removal may be due to other surface species formed in coordination with NO. A recent paper (Rochelle and Nelli, 1998) states that improved sorption of NO<sub>2</sub> due to added SO<sub>2</sub> is probably due to the formation of sulfur–nitrogen compounds that effectively sorb NO<sub>2</sub> and do not decompose upon further exposure to NO<sub>2</sub>. Thus, both enhanced NO<sub>2</sub> and NO sorption is observed at 25 °C (Rochelle and Nelli, 1998). Results for KOH-treated alumina do not indicate that SO<sub>2</sub> affects the sorption of NO<sub>x</sub>. At 250 °C



the data do not indicate any effect of  $\text{SO}_2$  on  $\text{NO}_x$  sorption for any of the sorbents. The tests were not reproduced due to experimental equipment constraints.

## CHAPTER 4

### CONCLUSIONS AND RECOMMENDATIONS

The gas-solid interactions of NO<sub>x</sub> and other common combustion-exhaust gases with selected sorbents were studied using an isothermal fixed-bed tubular-flow reactor and supporting analytical methods. The fixed-bed reactor was a specially designed and constructed tubular flow system with automated data collection of NO<sub>x</sub> concentrations from the inlets and outlets of three parallel sorbent tubes. Supporting analytical methods included X-ray photoelectron spectroscopy (XPS), ion-specific electrode (ISE) measurements (qualitatively confirmed by Fourier transform infrared spectroscopy (FTIR)), and BET surface-property measurements. In addition, the fixed-bed reactor was used to thermally decompose samples as a method to evaluate the stability and characteristics of surface nitrogen species as well as regeneration capacity.

Initial studies were based on a material previously studied as a NO<sub>x</sub> sorbent, magnesium oxide-coated vermiculite (MgO/v). Kimm (1995) has shown that NO, alone, is not sorbed by MgO/v. Kimm's experiments indicated that sorption of NO<sub>2</sub> resulted in NO formation in a 3:1 ratio. Given that NO did not sorb to MgO/v, initial experiments were performed using a feed-gas ratio of NO<sub>2</sub>:NO near 10:1. This ratio for combustion exhaust must assume some preliminary method is used to convert NO into NO<sub>2</sub>.

Experiments were performed to observe the effects of water-wetted beds of MgO/v. These tests indicated water-wetting increased NO<sub>2</sub> sorption and decreased NO

formation. However, as the bed temperature increased from 50 to 200 °C the effect of water decreased. NO<sub>x</sub>-saturation tests of sorbents indicated that water vapor affected NO<sub>x</sub> sorption at 200 °C. Previous research on similar solid materials yielded mechanisms that consider sorption of NO<sub>x</sub> as a gas-to-liquid (surfacial) interaction (Rochelle and Nelli, 1998). This effect at 200 °C indicates that another form of interaction other than that due to bulk liquid water was possible.

A comparison of MgO/v and  $\gamma$ -alumina sorbents in fixed-bed reactor tests indicates  $\gamma$ -alumina similarly converts sorbed NO<sub>2</sub> into NO in a 3:1 ratio. However,  $\gamma$ -alumina showed a significant increase in NO<sub>x</sub> sorption activity while presenting less pressure drop for the material tested. Additional advantages of  $\gamma$ -alumina are that it can be obtained in various forms and with specified chemical and physical properties that are not available for MgO/v.

Subsequent XPS analysis of NO<sub>x</sub>-exposed  $\gamma$ -alumina suggested that potassium impurities were active in the NO<sub>x</sub> sorption process. A literature search indicated that group-I alkali metal compounds have been tested and used to effectively sorb NO<sub>x</sub> originating from various sources (Jacobs and Hocheiser, 1958; Ma et al., 1995; American Public Health Association, 1939–1940). KOH-precipitated onto  $\gamma$ -alumina was tested in the fixed-bed reactor system and sorbed both NO and NO<sub>2</sub>. Accordingly,  $\gamma$ -alumina was treated with group-I alkali metal compounds (Na and K carbonates and hydroxides) and comparatively tested for optimum amounts of coating and NO<sub>x</sub> sorption over a range of temperatures and varied NO gas concentrations. From these tests it became apparent that the coating amount was limited by a threshold below which the pellets remained

structurally stable. Also, greater coating amounts drastically reduced the efficiency of NO<sub>x</sub> removal. Temperature effects on NO<sub>x</sub> sorption were small over the range from 100 to 200 °C.

The effect of varying the group-I alkali metal was evaluated for NO<sub>x</sub> sorption using lithium, sodium, potassium, rubidium, and cesium as carbonate and hydroxide compounds. These tests indicated that the activity of group-I compounds is related to the ionization potential of the group-I element. Thus, on a molar basis, cesium compounds most effectively sorbed NO<sub>x</sub>. Similar to MgO/v, all other sorbents did not sorb NO, in the absence of NO<sub>2</sub>. Surface area measurements of these materials and untreated  $\gamma$ -alumina indicated that a decrease in surface area due to treatment was related to the atomic radius of the corresponding element. In addition, BET measures of pore size distributions suggested that sorption of NO<sub>x</sub> is limited by closure of the sorbent pores.

After the observation that NO and NO<sub>2</sub> are sorbed by treated materials, two series of fixed-bed reactor tests compared the sorption of NO and NO<sub>2</sub> over a range of temperatures (25 to 250 °C) for three materials: untreated, K<sub>2</sub>CO<sub>3</sub>-treated, and KOH-treated alumina. The K<sub>2</sub>CO<sub>3</sub>-treated and KOH-treated were considered as possible NO<sub>x</sub>-sorbents because they are better NO<sub>x</sub> sorbents than their sodium analogues, and untreated alumina was evaluated as it is the support material. In the first series, the NO<sub>2</sub> concentration (500 ppm) was held constant and NO (10, 50, 200, and 500 ppm) was varied. All tests of the untreated alumina showed immediate NO production in a 3:1 ratio of the NO<sub>2</sub> sorbed. Sorption of NO<sub>2</sub> did not significantly vary as the NO<sub>x</sub> concentration was varied. For the two treated sorbent materials, the sorption of NO<sub>2</sub> did not

significantly differ as the input NO concentration varied. However, the sorption of NO increased at higher input NO concentration and at increased temperatures such that NO sorption became unlimited at 250 °C. ISE measurements of the samples exposed at 200 °C indicated a near 2:1 relation of increased nitrite formation to increased NO sorption.

In the second series, the NO concentration (500 ppm) was held constant and NO<sub>2</sub> (10, 50, 200, and 500 ppm) concentration was varied. The treated sorbent materials showed at 25 °C that NO sorption increased with increased input NO<sub>2</sub> concentration except for the 500 ppm input of NO<sub>2</sub>. Maximum cumulative NO sorbed was less at 500 than 200 ppm input NO<sub>2</sub> indicating a limit of NO sorption was reached. However, as temperature increased NO sorption increased such that at 250 °C NO sorption was a linear function of the input NO<sub>2</sub> concentration. For the untreated alumina, tests with 500 and 200 ppm input NO<sub>2</sub> showed immediate NO production in a 3:1 ratio. However, minor amounts of NO sorption by untreated alumina were observed for an input NO<sub>2</sub>:NO ratio of 500:50 and 500:10 with efficiencies of less than 5 percent of NO input.

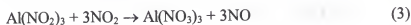
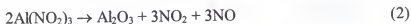
Additional fixed-bed reactor tests with supporting ISE analyses were performed as the "longbed" series to help derive general reaction mechanisms for three materials: untreated alumina, K<sub>2</sub>CO<sub>3</sub>-treated and KOH-treated alumina. The reactor tests exposed large samples of the three materials to 1950 ppm NO<sub>2</sub> and residual amounts of NO (6 ppm) at 25 °C. After exposure the samples were divided into sections and analyzed by ISE for nitrite and nitrate concentrations. Other reactor tests exposed smaller increments of the large sample masses to the same conditions to provide an indication of the change of NO<sub>x</sub> concentrations within the bed. These tests were performed over varied time

periods to observe gas and solid changes. The proposed mechanisms are given below with supporting evidence.

#### untreated alumina



In a second reaction the nitrite formed may react as follows



Combining sequential reactions provides the following overall reaction

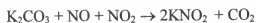


The proposed overall reaction predicts a molar ratio  $\text{NO}_2$  sorbed to NO formed of 3:1. This ratio was observed in most tests indicating the second reaction is not limiting. Also, ISE analyses found low or negligible nitrite concentrations on untreated alumina. In addition, instability of aluminum salts was observed in decomposition studies. Thus, the steady-state nitrite concentration should be small. Where the  $\text{NO}:\text{NO}_2$  feed-gas ratio was greater than 10:1 minor amounts of NO were sorbed as previously discussed. Under this condition a reversal of the second reaction is thought to occur.

#### $\text{K}_2\text{CO}_3$ -treated alumina



and



Greater concentrations of NO increase the amount of nitrite formed as suggested from ISE analyses. Eventually,  $\text{KNO}_2$  will reach a temporary steady state.



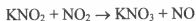
When  $\text{KNO}_2$  has achieved steady state the overall reaction can be represented by



Gas-phase data shows the trend to the 3  $\text{NO}_2$  sorbed: 1  $\text{NO}_{\text{formed}}$  is delayed but eventually occurs for both  $\text{K}_2\text{CO}_3$ -treated and  $\text{KOH}$ -treated alumina.

### **KOH-treated alumina**

Similar reactions of  $\text{KOH}$ -treated alumina to that of  $\text{K}_2\text{CO}_3$ -treated alumina are proposed.



For a steady-state concentration of  $\text{KNO}_2$ , overall reaction can be represented by



This overall reaction predicts that in the later stages of reaction, nitrite reaches steady state and a 3  $\text{NO}_2$  sorbed: 1  $\text{NO}_{\text{formed}}$  ratio should be observed. ISE analyses in the “longbed” series of  $\text{NO}_x$  exposure of over time indicate a steady nitrite concentration and the gas concentrations trend to a 3  $\text{NO}_2$  sorbed: 1  $\text{NO}_{\text{formed}}$  ratio.

For all of these sorbent materials the overall reaction is similar in that three  $\text{NO}_2$  molecules sorb to form two nitrate and one  $\text{NO}$  moieties. For untreated alumina the proposed mechanism suggests no significant interaction of  $\text{NO}$  in the presence of  $\text{NO}_2$ . Also, oxidation of nitrite formed by  $\text{NO}_2$  sorption is proposed to occur forming nitrate and gaseous  $\text{NO}$  or decomposing to  $\text{NO}_2$  and  $\text{NO}$  due to the presumed instability of aluminum

nitrite. Alkaline-treated alumina materials react with NO in the presence of NO<sub>2</sub> forming significant amounts of nitrite that increases with temperature. However, following build-up of nitrite, conversion of nitrite into nitrate with release of NO occurs as observed for untreated alumina.

Feasibility of sorbent regeneration was explored by two methods: washing the sorbent and thermal desorption. Washing the sorbent proved useless as the treatment material was removed and the pellet structure appeared degraded. Thermal desorption of NO<sub>x</sub> was applied to a sample of Cs<sub>2</sub>CO<sub>3</sub>-treated alumina previously exposed to 500 ppm NO<sub>2</sub> and residual NO (3 ppm) at 0.62 Lpm and 25 °C for 2 hours. Upon re-exposure under similar conditions as the initial exposure, NO<sub>x</sub> sorption was 93% of the cumulative amount sorbed in the initial exposure. Additional regeneration studies are suggested for further research.

Additional gases such as O<sub>2</sub>, CO<sub>2</sub>, H<sub>2</sub>O, or SO<sub>2</sub> in the NO<sub>x</sub>-laden stream were tested to observe their effects on NO<sub>x</sub> sorption. The presence of oxygen and carbon dioxide did not affect the sorption of NO<sub>x</sub> at 25 and 250 °C. In similar fractional amounts, water vapor improved the removal of NO and NO<sub>2</sub> for the sorbent studied. Sulfur dioxide reduces NO<sub>x</sub> sorption to untreated alumina but improves NO sorption to K<sub>2</sub>CO<sub>3</sub>-treated alumina at 25 °C.

Based on the conclusions presented above and the experience gained in performing this research, recommendations can be made that should further the understanding and application of these sorbent materials to the control of NO<sub>x</sub>.



1. The general mechanisms developed for untreated,  $K_2CO_3$ -treated, and KOH-treated alumina sorbents are based on gas-phase measurements of NO and  $NO_2$  and subsequent ISE analysis of nitrites and nitrates. A technique to measure the change of the surface species during the sorption process is Raman spectroscopy. This *in situ* technique could allow one to identify the interactive species more accurately that are involved in this  $NO_x$  sorption process. The sensitivity required for this technique may be a limiting factor and should be considered as an element in experimental design.
2. A brief demonstration test indicated that washing of sorbents as means of regeneration is not possible and that thermal desorption in an atmosphere of a reducing gas appears to be effective. Regeneration studies should be performed to demonstrate the long-term effects on sorbent properties of practical regeneration techniques.
3. These coated materials have shown promise as sorbents for use at temperatures well below combustion gas conditions (250 °C). Other uses of this material of interest to the USAF include controlling  $NO_x$  (primarily  $NO_2$ ) exhaust emitted during liquid rocket fueling. Currently, during the rocket fueling process wet scrubbing methods are used to control  $N_2O_4$  emissions. A dry sorption method could easily improve material handling issues as well as improve efficiency using adequate design.
4. Given the observed effects of the copollutants  $H_2O$  and  $SO_2$  on the sorption of  $NO_x$ , it is recommended that studies be carried out in which these copollutants

and their products are analyzed simultaneously with NO<sub>x</sub> species. These data will provide needed information to formulate modified or new sorption mechanisms with these gases present. Surface species may be identified by methods such as ion-chromatography or spectroscopic techniques to provide information about other surface species formed during NO<sub>x</sub> sorption in the presence of copollutants.

5. The materials studies can be further improved based on their physical characteristics. Given that pore size distribution measurements indicated that pore closure limited the sorption process, it is recommended that materials of varied physical properties be obtained and tested. As stated earlier, a desirable feature of alumina is that it can be obtained with specified physical properties at reasonable cost. In fact, alumina should allow for easy comparative studies of the effects of surface properties given the observed reproducibility of the obtained manufactured material. For example, because alumina acts as a support rather than sorbent in treated materials, it is important to optimize surface area.
6. The methods of surface treatment should be further studied. Treatment methods can significantly affect the chemical and physical characteristic of the final material. The treatment methods used in this study did evaluate parameters of treatment but other methods of treatment beyond impregnation and precipitation were not considered. Therefore, the common methods of

treatment and the expected results from those treatment methods should be analyzed and tested.

## REFERENCES

- Benedeck, K.; Flytzani-Stephanopoulos, M. *Cross-Flow Filter-Sorbent-Catalyst for Particulate, SO<sub>2</sub>, and NO<sub>x</sub> Control*. Final Report, DOE PETC DOE/PC/89805-T9. 1994.
- Berman, E.; Dong, J.; Lichtin, N. N. *Photopromoted and Thermal Decomposition of Nitric Oxide by Metal Oxides*. ESL-TR-91-32, HQ AFESC, Tyndall AFB, Florida. 1991.
- Bienstock, D.J.; Field, J.H.; Katell, S.; Plants, K.D. Evaluation of Dry Processes for Removing Sulfur Dioxide from Power Plant Flue Gases. *J.A.P.C.A.*, **1965**, 15(10), 459.
- Boehm, H.P. Acidic and Basic Properties of Hydroxylated Metal Oxide Surfaces. *Discuss. Faraday Soc.*, **1972**, 52, 264.
- Borgwardt, R.H.; Harvey, R.D. Kinetics of the Reaction of SO<sub>2</sub> with Calcined Limestone. *Environ. Sci. Tech.* **1972**, 6, 350.
- Bortz, S. J.; Podlenski, J. W. *Method and Apparatus for Reducing Nitrogen Dioxide Emissions in a Dry Sodium Scrubbing Process Using Humidification*. US Patent 5,165,902. 1992.
- Bowman, C.T. Kinetics of Nitric Oxide Formation on Combustion Processes. In *Fourteenth Symposium on Combustion*. The Combustion Institute, Pittsburgh, Pennsylvania. 1972. pp. 729-738.
- Brunauer, S.; Emmett, P.H.; Teller, E. Vapor Adsorption to Surfaces. *J. Am. Chem. Soc.* **1938**, 60, 309.
- Buonicore, A.J.; Theodore, L.; Davis, W.T. *Air Pollution Control Engineering Manual*. Eds. Buonicore, A.J.; Theodore, L.; Davis, W.T. Van Nostrand Reinhold, New York, New York, 1991. pp. 1-13.
- Campbell, L. E.; Danziger, R.; Guth, E. D.; Padron, S. *Process for the Reaction and Absorption of Gaseous Air Pollutants, Apparatus Therefore and Method of Making Same*. US Patent 5,665,321. 1997.

- Carmichael, G.R.; Peters, L.K. An Eulerian Transport/Transformation/Removal Model for SO<sub>2</sub> and Sulfate - I. Model Development. *Atmos. Environ.* **1984**, *18*, 937.
- Cook, W.A. Chemical Procedures in Air Analysis for Determination of Poisonous Atmospheric Contaminants, *American Public Health Association Yearbook* **1936**; 26, 3, 80-83.
- Cooper, D.C.; Alley, F.C. *Air Pollution Control: A Design Approach*. Waveland Press Inc., Prospect Heights, Illinois, 1986. pp. 451-480.
- Coster, D.J.; Fripiat, J.J. Effect of Bulk Properties on the Rehydration of Aluminas. *Langmuir*, **1995**, *11*, 2615.
- Counce, R.M.; Perona, J.J. A Mathematical Model for Nitrogen Oxide Absorption in a Sieve-Plate Column. *Ind. Eng. Chem. Proc. Des. Dev.* **1980**, *19*, 426.
- CRC, 1992. *CRC Handbook of Chemistry and Physics*, 73rd Edition, 1992.
- Datta, A. Evidence for Cluster Sites on Catalytic Alumina. *J. Phys. Chem.*, **1989**, *93*, 7053.
- Debbage, L.; Kelley, E.; Guth, E.D.; Campbell, L.E.; Danziger, R.N.; Padron, S. *Apparatus for Removing Contaminants from Gaseous Stream*. US Patent 5,607,650. 1997.
- Fiero, J.L.G., ed. 1990. *Spectroscopic Characterization of Heterogenous Catalysts, Part A*. Elsevier. pp. 202-208.
- Flury, F.; Zernick, F. *Schadliche Gas*. Berlin, Springer, 1931.
- Ganz, S.N. Sorption of Nitrogen Oxides by Solid Sorbents. *J. Appl. Chem. USSR*. **1958**, *31*(1), 128.
- Gilbert, R.E.; Cox, D.F.; Hoflund, G.B. Computer-interfaced Digital Pulse Counting Circuit. *Rev. Sci. Instrum.*, **1982**, *53*, 447.
- Glaser, R.A. *Smog and Plant Structure in Los Angeles County. Reports Group, School of Engineering and Applied Science*. University of California at Los Angeles, March 1970. Report No. 70-17, pp. 1-39.
- Golden, T.C.; Kalbassi, M.A.; Taylor, F.W.; Allam, R.J. *Use of Zeolites and Alumina in Adsorption Process*. US Patent 5,779,767. 1998.
- Grano, D. *Clean Air Act Requirements: Effect on Emissions of NO<sub>x</sub> from Stationary Sources*. ACS Symposium Series, Vol. 587, 1995, p. 14.

- Greenwood, N.N.; Earnshaw, A. Eds. *Chemistry of the Elements*. Pergamon Press, Oxford, 1984, pp. 273-278.
- Grim, R.E. *Clay Mineralogy*, McGraw-Hill Book Co., New York, New York, 1953. pp. 102-103.
- Haslbeck, J.L.; Neal, L.G.; Perng, C.P.; Wang, C.J. *Evaluation of the NOXSO Combined NO<sub>x</sub>/SO<sub>2</sub> Flue Gas Treatment Process*. US DOE Report No. DOE/PC/7325-T2; 1985.
- Haslbeck, J.L.; Wang, C.J.; Tseng, H.P.; Tucker, J.D. *Evaluation of the NOXSO Combined NO<sub>x</sub>/SO<sub>2</sub> Flue Gas Treatment Process*. US DOE Report No. DOE/FE/60148-T5; 1984.
- Heinsohn, R.J.; Kabel, R.L. *Sources and Control of Air Pollution*. Prentice Hall, Upper Saddle River, NJ, 1999. pp. 89-125.
- Henry, M.C.; Ehrlich, R.; Blair, W.H. Effect of Nitrogen Dioxide on Resistance of Squirrel Monkeys to Klebsiella pneumoniae Infection. *Arch. Environ. Health*, **1965**, *18*, 580.
- Hermance, H.W.; Russell, C.A.; Bauer, E.J.; Egan, T.F.; Wadlow, H.V. Relation of Air-Borne Nitrate to Telephone Equipment Damage. *Environ. Sci. Techn.* **1970**.
- Heywood, J.B. *Internal Combustion Engine Fundamentals*. McGraw-Hill Book Co., New York, New York, 1988. p. 571.
- Hill, A.C.; Bennett, J.H. Inhibition of Apparent Photosynthesis by Nitrogen Oxides. *Atmos. Environ.* **1970**.
- Himi, Y.; Muramatsu, F. Sampling Method for Determination of Nitrogen Oxides in Flue Gas. *Japan. Analyst*, **1969**, *18*(6), 710.
- Jacobs, M.B. *The Analytical Chemistry of Industrial Poisons, Hazards, and Solvents*; 2nd ed., Interscience Publishers, New York, New York, 1949; Vol. 1, pp. 79-99.
- Jacobs, M.B.; Hochheiser, S. Continuous Sampling and Ultramicrodetermination of Nitrogen Dioxide in Air. *Analytical Chemistry*, **1958**, *30*, 426.
- James, N.J.; Hughes, R. Rates of NO<sub>x</sub> Absorption in Calcined Limestones and Dolomites. *Environ. Sci. Techn.* **1977**, *11*(13), 1191.
- Jimenez-Gonzalez, A.; Schmeisser, D. Preparation and Spectroscopic Characterization of  $\gamma$ -Al<sub>2</sub>O<sub>3</sub> Thin Films. *Surface Science*, **1991**, *250*, 59.

- Johnson, S.A.; Katz, C.B. *Feasibility of Reburning for Controlling NO<sub>x</sub> Emissions from Air Force Jet Engine Test Cells*. ESL-TR-89-33, HQ AFESC, Tyndall AFB, Florida; 1989.
- Jones, Dale G. *Apparatus for Removing Oxides of Nitrogen and Sulfur from Combustion Gases*. US Patent 5,116,587. 1992.
- Keiser, E.H.; McMaster, L. On the Detection of Ozone, Nitrogen Peroxide, and Hydrogen Peroxide on Gas Mixtures. *American Chemical Society*. 1908, 39, 96.
- Kikkiniades, E.S.; Yang, R.T. Simultaneous SO<sub>2</sub>/NO<sub>x</sub> Removal and SO<sub>2</sub> Recovery of Synthesis Gas with Zinc Ferrite. *Ind. Eng. Chem. Res.* 1991, 30(8), 1981.
- Kimm, L.T. Control of Nitrogen Oxide Emissions from Jet Engine Test Cell Exhaust using a Magnesium Oxide-Vermiculite Sorbent. Ph.D. Dissertation in Environmental Engineering, University of Florida, Gainesville, Florida, 1995.
- Kimm, L.T.; Allen, E.R.; Wander, J.D. Control of NO<sub>x</sub> Emissions from Jet Engine Test Cells. *Proceedings of the 88th Annual Air and Waste Management Association Meeting*; San Antonio, Texas, 1995.
- Kittrell, J.R. *High Temperature NO<sub>x</sub> Control Process*. ESL-TR-89-36, HQ AFESC, Tyndall AFB, Florida; 1991.
- Knozinger, H. Specific Poisoning and Characterization of Catalytic Active Oxide Surfaces. In *Advances in Catalysis*, Academic Press, New York, New York, Vol. 25, 1976, pp. 184-267.
- Knozinger, H.; Ratnasamy, R. Catalytic Aluminas: Surface Models and Characterization of Surface Sites. In *Catalysis Reviews: Science and Engineering*, Marcel Dekker Inc., New York, New York, Vol. 17, No. 1, 1976, pp. 31-70.
- Komppa, V. Dry Adsorption Process for Removal of SO<sub>x</sub> and NO<sub>x</sub> in Flue Gases. *Paperii ja Puu*, 1986, 5, 401.
- Krasna, I.; Rittenburg, D. The Inhibition of Hydrogenase by Nitric Oxide. *Proc. Nat. Acad. Sci.* 1954, 70, 225.
- Krizek, J. Determination of Nitrogen Oxides in Small Concentrations. *Chem. Prumysl.*, 1966, 16(9), 558.
- Lee, M.R.; Allen, E.R.; Wander, J.D. Evaluation of Coated Alumina for the Removal of Nitrogen Oxides (NO<sub>x</sub>). *Proceedings of the Air and Waste Management Association*. Paper No. 98-RA93A.03. San Diego, California, June 14-19, 1998a

- Lee, M.R.; Allen, E.R.; Wolan, J.T.; Hoflund, G.B. NO<sub>2</sub> and NO Adsorption Properties of KOH-Treated  $\gamma$ -Alumina. *Ind. Eng. Chem. Res.* **1998b**, 37, 3375.
- Lever G.; Etchart, C.P.; Tahiani, F; *Alumina-Alkali Metal Aluminum Silicate Agglomerate Acid Adsorbents*. US Patent 5,096,871. 1992.
- Lott, S.E.; Gardner, T.J.; McLaughlin, L.I.; Oelfke, J.B.; Matlock, C.A. *Nitrogen Oxide Adsorbing Material*. US Patent 5,795,553. 1998.
- Lunsford, J.H. A Study of Surface Interactions on  $\gamma$ -Alumina, Silica-Alumina, and Silica-Magnesia using the EPR Spectra of Adsorbed Nitric Oxide. *J. Catalysis*, **1969**, 14, 379.
- Lyon, R.K. *New Technology for Controlling NO<sub>x</sub> from Jet Engine Test Cells*. ESL-TR-89-15, HQ AFESC, Tyndall AFB, Florida; 1991.
- Ma, W.T.; Chang, A.M.; Haslbeck, J.L.; Neal, N.G. NOXSO SO<sub>2</sub>/NO<sub>x</sub> Flue Gas Treatment Process Adsorption Chemistry and Kinetics. In *Novel Adsorbents and their Environmental Application*. AIChE Symposium Series 309, Vol. 91, 1995, p. 18.
- Ma, W.T.; Haslbeck, J.L.; Neal, L.G.; Yeh, J.T. Life Cycle of the NOXSO SO<sub>2</sub> and NO<sub>x</sub> Flue Gas Treatment Process: Process Modeling. *Sep. Tech.*, **1991**, 1, 195.
- Markussen, J.M.; Livengood, C.D. Alternative Flue Gas Treatment Technologies for Integrated SO<sub>2</sub> and NO<sub>x</sub> Control. *Proceedings of the 57th Annual American Power Conference*, Chicago, Illinois; 1995.
- McLendon, V.; Richardson, F. Oxides of Nitrogen as a Factor in Color Changes of Used and Laundered Cotton Articles. *Amer. Dyest. Rep.* **1965**, 54, 305.
- Morris, M.A.; Young, M.A.; Molig T. The Effect of Air Pollutants on Cotton. *Text. Res.* **1964**, 34, 563.
- Murphy, J.F. Alumina in Air Pollution Control. *Proceedings of the 102nd AIME Annual Meeting*. Chicago, Illinois, 1972.
- Nelli, C.H.; Rochelle, G.T. Nitrogen Dioxide Reaction with Alkaline Solids. *Ind. Eng. Chem. Res.*, **1996**, 35, 999.
- Nelson, B.W.; Nelson, S.G.; Higgins, M.O.; Brandum, P.A. *A New Catalyst for NO<sub>x</sub> Control*. ESL-TR-89-11, HQ AFESC, Tyndall AFB, Florida; 1989.



- Nelson, B.W.; Nelson, S.G.; Van Stone, D.A. *Controlling Combustion-Source Emissions at Air Force Sites with a New Filter Concept*. AL/EQ-TR-1994-0006, Armstrong Laboratory, Tyndall AFB, Florida; 1994.
- Nelson, B.W.; Nelson, S.G.; Van Stone, D.A. *Development and Demonstration of a New Filter System to Control Emissions During Jet Engine Testing*. CEL-TR-92-49, HQ AFESC, Tyndall AFB, Florida; 1992.
- Nelson, S.G. *Toxic Gas Sorbent and Process for Making Same*. US Patent 4,721,582. 1987.
- Nelson, S.G.; Van Stone, D.A.; Little, R.C.; Peterson, R.A. *Laboratory Evaluation of a Reactive Baffle Approach to NO<sub>x</sub> Control*. AL/EQ-TR-1993-0017, HQ AFESC, Tyndall AFB, Florida; 1993.
- Nyquist, R.A.; Kagel, R.O. *Infrared Spectra of Inorganic Compounds*. Academic Press, New York, New York, 1971.
- Parkyn, N.D. Adsorption Sites on Oxides, Infra-red Studies of Adsorption of Oxides of Nitrogen. *Proceedings of the Fifth International Congress on Catalysis*. Miami Beach, Florida, 1972.
- Petrik, M.A. *Use of Metal Oxide Electrocatalysts to Control NO<sub>x</sub> Emissions from Fixed Sources*. ESL-TR-89-29, HQ AFESC, Tyndall AFB, Florida; 1991.
- Pinnavaia, T.J.; Amarasekera, J.; Polansky, C.A. *Layered Double Hydroxide Sorbents for the Removal of SO<sub>x</sub> from Flue Gas Resulting from Coal Combustion*. US Patent 5,120,508. 1992.
- Regalbutto, J.R. Comparison of NO<sub>x</sub> Abatement Strategies Utilizing Adsorption. In *Final Task Report to the Gas Research Institute*, USDOC PB95-171575, June 1994.
- Rochelle, G.T.; Nelli, C.H. Simultaneous Sulfur Dioxide and Nitrogen Dioxide Removal by Calcium Hydroxide and Calcium Silicate Solids. *J. AWMA*, 1998, 48, 819.
- Ruthven, D.M. A Simple Method for Calculating Mass Transfer Factors for Heterogeneous Catalytic Gas Reactions. *Chemical Engineering Science*. 1968, 23, 759.
- Savitzky, A.; Golay, J.E. Smoothing and Differentiation of Data by Simplified Least Squares Procedures. *Analytical Chemistry*. 1984, 36, 1627.
- Schlesinger, M.D.; Illig, E.G. *The Regeneration of Alkalized Alumina, Attritioning and SO<sub>2</sub> Sorption Rates*. USB.M. Report No. 7275, 1969.

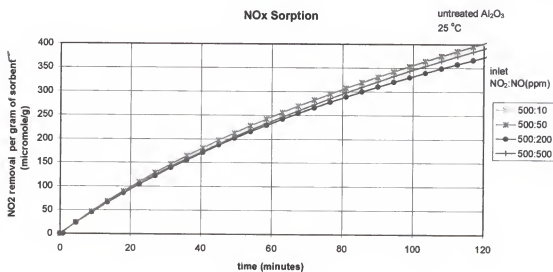
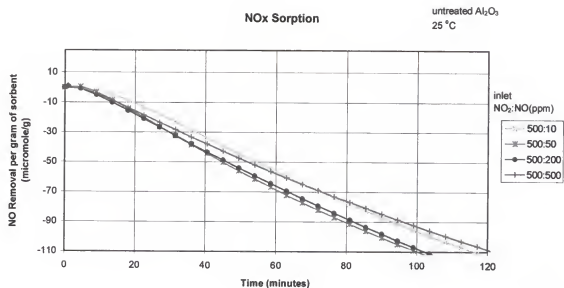
- Shy, C.M.; Creason, J.P.; Pearlman, M.E.; McClain, K.E.; Benson, F.B.; Young, M.M. The Chattanooga School Study: Effects of Community Exposure to Nitrogen Dioxide. Incidence of Acute Respiratory Illness. *J.A.P.C.A.* **1970**, *20*, 582.
- Sigsby, J.E.; Black, F.M.; Bellar, T.A.; Klosterman, D.L. Chemiluminescent Method for Analysis of Nitrogen Compounds in Mobile Source Emissions (NO, NO<sub>2</sub>, and NH<sub>3</sub>). *Environmental Science and Technology*. **1973**, *7*(1), 51.
- Sircar, S.; Rao, M.B.; Golden, T.C. Drying of Gases and Liquids by Activated Alumina. In *Adsorption on New and Modified Inorganic Sorbents. Studies in Surface Science and Catalysis*. Eds. Dabrowski, A. and Tertykh, V.A., Vol. 99, 1996, p. 629.
- Smith, J.M., *Chemical Engineering Kinetics*. McGraw-Hill Book Co., New York, New York, 1981, pp. 311-333.
- Staudt, J.E. Post-Combustion NO<sub>x</sub> Control Technologies for Electric Power Plants. *89th Annual Meeting of the Air and Waste Management Association*. 96-RP139.02. Nashville, Tennessee, June 23-28, 1996.
- Terenin, A.N.; Roev, L. Infrared Spectra of Nitric Oxide Adsorbed on Transition Metals, their Salts and Oxides. *Spectrochimica Acta*, **1959**, *15*, 946.
- US DOE. *Clean Coal Technology Demonstration Program*. Report No. DOE/FE-0351; 1997
- US EPA. *Air Quality Criteria for Oxides of Nitrogen*. Report No. EPA/600/8-91/049aF; 1993.
- US EPA. *Alternative Control Techniques Document-NO<sub>x</sub> Emissions from Utility Boilers*. Report. No. EPA-453/R-94-023; 1994.
- US EPA. *The Regional Transport of Ozone*. Report No. EPA-456/F-98-006; 1998.
- Van Haut, H.; Stratmann, H. Experimental Investigations of the Effect of Nitrogen Dioxide on Plants. *Transactions of the Land Inst. of Pollution Control and Soil Conservation of the Land of North Rhine-Westphalia*, **1967**, *7*, 50.
- Yeh, J.T.; Ma, W.T.; Pennline, H.W.; Haslbeck, J.L.; Joubert, J.I.; Gromicko, F.N. Integrated Testing of the NOXSO Process: Simultaneous Removal of SO<sub>2</sub> and NO<sub>x</sub> from Flue Gas. *Chem. Eng. Comm.*, **1992**, *114*, 65.
- Zeldovitch, J. The Oxidation of Nitrogen in Combustion and Explosions. *Acta Physiochem.* **1946**, *21*(4).

Zemlyanov, D.Y.; Hornung, A.; Weinburg, G.; Wild, U.; Schlog, R. Interaction of Silver with a NO/O<sub>2</sub> Mixture: A Combined X-ray Photoelectron Spectroscopy and Scanning Electron Microscopy Study. *Langmuir*, **1998**, *14*, 3242.

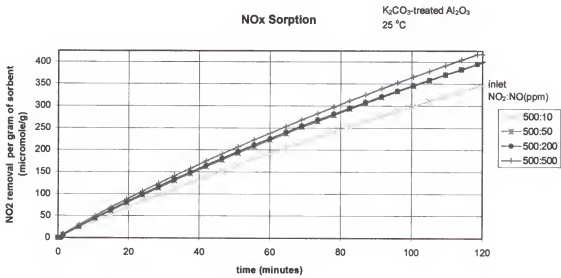
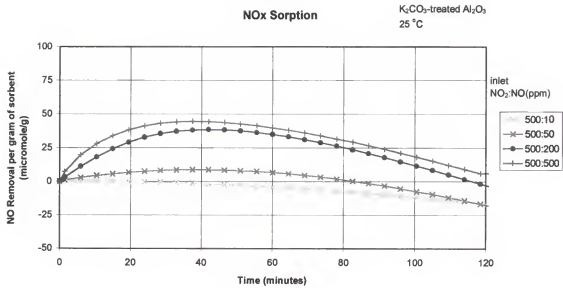
Ziebarth M.S.; Hager, M.J.; Beeckman, J.W.; Plecha, S.. *SOx/NOx Sorbent and Process of Use*. US Patent 5,585,082. 1996.

## APPENDIX A

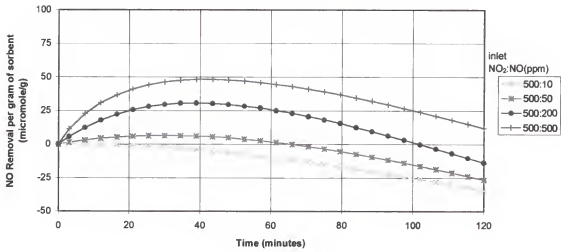
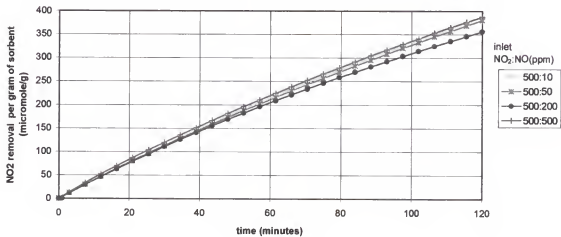
NOX SORPTION: CONSTANT NO<sub>2</sub> (500 PPM), VARIED NO CONCENTRATION



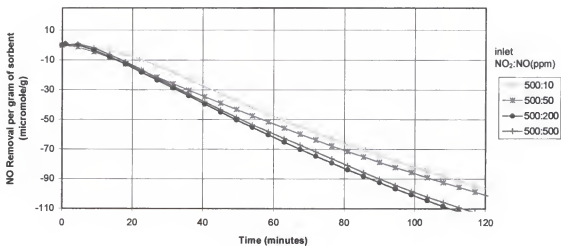
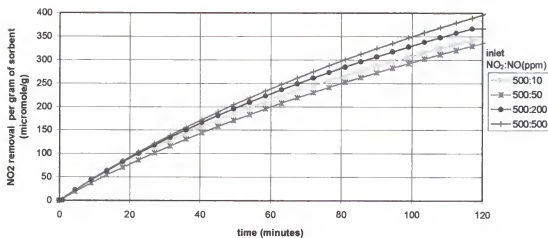
Untreated alumina, 25 °C.



$K_2CO_3$ -treated alumina, 25 °C.

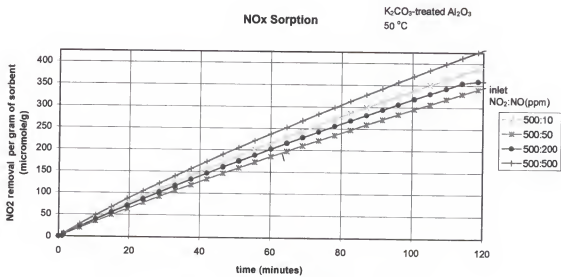
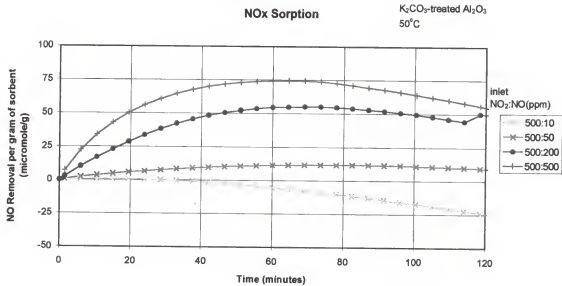
NO<sub>x</sub> SorptionKOH-treated Al<sub>2</sub>O<sub>3</sub>  
25 °CNO<sub>x</sub> SorptionKOH-treated Al<sub>2</sub>O<sub>3</sub>  
25 °C

KOH-treated alumina, 25 °C.

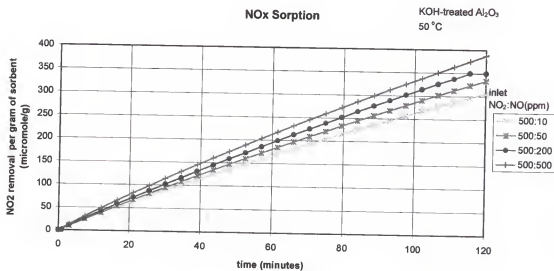
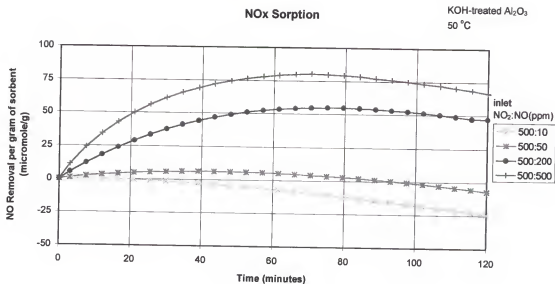
NO<sub>x</sub> Sorptionuntreated Al<sub>2</sub>O<sub>3</sub>  
50 °CNO<sub>x</sub> Sorptionuntreated Al<sub>2</sub>O<sub>3</sub>  
50 °C

Untreated alumina, 50 °C.



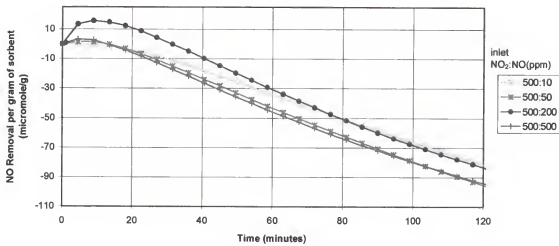


$K_2CO_3$ -treated alumina, 50 °C.

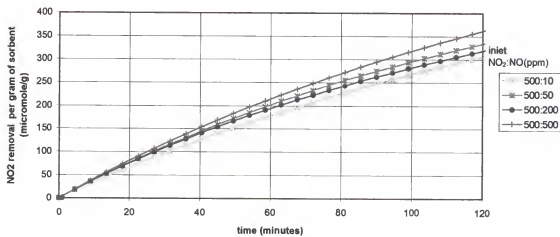


KOH-treated alumina, 50 °C.

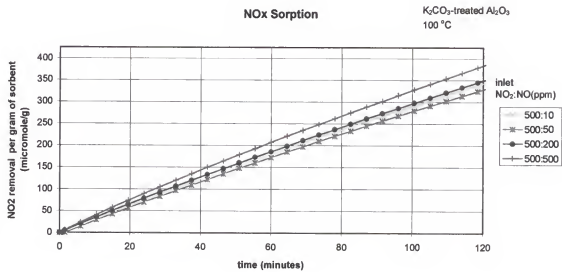
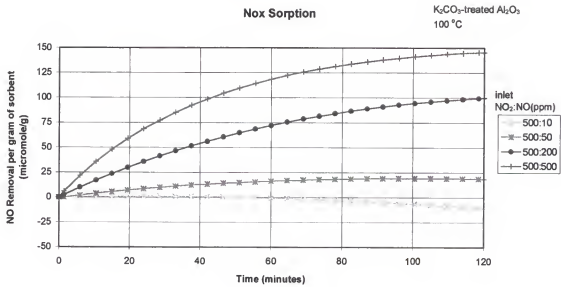
## Nox Sorption

untreated  $\text{Al}_2\text{O}_3$   
100 °C

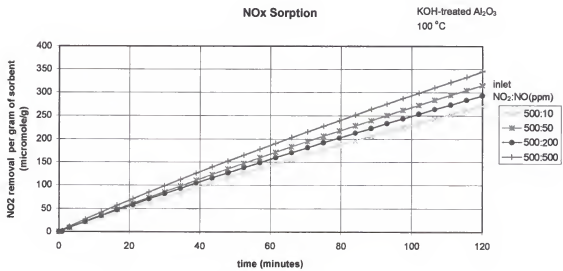
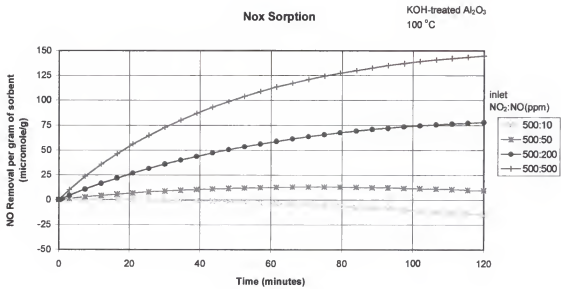
## NOx Sorption

untreated  $\text{Al}_2\text{O}_3$   
100 °C

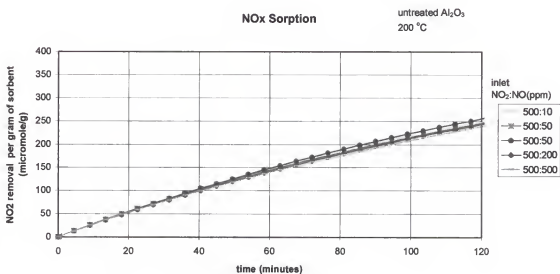
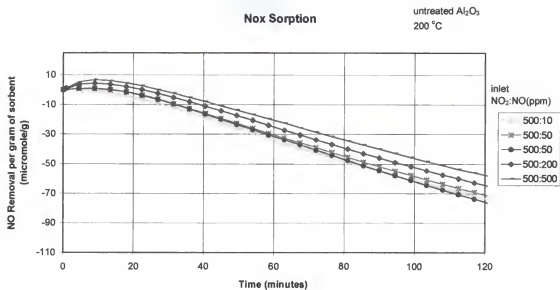
Untreated alumina, 100 °C.



$K_2CO_3$ -treated alumina, 100 °C.

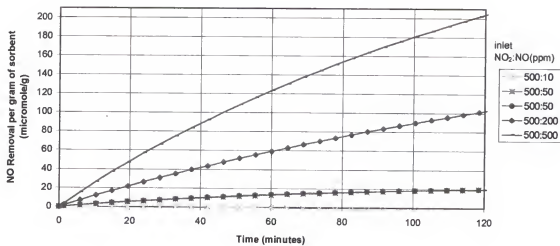


KOH-treated alumina, 100 °C.

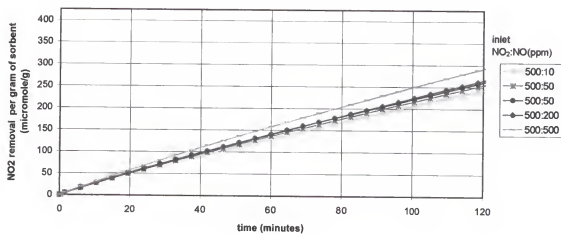


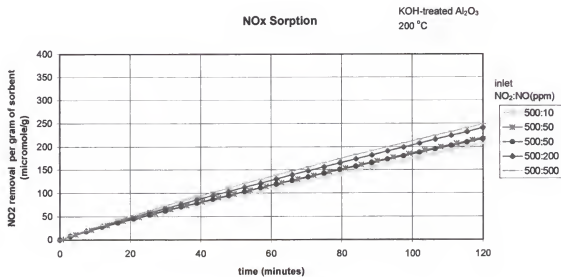
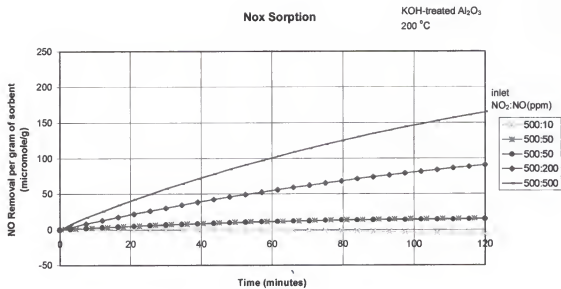
Untreated alumina, 200 °C.

## Nox Sorption

K<sub>2</sub>CO<sub>3</sub>-treated Al<sub>2</sub>O<sub>3</sub>  
200 °C

## NOx Sorption

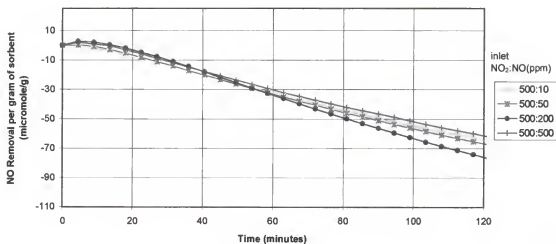
K<sub>2</sub>CO<sub>3</sub>-treated Al<sub>2</sub>O<sub>3</sub>  
200 °CK<sub>2</sub>CO<sub>3</sub>-treated alumina, 200 °C.



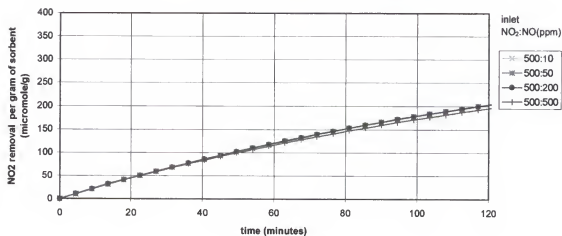
KOH-treated alumina, 200 °C



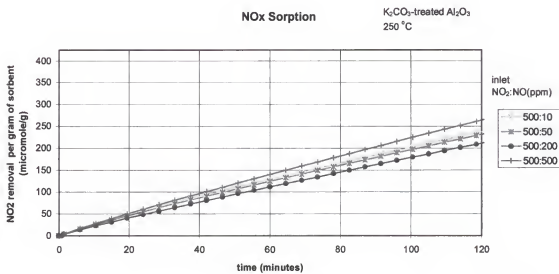
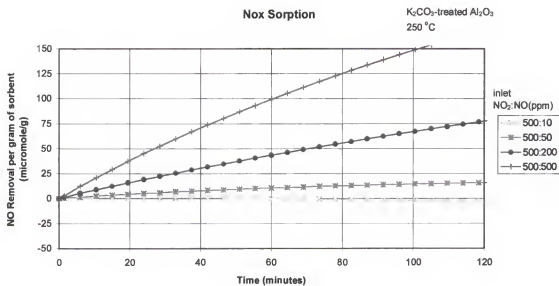
## NOx Sorption

untreated  $\text{Al}_2\text{O}_3$   
250 °C

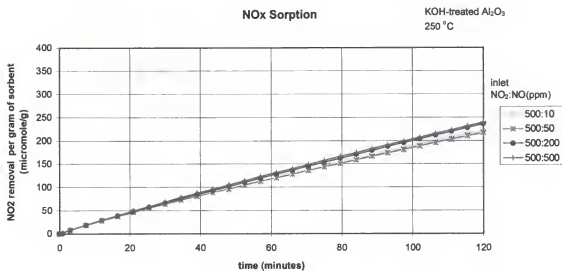
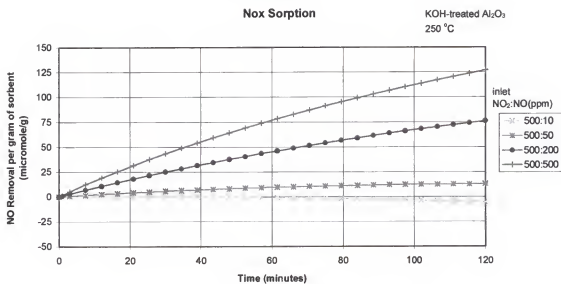
## NOx Sorption

untreated  $\text{Al}_2\text{O}_3$   
250 °C

Untreated alumina, 250 °C.



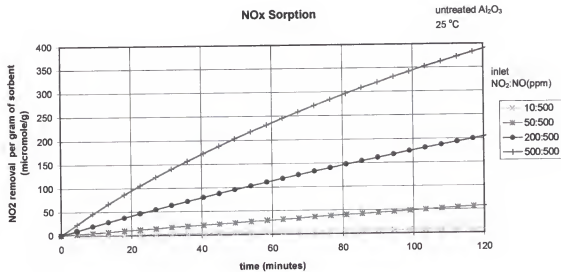
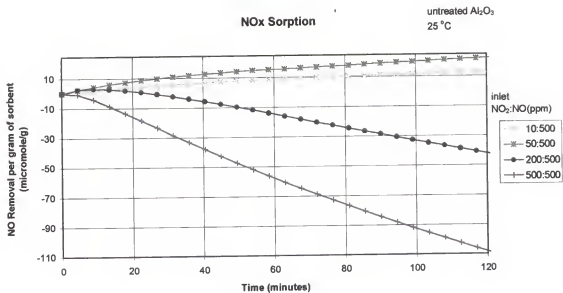
$K_2CO_3$ -treated alumina, 250 °C.



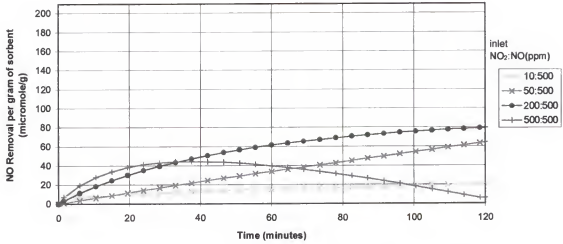
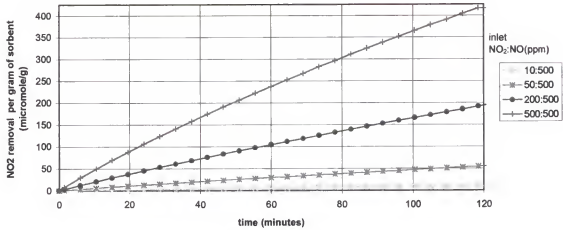
KOH-treated alumina, 250 °C

## APPENDIX B

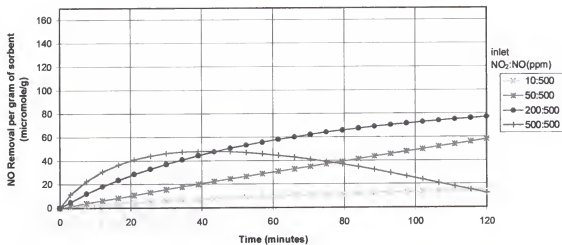
NOX SORPTION: CONSTANT NO (500 PPM), VARIED NO<sub>2</sub> CONCENTRATION



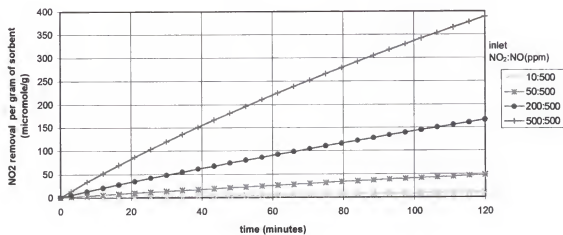
Untreated alumina, 25 °C.

NO<sub>x</sub> SorptionK<sub>2</sub>CO<sub>3</sub>-treated Al<sub>2</sub>O<sub>3</sub>  
25 °CNO<sub>x</sub> SorptionK<sub>2</sub>CO<sub>3</sub>-treated Al<sub>2</sub>O<sub>3</sub>  
25 °C. K<sub>2</sub>CO<sub>3</sub>-treated alumina, 25 °C.

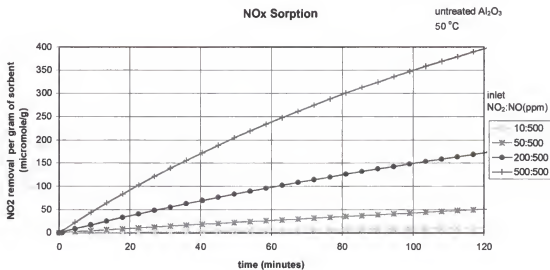
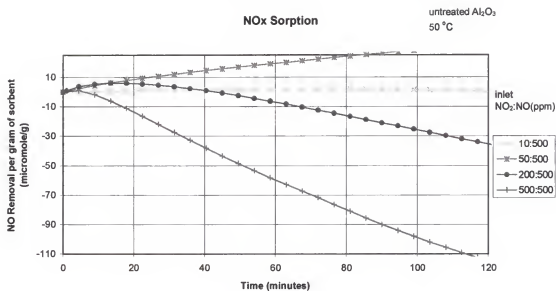
## NOx Sorption

KOH-treated  $\text{Al}_2\text{O}_3$   
25 °C

## NOx Sorption

KOH-treated  $\text{Al}_2\text{O}_3$   
25 °C

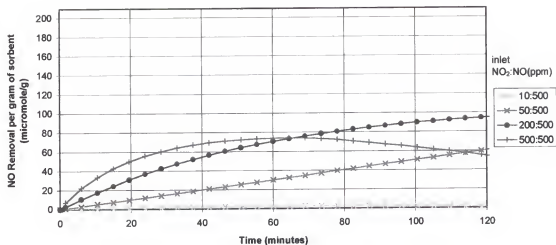
KOH-treated alumina, 25 °C.



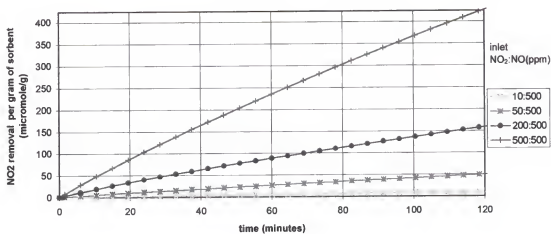
untreated alumina, 50 °C.



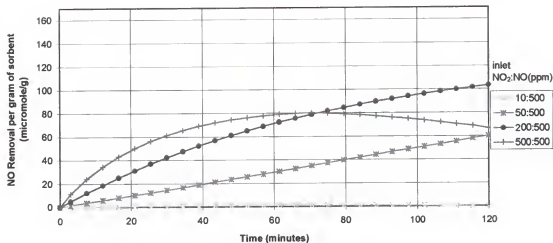
## NOx Sorption

 $K_2CO_3$ -treated  $Al_2O_3$   
50 °C


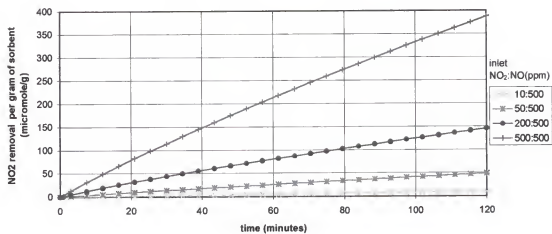
## NOx Sorption

 $K_2CO_3$ -treated  $Al_2O_3$   
50 °C

 $K_2CO_3$ -treated alumina, 50 °C.

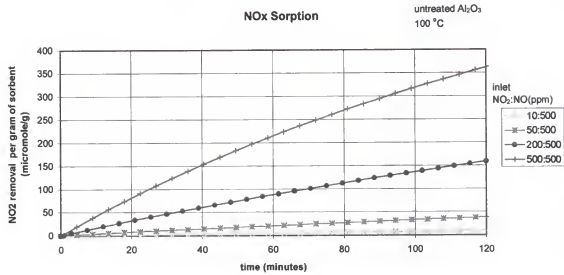
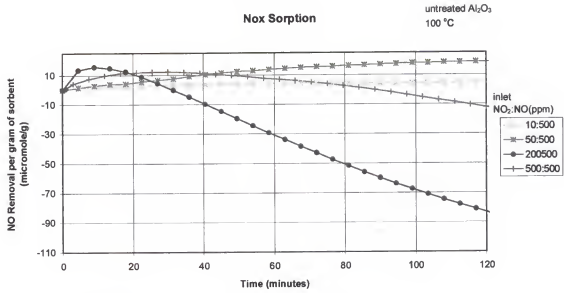
## NOx Sorption

KOH-treated  $\text{Al}_2\text{O}_3$   
50 °C

## NOx Sorption

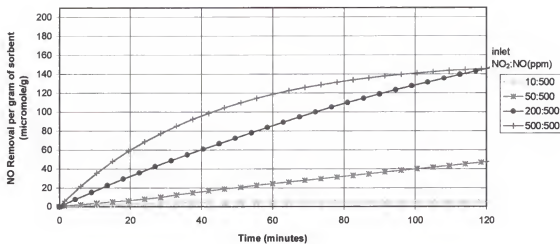
KOH-treated  $\text{Al}_2\text{O}_3$   
50 °C

KOH-treated alumina, 50 °C.

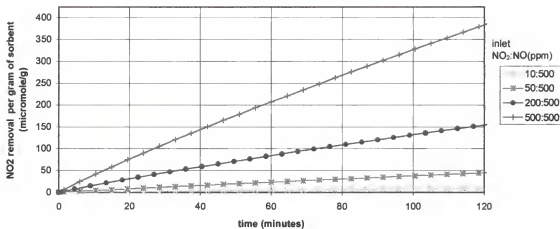


Untreated alumina, 100 °C.

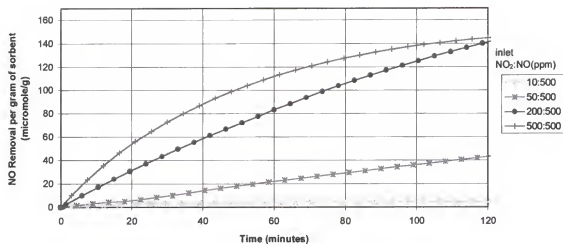
## Nox Sorption

 $K_2CO_3$ -treated  $Al_2O_3$   
 100 °C


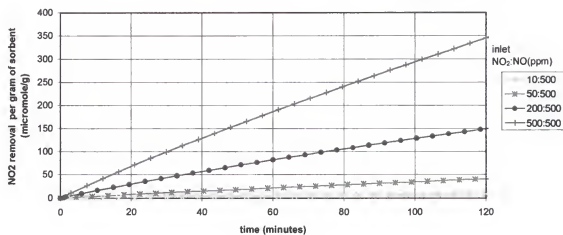
## NOx Sorption

 $K_2CO_3$ -treated  $Al_2O_3$   
 100 °C

 $K_2CO_3$ -treated alumina, 100 °C.

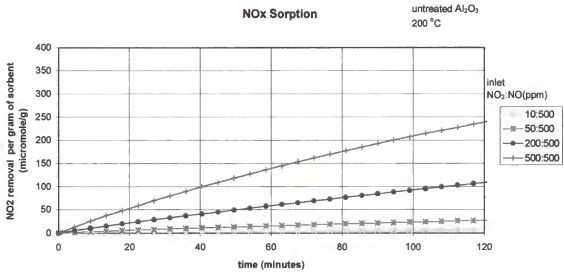
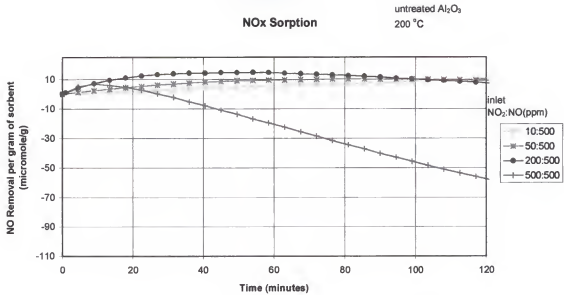
## Nox Sorption

KOH-treated  $\text{Al}_2\text{O}_3$   
100 °C

## NOx Sorption

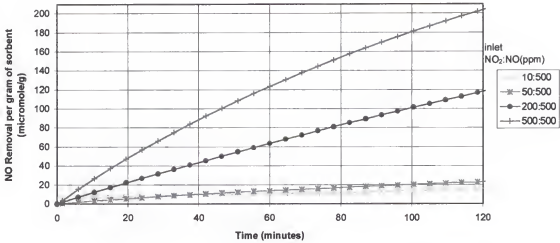
KOH-treated  $\text{Al}_2\text{O}_3$   
100 °C

KOH-treated alumina, 100 °C.

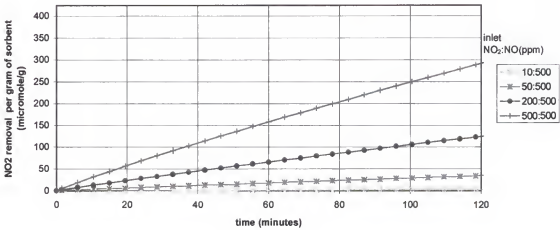


Untreated alumina, 200 °C.

## NOx Sorption

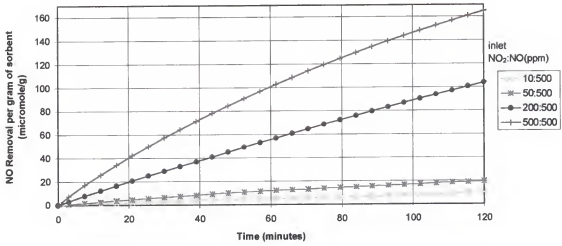
K<sub>2</sub>CO<sub>3</sub>-treated Al<sub>2</sub>O<sub>3</sub>  
200 °C

## NOx Sorption

K<sub>2</sub>CO<sub>3</sub>-treated Al<sub>2</sub>O<sub>3</sub>  
200 °CK<sub>2</sub>CO<sub>3</sub>-treated alumina, 200 °C.

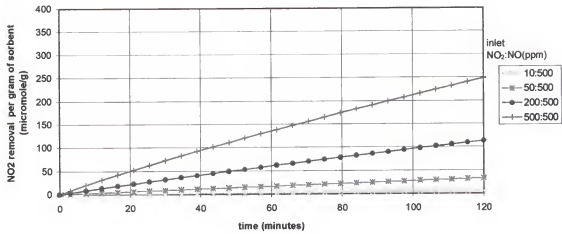
# **NOx Sorption**

KOH-treated  $\text{Al}_2\text{O}_3$   
200 °C



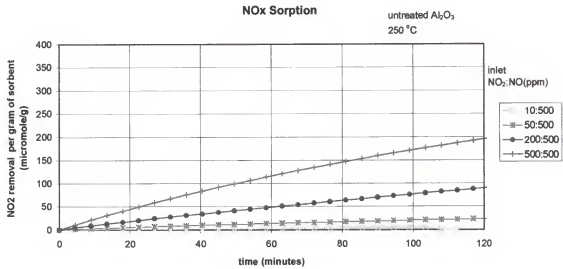
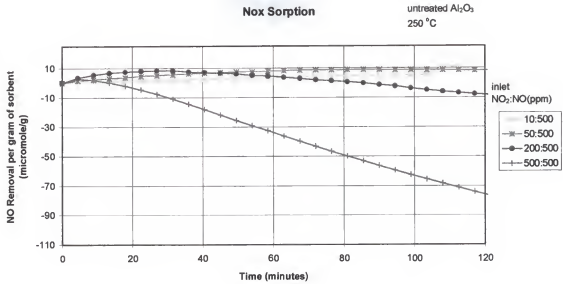
# **NOx Sorption**

KOH-treated  $\text{Al}_2\text{O}_3$   
200 °C

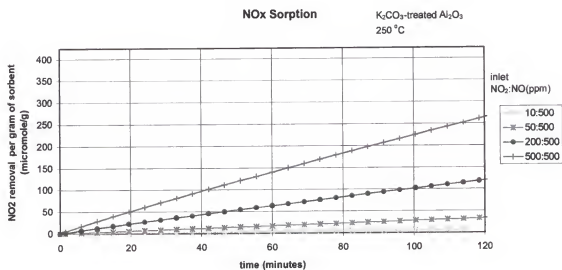
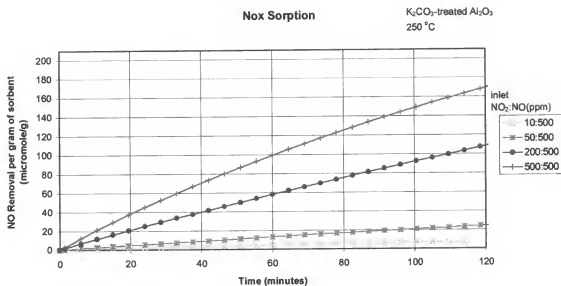


KOH-treated alumina, 200 °C.



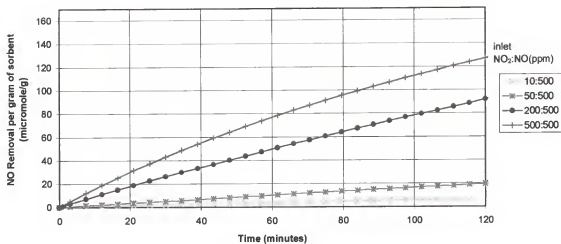


Untreated alumina, 250 °C.

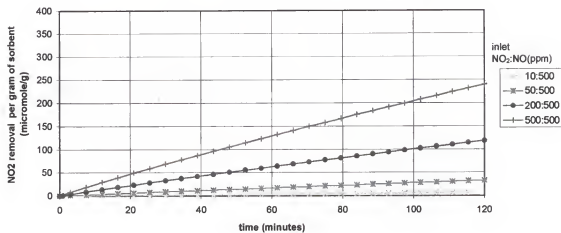


$K_2CO_3$ -treated alumina, 250 °C.

## Nox Sorption

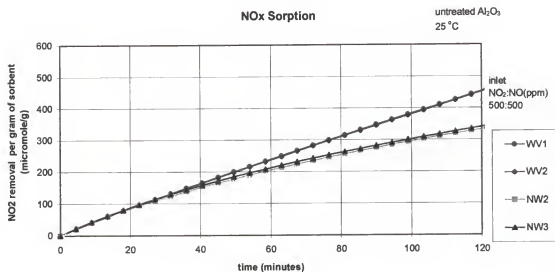
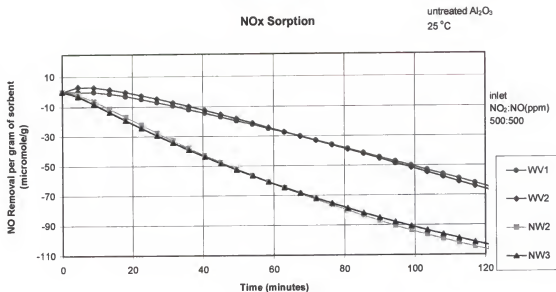
KOH-treated  $\text{Al}_2\text{O}_3$   
250 °C

## NOx Sorption

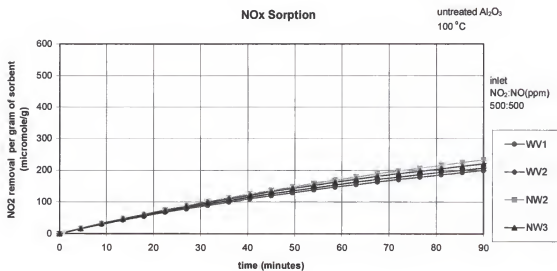
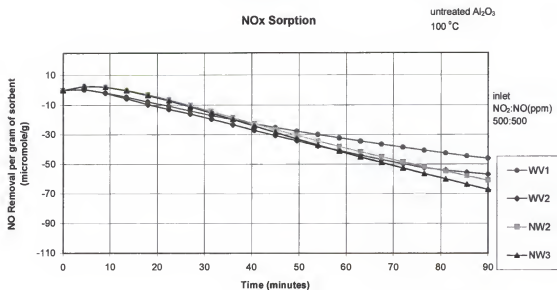
KOH-treated  $\text{Al}_2\text{O}_3$   
250 °C

KOH-treated alumina, 250 °C.

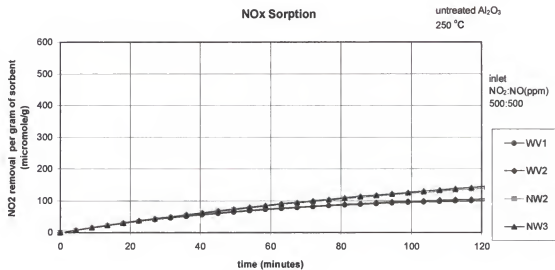
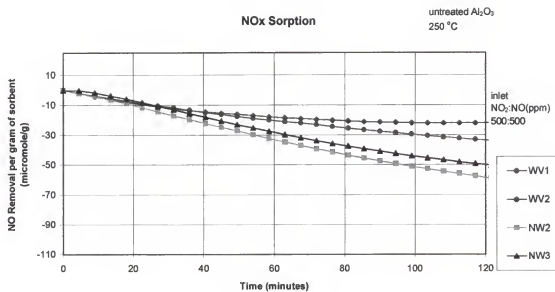
APPENDIX C  
ADDED GASES, SO<sub>2</sub> AND H<sub>2</sub>O



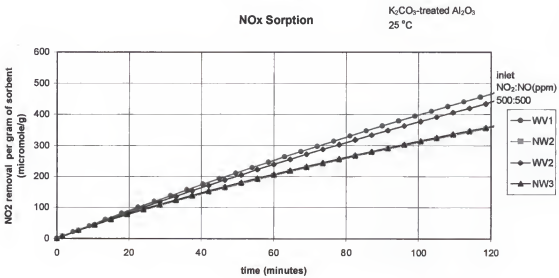
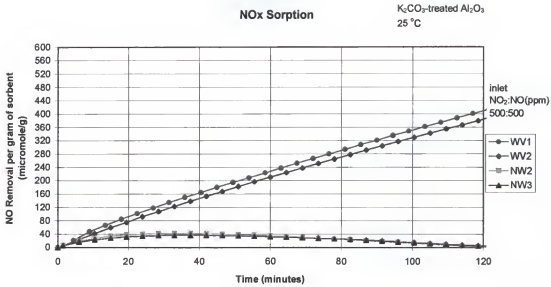
NOx sorption in the presence of water vapor (2.3%) for untreated alumina at 25 °C.



NOx sorption in the presence of water vapor (2.3%) for untreated alumina at 100 °C.

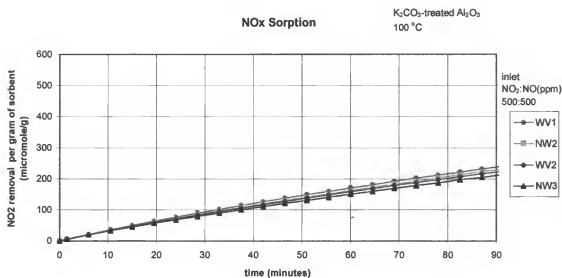
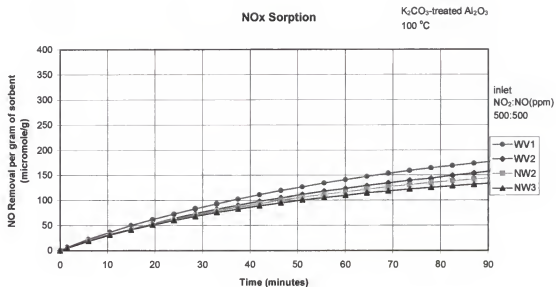


NOx sorption in the presence of water vapor (2.3%) for untreated alumina at 250 °C.

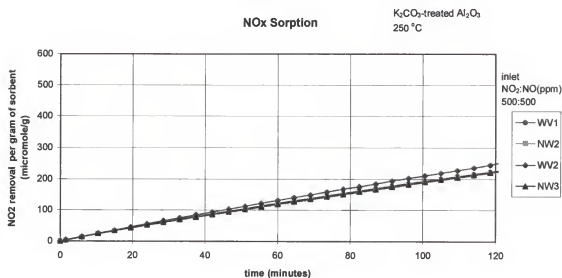
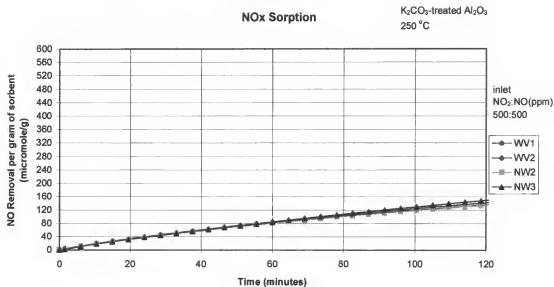


NOx sorption in the presence of water vapor (2.3%) for  $K_2CO_3$ -treated alumina at 25 °C.

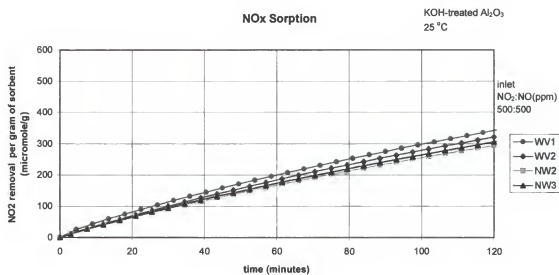
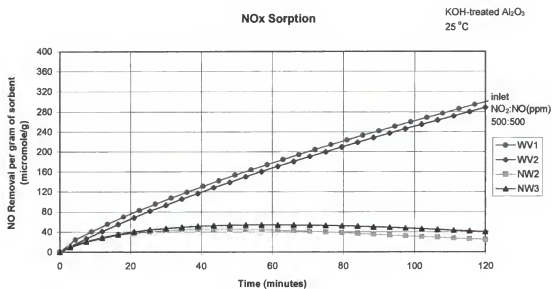




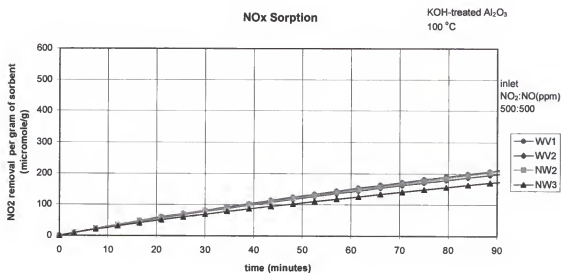
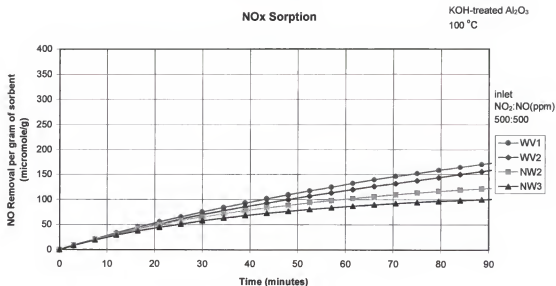
NOx sorption in the presence of water vapor (2.3%) for  $K_2CO_3$ -treated alumina at 100 °C.



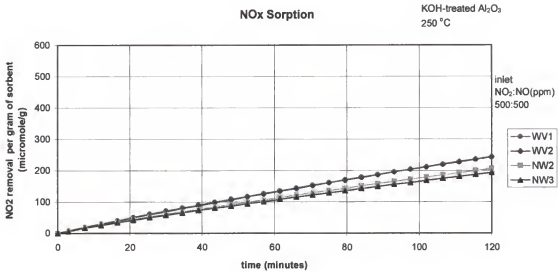
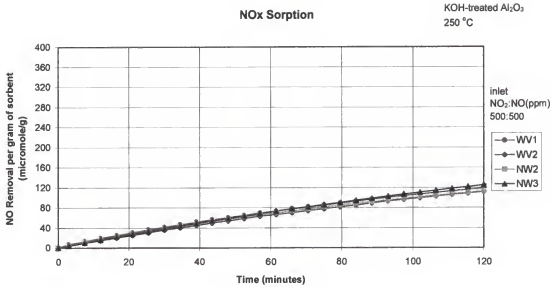
NOx sorption in the presence of water vapor (2.3%) for  $K_2CO_3$ -treated alumina at 250 °C.



NOx sorption in the presence of water vapor (2.3%) for KOH-treated alumina at 25 °C.

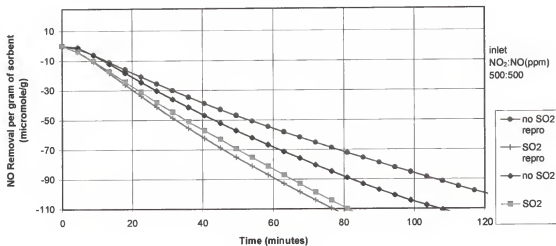


NOx sorption in the presence of water vapor (2.3%) for KOH-treated alumina at 100 °C.

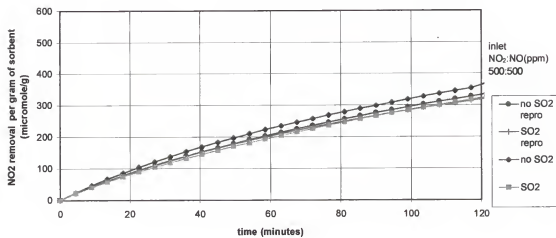


NOx sorption in the presence of water vapor (2.3%) for KOH-treated alumina at 250 °C.

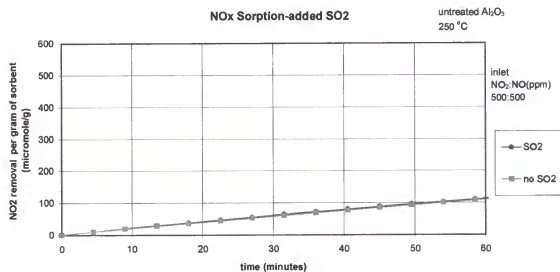
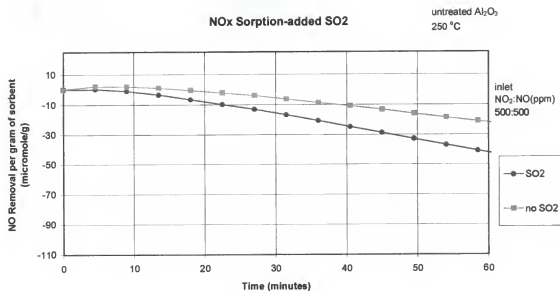
## NOx Sorption

untreated  $\text{Al}_2\text{O}_3$   
25 °C

## NOx Sorption

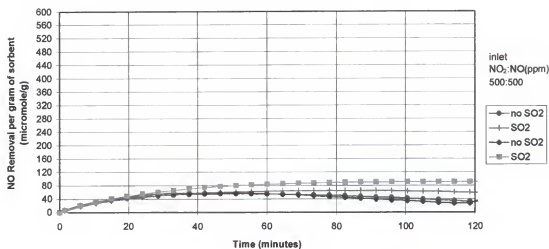
untreated  $\text{Al}_2\text{O}_3$   
25 °C

$\text{NO}_x$  sorption in the presence of  $\text{SO}_2$  (83 ppm) for untreated alumina at 25 °C.

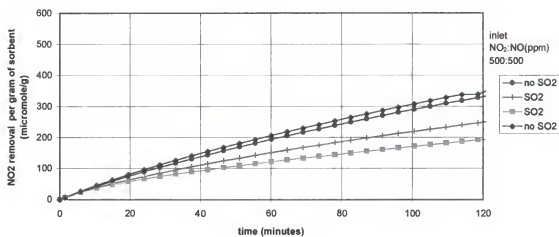


NO<sub>x</sub> sorption in the presence of SO<sub>2</sub> (83 ppm) for untreated alumina at 250 °C.

## NOx Sorption

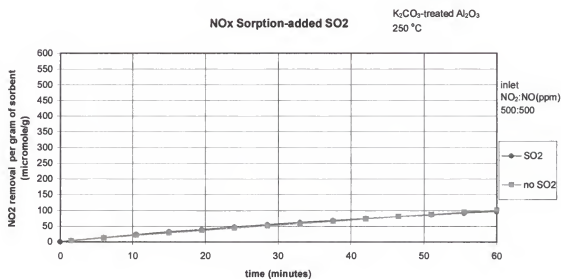
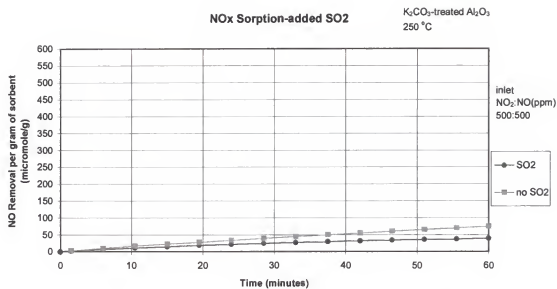
K<sub>2</sub>CO<sub>3</sub>-treated Al<sub>2</sub>O<sub>3</sub>  
25 °C

## NOx Sorption

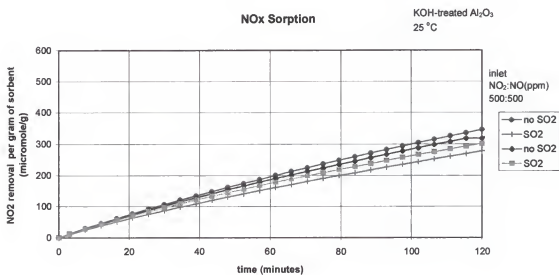
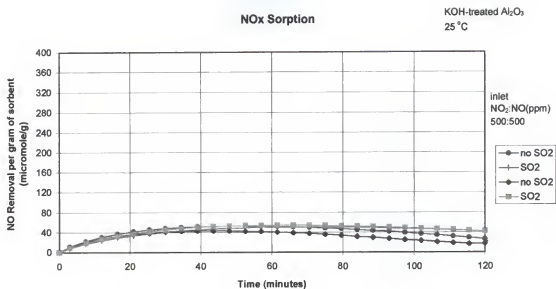
K<sub>2</sub>CO<sub>3</sub>-treated Al<sub>2</sub>O<sub>3</sub>  
25 °C

NO<sub>x</sub> sorption in the presence of SO<sub>2</sub> (83 ppm) for K<sub>2</sub>CO<sub>3</sub>-treated alumina at 25 °C.

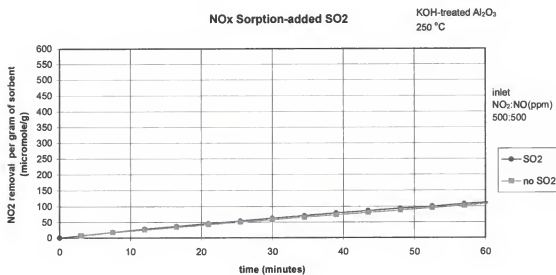
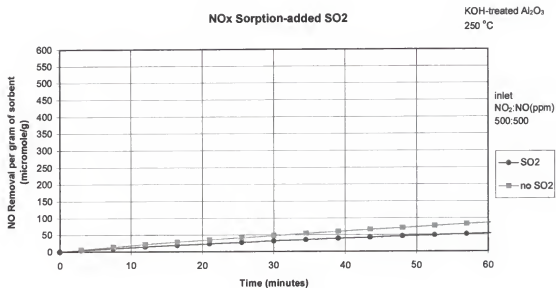




NOx sorption in the presence of SO<sub>2</sub> (83 ppm) for  $K_2CO_3$ -treated alumina at 250 °C.



NO<sub>x</sub> sorption in the presence of SO<sub>2</sub> (83 ppm) for KOH-treated alumina at 25 °C.



NO<sub>x</sub> sorption in the presence of SO<sub>2</sub> (83 ppm) for KOH-treated alumina at 250 °C.

## BIOGRAPHICAL SKETCH

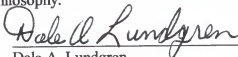
Maxwell Lee was born in Atlanta, Georgia on December 12, 1969. After graduation from Northside High School, in Atlanta, Georgia, in 1987 he moved to Tallahassee, Florida and attended Tallahassee Community College. After receiving a 2-year Associate Arts he entered the Civil Engineering program of Florida State University in 1990. In 1992 he transferred to the Environmental Engineering Program at the University of Florida. He received his Bachelor of Science degree with honors from the Environmental Engineering Department in December of 1994. Upon graduation he entered the graduate program of the University of Florida, Environmental Engineering Department. In 1995 he applied for and received direct entrance into the Doctoral Program specializing in Air Pollution with his Principal Advisor, Dr. Eric Allen. He received a National Science Foundation Pre-Doctoral MEDI Fellowship in the Spring of 1996. He began research on the USAF contract (F08637-C-6015) with the University of Florida entitled "Improved Control of Nitrogen Oxides) in 1996 which has been the cornerstone of his dissertation.

I certify that I have read this study and that in my opinion it conforms to acceptable standards of scholarly presentation and is fully adequate, in scope and quality, as a dissertation for the degree of Doctor of Philosophy.




Eric R. Allen, Chair  
Professor Emeritus of Environmental  
Engineering Sciences

I certify that I have read this study and that in my opinion it conforms to acceptable standards of scholarly presentation and is fully adequate, in scope and quality, as a dissertation for the degree of Doctor of Philosophy.



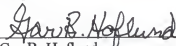
Dale A. Lundgren  
Professor Emeritus of Environmental  
Engineering Sciences

I certify that I have read this study and that in my opinion it conforms to acceptable standards of scholarly presentation and is fully adequate, in scope and quality, as a dissertation for the degree of Doctor of Philosophy.



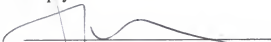
W. Emmett Bolch Jr.  
Professor of Environmental  
Engineering Sciences

I certify that I have read this study and that in my opinion it conforms to acceptable standards of scholarly presentation and is fully adequate, in scope and quality, as a dissertation for the degree of Doctor of Philosophy.



Gar B. Hoflund  
Professor of Chemical Engineering

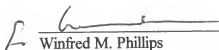
I certify that I have read this study and that in my opinion it conforms to acceptable standards of scholarly presentation and is fully adequate, in scope and quality, as a dissertation for the degree of Doctor of Philosophy.



Joseph D. Wander  
Adjunct Associate Professor of  
Environmental Engineering Sciences

This dissertation was submitted to the Graduate Faculty of the College of Engineering and to the Graduate School and was accepted as partial fulfillment of the requirements for the degree of Doctor of Philosophy.

May, 1999

  
Winfred M. Phillips  
Dean, College of Engineering

\_\_\_\_\_  
M. J. Ohanian  
Dean, Graduate School